Doctoral theses at NTNU, 2020:328

Arnt-Ole Tvenning

Drusenoid pigment epithelial detachments and age-related macular degeneration

Evaluation of treatment, observation of the natural history, and the use of artificial intelligence to detect and visualize the disease

Doctoral thesis

Arnt-Ole Tvenning

NTNU
Norwegian University of Science and Technology

Doctoral theses at NTNU, 2020:328

NTNU
Norwegian University of Science and Technology
Thesis for the Degree of
Philosophiae Doctor
Faculty of Medicine and Health Sciences
Department of Neuromedicine and Movement Science

ISBN 978-82-326-5002-6 (printed ver.)
ISBN 978-82-326-5003-3 (electronic ver.)
ISSN 1503-8181

NTNU
Norwegian University of Science and Technology

Arnt-Ole Tvenning

Drusenoid pigment epithelial detachments and age-related macular degeneration

Evaluation of treatment, observation of the natural history, and the use of artificial intelligence to detect and visualize the disease

Thesis for the Degree of Philosophiae Doctor

Trondheim, October 2020

Norwegian University of Science and Technology
Faculty of Medicine and Health Sciences
Department of Neuromedicine and Movement Science

NTNU
Norwegian University of
Science and Technology

NTNU
Norwegian University of Science and Technology

Thesis for the Degree of Philosophiae Doctor

Faculty of Medicine and Health Sciences
Department of Neuromedicine and Movement Science

ISBN 978-82-326-5002-6 (printed ver.)
ISBN 978-82-326-5003-3 (electronic ver.)
ISSN 1503-8181

Doctoral theses at NTNU, 2020:328

Printed by NTNU Grafisk senter

Drusenoid pigmentepitelavløsning og aldersrelatert makuladegenerasjon

Evaluering av behandling, det naturlige sykdomsforløp, og bruken av kunstig intelligens til å identifisere og visualisere sykdommen

Tematisk tittel *Store avleiringer under den gule flekken i øyet*
Behandling, naturlig forløp og kunstig intelligens

Pasienter med aldersrelatert makuladegenerasjon og væskeansamling (serøs pigmentepitelavløsning) eller avleiring av fettstoffer (drusenoid pigmentepitelavløsning) i den gule flekken i øyet har en høy risiko for utvikling av et endestadium av sykdommen med tap av sanseceller eller nydannelse av blodårer, og tap av synsfunksjon. I den første studien i avhandlingen testet vi behandling mot nydannelse av blodårer ved serøs og drusenoid pigmentepitelavløsning. Noen studier kunne indikere at behandling stabiliserte sykdommen selv om nydannelse av blodårer ikke kunne påvises, men det fantes ingen randomiserte kontrollerte studier som hadde testet dette. Vi tenkte at pasientene kunne ha nydannelse av blodårer som ikke kunne påvises med dagens bildeteknologi. De fleste pasientene som hadde serøs pigmentepitelavløsning ble ikke inkludert i studiet på grunn av at de hadde nydannelse av blodårer, de resterende pasientene hadde drusenoid pigmentepitelavløsning. Etter at studien var startet kom det ny kunnskap om en bildeteknologi som kunne identifisere forstadiene til et endestadium av sykdommen som det ikke finnes behandling for, og da 75% av pasientene i studien hadde dette stoppet vi videre inkludering og behandling. På grunn av et lite antall studiedeltakere kunne vi ikke konkludere om behandlingseffekt. Studiedeltakerne som allerede var inkludert ble fulgt i 2 år, og både de som hadde fått behandling og de som ble observert mistet synsfunksjon og hadde progresjon mot et endestadium av sykdommen med totalt bortfall av sanseceller i den gule flekken. Erfaringene fra denne studien viste at kunnskapen om pasienter med drusenoid pigmentepitelavløsning ikke var tilstrekkelig med dagens bildeteknologi, og dette var grunnlaget for den andre studien i avhandlingen.

I den andre studien i avhandlingen fulgte vi pasienter som hadde drusenoid pigmentepitelavløsning med den nye bildeteknologien og målte synsfunksjon. Vi tenkte at store drusenoide pigmentepitelavløsninger hadde en negativ påvirkning på synsfunksjonen og sansecellene i netthinnen. 1-års resultatene viste en sammenheng med økende størrelse på drusenoide pigmentepitelavløsninger og redusert syn og tap av sanseceller også før utvikling av endestadium av sykdommen. Dette arbeidet er publisert i et velrenommert tidsskrift.

I den tredje studien i avhandlingen trente vi en kunstig intelligens til å skille aldersrelatert makuladegenerasjon fra friske i tredimensjonale bilder av netthinnen. Den kunstige intelligensen ble ikke instruert i hva som kunne være sykdomstegn i bildene, og dette måtte den lære selv. Ved hjelp av en ny visualiseringsmetode kunne vi få innblikk i hva den kunstige intelligensen identifiserte som sykdom, og på denne måten kan det være mulig å oppdage nye sykdomstegn. Visualiseringsmetoden viste oss at den kunstige intelligensen brukte etablerte kjennetegn ved identifisering av sykdom, men også ikke fullt så etablerte kjennetegn som nervefiberlaget i netthinnen og blodårehinnen.

Den første studien i avhandlingen var en randomisert kontrollert studie. Den andre studien rapporterte 1-års resultatene fra en større observasjonsstudie av pasienter med aldersrelatert makuladegenerasjon og drusenoid pigmentepitelavløsning i helse Midt-Norge og helse Vest med 5 års planlagt oppfølgingstid. Den tredje studien var et samarbeid med institutt for datateknologi og informatikk for å utvikle og teste en kunstig intelligens til å identifisere og visualisere aldersrelatert makuladegenerasjon.

Kandidat: *Arnt-Ole Tvenning*
Institutt: *Nevromedisin og bevegelsesvitenskap*
Veiledere: *Dordi Austeng (Hovedveileder) og Jørgen Krohn (Biveileder)*
Finansieringskilde: Dette prosjektet er støttet av Stiftelsen Dam

Ovennevnte avhandling er funnet verdig til å forsvares offentlig
for graden ph.d. i medisin
Disputas finner sted fredag 30. oktober 2020, kl. 12.15

Table of contents

Acknowledgments

This thesis has been made possible by the patients and their interest in progressing research. The Dam Foundation is acknowledged for financially supporting our research, even though the project had to change course.

None of this would have been possible without the love, support, and patience of my wife Tonje and our two wonderful daughters Arja & Lydia. I am especially grateful that we have been doctoral candidates together and for our numerous late-night discussions about life and research. I am also thankful for the interest and support of my parents and sisters.

My supervisors Dordi Austeng and Jørgen Krohn, are thanked for their belief in me and the research during the many ups and downs over six (!) years. The numerous discussions, guidance, support, motivation, and valuable feedback have not only made the research better but far more rewarding.

I would also like to thank Marit Fagerli, who was the head of the ophthalmology department at St. Olavs Hospital for most of the research years. It is challenging to be a medical doctor and a researcher at the same time, and I appreciate that you encouraged, supported, and enabled me to be both.

Tor Elsås and Christian Hedels have been invaluable discussion partners over the years, and I would like to thank you for your interest and dedication.

I would also like to thank Vegard Forsaa, Agni Malmin, Liliane Skeidseid, and their research assistants at Stavanger University Hospital for their collaboration.

Tora Morken started our research collaboration with the Artificial Intelligence lab at NTNU, and I appreciate your persistence in encouraging me to be a part of this. The utilization of artificial intelligence in research might be essential in the future, and the way forward is exciting. The collaboration introduced me to Stian Hanssen with whom I have worked closely with and has reignited my belief in multidisciplinary research.

I would also like to thank Turid Follestad, who has been a discussion partner in the statistical modeling of the data.

Randi Bonesrønning has been invaluable in making sure that the study participants had appointments at the right time, and I much appreciate your efforts.

I also thank the Eye Research Group at St. Olavs Hospital, for your constructive feedback and discussions on manuscripts and posters over the years.

Last but not least, I wish to thank the optician Jan Løndal, the nurses, and the secretaries for their help during the research project.

Abbreviations

AMD: age-related macular degeneration

AREDS: age-related eye disease study group

AUC: area under the receiver operator curve

A2A: Age-Related Eye Disease 2 Ancillary SD-OCT study

BCVA: best-corrected visual acuity

CNN: convolutional neural network

CNV: choroidal neovascularization

cORA: complete outer retinal atrophy

cRORA: complete retinal pigment epithelium and outer retinal atrophy

DPED: drusenoid pigment epithelial detachment

ETDRS: early treatment diabetic retinopathy study letters

iRORA: incomplete retinal pigment epithelium and outer retinal atrophy

NORPED: Norwegian Pigment Epithelial Detachment Study

PED: pigment epithelial detachment

PDT: photodynamic therapy

RPE: retinal pigment epithelium

SD-OCT: spectral-domain optical coherence tomography

VEGF: vascular endothelial growth factor

List of papers

Paper I

Tvenning AO, Hedels C, Krohn J, Austeng D. Treatment of large avascular retinal pigment epithelium detachments in age-related macular degeneration with aflibercept, photodynamic therapy, and triamcinolone acetonide. Clin Ophthalmol. 2019;13:233-241. doi:10.2147/OPTH.S188315.

Paper II

Tvenning A-O, Krohn J, Forsaa V, Malmin A, Hedels C, Austeng D. Drusenoid pigment epithelial detachment volume is associated with a decrease in best-corrected visual acuity and central retinal thickness. The Norwegian Pigment Epithelial Detachment Study (NORPED) report no. 1. Acta Ophthalmol. doi:10.1111/aos.14423.

Paper III

Tvenning AO and Hanssen S, Austeng D, Morken TS. Retinal nerve fibre and choroid layers are signified as age-related macular degeneration by deep learning in classification of spectral-domain optical coherence tomography macular volumes. In manuscript.

Summary

Patients with age-related macular degeneration (AMD) and serous or drusenoid pigment epithelial detachments (PEDs) have a high risk of progression to geographic atrophy, choroidal neovascularization, and a loss of visual function. The abundance of lipids and proteins constituting drusenoid PEDs makes it challenging to visualize the choroidal blood circulation and probably also the choroidal neovascularization with the imaging technology available today. Case reports and studies have shown that treatment of serous and drusenoid PEDs with anti-vascular endothelial growth factor (anti-VEGF) or photodynamic therapy (PDT) could stabilize or improve visual function in the absence of choroidal neovascularization on angiography. There were none randomized controlled trials that had tested treatment with anti-VEGF or PDT for serous or drusenoid PEDs, and this was the foundation for our first study. However, most of the patients with serous PEDs were ineligible because of CNV, and one patient had a misdiagnosis and was excluded from statistical analysis because of central serous chorioretinopathy. In addition, new studies described precursors of end-stage geographic atrophy on spectral-domain optical coherence tomography (SD-OCT), and because 75 % of the included patients were in the progression of atrophy, further inclusion and treatment were stopped. The ability to describe atrophy on SD-OCT years before they were visible on color fundus photography made it evident that the knowledge about the natural history of drusenoid PEDs with today's imaging technology was insufficient, and the prospective observational Norwegian Pigment Epithelial Detachment Study (NORPED) was formed. The 1-year result showed that there was progressive atrophy with a decrease in best-corrected visual acuity and central retinal thickness during the earlier growth phase of drusenoid PEDs, and none developed choroidal neovascularization. A large amount of data was gathered with multimodal imaging in the NORPED study, some of which are better suited for machine learning. SD-OCT volumes have an abundance of information that could potentially represent new features of AMD. With the collaboration of the Department of Computer Science, we developed a deep learning model to detect AMD, and through the adaptation of a novel high-resolution visualization method, show the points of interest

in the images associated with the disease. The deep learning model identified AMD and controls with high performance. Known image regions associated with AMD such as drusen, the photoreceptor layers, and the retinal pigment epithelium layer were points of interest in the SD-OCT image associated with AMD. Interestingly, the retinal nerve fiber and choroid layer were also points of interest, and their association with AMD remains to be determined. High-resolution visualization methods in deep learning do not only provide feedback to the clinician but might also increase our knowledge of the disease.

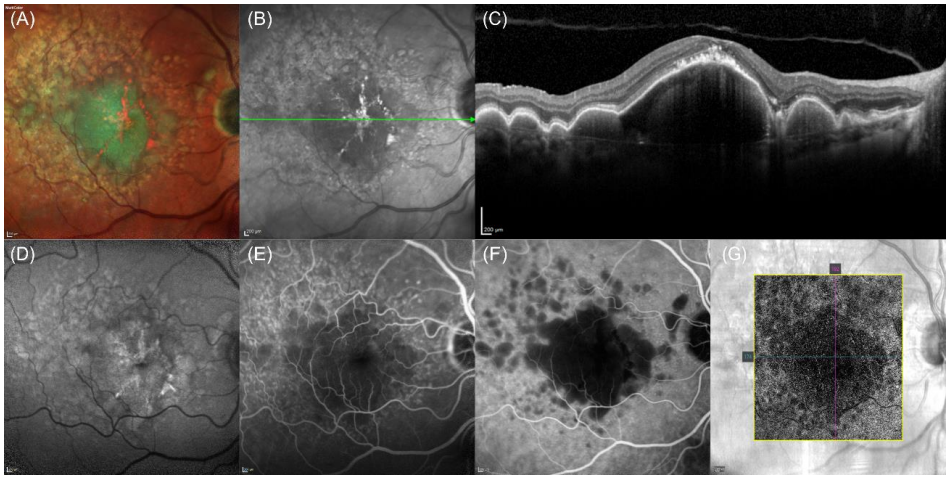

Figure 1 Multimodal imaging of a drusenoid pigment epithelial detachment. (A) Multicolor image. (B) Near-infrared reflectance image. (C) Optical coherence tomography scan. (D) Fundus autofluorescence image. (E) Fluorescein angiography image. (F) Indocyanine green angiography image. (G) Optical coherence tomography angiography scan. Scale bar = 200 µm. (Tvenning et al. 2020). .

1. Introduction

Drusenoid pigment epithelial detachment (DPED) is an uncommon manifestation of age-related macular degeneration (AMD) with an excessive accumulation of soft drusen material and fluid inside Bruch's membrane under the retinal pigment epithelium (RPE) (Figure 1C) (Cukras et al. 2010). Patients with DPEDs have a high risk of losing visual acuity due to choroidal neovascularization (CNV) and central geographic atrophy (Roquet et al. 2004; Cukras et al. 2010). The drusenoid material partially blocks visualization of the underlying choroidal vasculature (Figure 1E-G) (Arnold et al. 1997), and probably also CNVs. Our hypothesis for the first study in this thesis was that treatment with anti-vascular endothelial growth factor or in combination with photodynamic therapy (PDT) and triamcinolone acetonide could be beneficial in patients with large pigment epithelial detachments (PED) and no visible CNV on angiography. This study was designed to include both patients with DPEDs and serous

PEDs secondary to AMD. However, most patients with serous PEDs were ineligible because of CNV, and one patient had a misdiagnosis and was excluded from statistical analysis because of central serous chorioretinopathy. The remaining patients had DPED. During the first year of the study, descriptions of spectral-domain optical coherence tomography (SD-OCT) findings that preceded central geographic atrophy on color fundus photography were published (Wu et al. 2014). An interim analysis of our six months data showed that 75% of our included patients were in the progression of atrophy, and further inclusion and treatment of patients were stopped. We believed that the patients were too far in the progression of atrophy to justify the potential risk of treatments. In addition, treatments with PDT could hasten the progression of atrophy, and the role of anti-vascular endothelial growth factor (anti-VEGF) in the progression of atrophy remains to be determined. The included patients were followed for two years, and their progression of atrophy on SD-OCT was described.

The possibility to find precursors on SD-OCT many years before the development of central geographic atrophy on color fundus photography was the foundation for our observational study, the Norwegian Pigment Epithelial Detachment study (NORPED). Finding precursors of central geographic atrophy in eyes at risk of developing this endpoint are the first steps for future treatment trials. The NORPED study has a planned follow-up period of 5 years and aims to describe the natural history of DPEDs in central and western Norway. Our hypothesis for the second study, as previously suggested by Mrejen et al. (Mrejen et al. 2013), was that the increasing DPED volume, and subsequent distance to the choriocapillaris, would be associated with progressive outer retinal atrophy and a decrease in best-corrected visual acuity (BCVA) and central retinal thickness. Multimodal images were obtained of patients in the NORPED-study, and this abundance of information, particularly in the SD-OCT volumes, is suited for analysis by artificial intelligence and deep learning (Schmidt-Erfurth et al. 2018). Deep learning models have shown performance equal to or better than human experts in the field in diagnosing retinal disease on color fundus photography or SD-OCT images (Ting et al. 2017; De Fauw et al. 2018; Kermany et al. 2018). The deep learning models are not instructed in what parts of an image represent disease, and they extract these features out of the diseased images compared to the control images (Schmidt-Erfurth et al. 2018). With our third study, we wanted to understand what parts of an SD-OCT image

that were important in the identification of AMD. The most commonly used visualization methods in deep learning are of low-resolution, or they alter the architecture of the models, potentially limiting their performance. We modified a novel visualization method capable of showing precise points of interest associated with AMD in the SD-OCT images (Mopuri et al. 2019).

Thus, with three different studies and designs, we have tried to evaluate treatment, observe the natural history of the disease with new technology, and utilize artificial intelligence to detect AMD and visualize the SD-OCT image regions associated with the disease.

The next sections of this chapter intend to establish the background and knowledge available of DPEDs at the start of the first study. In addition, to understand DPED pathophysiology, we will look at the physiology and aging of the macula, the pathophysiology of AMD, and previously attempted and current treatments. Artificial intelligence, deep learning, and visualization methods will be explained, with current applications and previous studies on AMD.

1.1 Physiology and aging of the macula

In the human macula, the rods outnumber the cones. Cones are responsible for sharp and color vision, while the rods are responsible for night and peripheral vision. The perifovea is predominantly rods, while the fovea constitutes only cones (Curcio et al. 1990). Rods and cones are highly metabolically active and require the support of RPE and Müller cells to recycle vitamin A to regenerate photopigments (Muniz et al. 2007).

Müller cells are macroglial cells that span the retina from the ganglion cell layer to the outer retina, where they envelop retinal neurons, rods, and cones (Reichenbach & Bringmann 2013). In animal studies, these cells phagocytize outer-segment discs (Long et al. 1986) and transport docosahexaenoic acid to photoreceptors (Politi et al. 2001). Docosahexaenoic fatty acids have a high concentration in retinal phospholipids and are vital for visual function by modulating the rhodopsin content and shape of the discs and photoresponses (Jastrzebska et al. 2011; Shindou et al. 2017). The cones and rods

regenerate chromophores of photopigments through two cycles. All-trans retinol of the rods is recycled to 11-cis-retinal in the RPE, while all-trans retinol from the cones is recycled by the Müller cells in animal studies (Muniz et al. 2007). The Müller cells are active in normal retinal physiology, but also all types of retinal degeneration. Waste products, nutrients, water, ions, and other molecules are transported through Müller cells between retinal neurons and blood vessels. Importantly, they have a symbiotic relationship with retinal neurons in their column and provide homeostatic and metabolic support (Bringmann et al. 2006; Reichenbach & Bringmann 2013). Müller cells have a 1:1 ratio to cones in the macula of macaque monkeys, in addition to a variable number of rods and retinal neurons, which might be similar in humans, and essential for cone-mediated vision (Ahmad et al. 2003; Bringmann et al. 2006). Müller cells become activated by pathogenic stimuli, and these cells are neuroprotective while secreting neurotrophic factors, growth factors, and antioxidants, but can also contribute to degeneration and gliosis (Bringmann et al. 2009). Müller cells are also an intracellular reservoir for the carotenoid xanthophyll pigments lutein and zeaxanthin that are the most likely precursors for soft drusen and basal linear deposits in AMD (Powner et al. 2010).

The RPE is a cuboidal monolayer adjacent to rod and cone photoreceptors and is a multifunctional and indispensable component in the maintenance of neuroretina homeostasis. It has a proximity to the highly vascularized capillary bed of the choroid layer and forms a part of the outer blood-retina barrier through tight-junctions (Peyman & Bok 1972). The RPE regulates nutrients and waste product transport to and from the retina (Boulton & Dayhaw-Barker 2001). Specifically, the RPE transports ions and water from the retina to the choroid, secrete antioxidants, absorb high-energy light, maintains attachment of the retina, process and transport retinoids, and phagocytose rod and cone outer segments (Bok 1993; Boulton & Dayhaw-Barker 2001). The RPE cell does not under normal circumstances renew itself by cell division. With aging, there is RPE cell death, and the remaining RPE cells lose melanin granules, accumulate intracellular phototoxic lipofuscin, deposits basal deposits on or within Bruch's membrane, and form drusen (Boulton & Dayhaw-Barker 2001).

Bruch's membrane is a five-layered connective tissue between the choriocapillaris and the RPE, and nutrients and waste products must traverse this membrane to maintain retinal homeostasis. With aging, Bruch's membrane undergoes lipidization, cross-linking, calcification, and subsequent thickening that is thought to predispose to the deposition of drusen material in AMD (Pauleikhoff et al. 1990; Curcio et al. 2001).

With aging and also in the presence of advanced AMD (central geographic atrophy and/or CNV), a relative sparing of cones compared to rods occurs (Gao & Hollyfield 1992; Litts et al. 2016), probably because of the symbiotic support system with Müller cells, that unlike the RPE cells does not primarily rely on the choriocapillaris.

1.2 Age-related macular degeneration

1.2.1 Definition

In the Age-Related Eye Disease Study Research Group (AREDS), AMD was clinically defined in four different AREDS categories (Age-Related Eye Disease Study Research Group 2001) (Table 1). Ferris et al. proposed later, after a consensus meeting, a 5-stage clinical AMD classification scale based on the risk of progression: 1) No apparent aging changes: no drusen and no AMD pigment abnormalities, 2) normal aging: only druplets (small drusen ≤ 63 µm) and no AMD pigment abnormalities, 3) early AMD: medium drusen ≥ 63 µm ≤ 125 µm and no AMD pigment abnormalities, 4) intermediate AMD: large drusen ≥ 125 µm and/or any AMD pigment abnormalities, 5) advanced AMD: CNV and/or geographic atrophy (Ferris et al. 2013).

1.2.2 Epidemiology and risk factors

AMD accounts for 5.9% of blindness worldwide, and the proportion increases to over 14% in high-income countries with an older population (Bourne et al. 2014; Flaxman et al. 2017). The global prevalence of blindness because of AMD in 1990 was reduced

	First eye			Second eye
	Drusen size	Drusen Area	Pigment abnormalities	
1	None or <63µm	<125µm in diameter circle	None	Same as the first eye
2	<63µm or ≥63µm to <125µm, or none if pigment abnormalities	≥125µm in diameter circle	Absent or present, but no geographic atrophy	Same as the first eye or category 1
3	≥63µm to <125µm or ≥125µm. None required if central geographic atrophy.	≥360µm diameter circle if soft drusen, ≥656µm if soft drusen are absent	Absent or present, but central geographic atrophy absent	Same as the first eye or category 1 and 2
4	Same as category 3	Same as category 3	Same as category 3	CGA, CNV, or visual acuity <20/32 due to AMD.

Table 1 Age-Related Eye Disease Study Group (AREDS) categories
AMD, age-related macular degeneration; CGA, central geographic atrophy; CNV, choroidal neovascularization.

from 0.24 % (2.247.000 people) to 0.10 % (1.960.000 people) in 2015, maybe because of the introduction of anti-VEGF. However, the number of people affected did not change proportionally because of the increase of the elderly in the population (Flaxman et al. 2017).

After the introduction of anti-VEGF therapy to treat CNV associated with AMD, the incidence of legal blindness had a 50% reduction in Denmark from 2000 to 2010 (Bloch et al. 2012). The projected number of people with AMD in 2020 is 196 million, with a projected increase to 288 million by 2040 (Wong et al. 2014).

Aging is the most significant risk factor for AMD, followed by heredity and smoking (Thornton et al. 2005; Chakravarthy et al. 2010). The largest intraocular risk factors for

progression to advanced AMD are the size and location of drusen and RPE abnormalities (Joachim et al. 2015).

1.2.3 Pathophysiology

AMD is a vascular-metabolic-inflammatory disease (Seddon et al. 2016; Copland et al. 2018; Curcio 2018b). It is defined histologically by the presence of basal linear deposits primarily composed of lipoproteins secreted by the RPE, and basal laminar deposits (Figure 2) (Sarks et al. 2007; Wang et al. 2010). Focal aggregations of basal linear deposits constitute soft drusen (Sarks et al. 2007).

The development of soft drusen and basal linear deposits in AMD is not fully understood. However, the macula is highly metabolically active, requiring the support of both RPE and Müller cells for normal function, recycling of photopigments, and removal of waste products. The disturbance of this homeostasis forms the basis for understanding the disease processes of AMD and drusen formation.

An essential anatomical location for AMD is Bruch's membrane. Bruch's membrane has increased resistance to fluid with age (Ethier et al. 2004), and importantly also an impaired macromolecule (including lipoprotein) transport (Moore & Clover 2001). Soft drusen and basal linear deposits are thought to deposit within Bruch's membrane after impaired transport over an aged Bruch's membrane-choriocapillaris endothelium (Sarks 1980). The deposition of basal linear deposits and soft drusen material on Bruch's membrane constitute the "Oil Spill on aging Bruch's membrane" theory (Curcio 2018b).

After the discovery of extracellular deposits in the subretinal space on SD-OCT, named subretinal drusenoid deposits, new theories about the pathophysiology of AMD has emerged. Subretinal drusenoid deposits appear to be distributed where the density of rod photoreceptors is highest (Zweifel et al. 2010b; Zarubina et al. 2016), while drusen and basal linear deposits are more abundant in the central macula where there is a cone photoreceptor dominance.

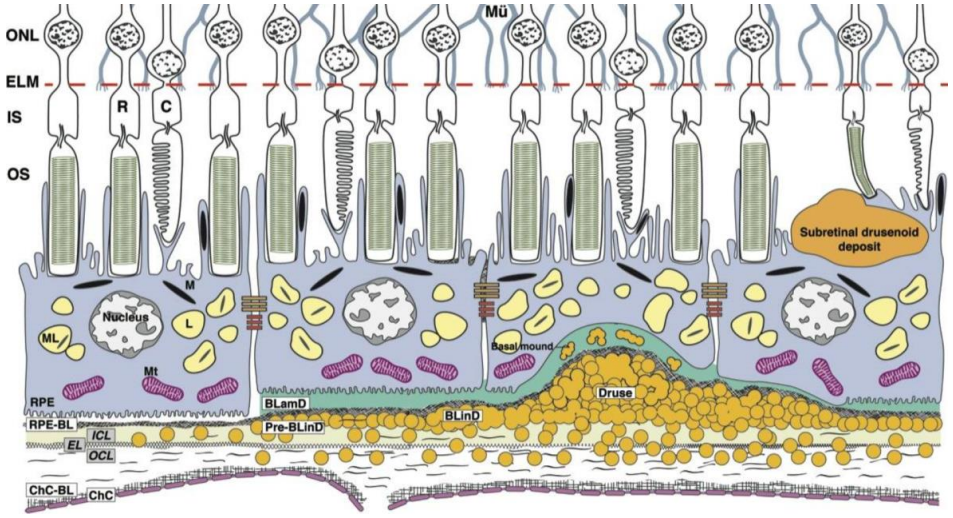

Figure 2 AMD by the layers. BrM consists of the ICL, EL, and OCL. Soft drusen and BLinD are two forms (lump and layer) of the same AMD-specific extracellular deposit. BLamD is a thickening of the RPE-BL. Basal mound is soft druse material within BLamD. Subretinal drusenoid deposit localizes to the subretinal space (between photoreceptors and RPE). RPE cells contain melanosomes, lipofuscin and melanolipofuscin, and mitochondria that provide signals for color fundus photography, fundus autofluorescence, and OCTs. Abbreviations from inner to outer: ONL, outer nuclear layer; ELM, external limiting membrane; IS, inner segments of photoreceptors; OS, outer segments of photoreceptors; R, rods; C, cones; L, lipofuscin; M, melanosome; ML, melanolipofuscin; Mt, mitochondria; Mu, Müller glia; circles, lipoprotein particles. (Curcio 2018b).

This discovery has led to a hypothesis that soft drusen biogenesis might be from the cone photoreceptors because of the different topography of subretinal drusenoid deposits and soft drusen (Figure 3) (Curcio et al. 2013; Curcio 2018a).

The main component of soft drusen in Bruch's membrane is large lipoproteins that are secreted by the RPE. The most abundant fatty acid in lipoproteins is linoleate (Wang et al. 2009), which is derived from diet, and not docosahexaenoate that is derived from

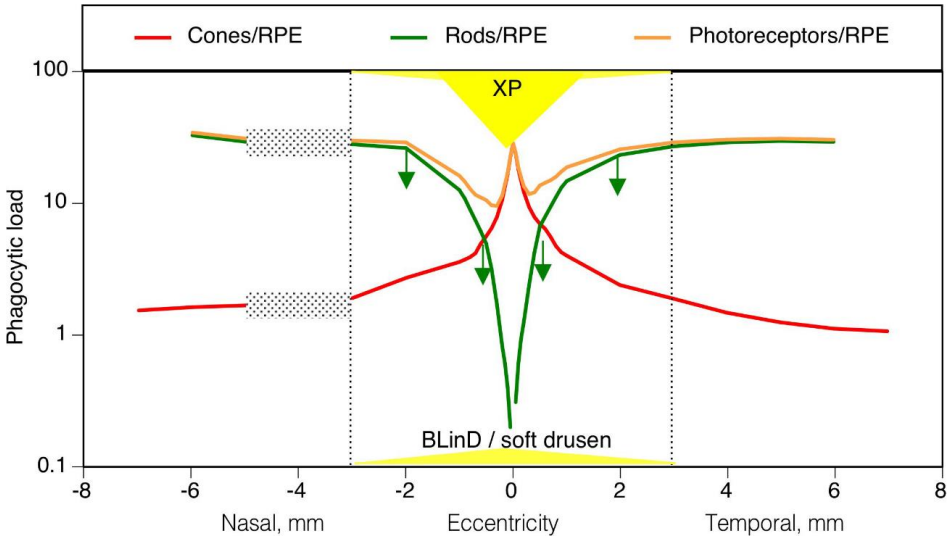

Figure 3 Topography of human macular photoreceptors, retinal pigment epithelium, XP, and BLinD/soft drusen. Dotted lines indicate the limits of the 6-mm-diameter macula. Stippled rectangles indicate the optic nerve head. Green downward arrows indicate the annulus of deepest rod loss in aging. The lateral extents of XP and BLinD/soft drusen are drawn to scale on the eccentricity axis and not-to-scale on the y-axis. (Curcio 2018a). *CC BY-NC-ND 4.0*.

outer segments (Curcio 2018b). The RPE and Müller cells recycle docosahexaenoate back to the photoreceptors (Bazan et al. 1992).

It is thought that the lipoproteins in soft drusen have two sources, from plasma proteins delivering lipophilic nutrients, and phagocytized outer segments. The lipoproteins are thought to enable offloading of unneeded lipids from the retina to the systemic circulation, thereby avoiding lipotoxicity (Curcio 2018b). The leading candidate of the origin to the fatty acid linoleate in lipoproteins is the delivery of the Xanthophyll pigments, through the RPE, to the Müller cells that support cone photoreceptors, which replenish from the diet (Curcio 2018a).

Xanthophyll pigments have been hypothesized to be a marker for Müller cell protection and enhancement of foveal cone visual function (Curcio 2018a). However, the

Xanthophyll pigments are probably also the primary source of peroxidizable and cytotoxic lipids in soft drusen lipoproteins.

AMD has genetic associations with the immune system (CFH and CFI), to a protein found in the retina whose function remains to be determined (ARMS2), and high-density lipoprotein cholesterol in the blood and their metabolism (LIPC, LPL, and ABCA1) (Chen et al. 2010; Grassmann et al. 2017; Toomey et al. 2018).

The immunological aspects in AMD development and progression are still not understood but may be important therapeutic targets to halt the progressive atrophy of RPE and photoreceptors (Copland et al. 2018). The eye has an immune privilege, which is maintained by the blood-retinal barrier and blood-aqueous barrier and has a tolerance of foreign antigens because of local immunosuppressive factors (Ambati et al. 2013). However, with aging, there is accumulative oxidative stress to retinal and choroidal tissues that result in para-inflammation to maintain homeostasis, and if dysregulated, it can contribute to an inflammatory component in the pathogenesis of AMD (Anderson et al. 2002; Chen & Xu 2015). There is an accumulation of retinal microglia or infiltrating monocytes in the subretinal space or at the choroid-RPE interface in AMD (Gupta et al. 2003). Many of the proteins in the complement system have been identified in drusen (Anderson et al. 2002), and complement pathway components have also been found to be locally expressed by cells in the choroid and in the RPE (Anderson et al. 2010). The strong genetic association to the innate immune system, particularly with CFH, are associated with AMD (Klein et al. 2005; Fritsche et al. 2014). CFH is an inhibitor of the complement cascade (Rodriguez de Cordoba et al. 2004), and the amino acid substitution in the CFH gene at position 402 (CFHY402H) might increase the immune response in AMD (Shaw et al. 2012). AMD patients homozygous for CFHY402H have also been found to have elevated levels of pro-inflammatory C - reactive protein in the choroid (Johnson et al. 2006). Another study has found increased levels of aged $CD56^{+}$ $CD28^{-}$ T cells in the peripheral blood in person with AMD compared to aged controls (Faber et al. 2013), suggesting that the adaptive immune system may play a part in the pathogenesis of AMD.

The exact mechanism of CNV formation in AMD is still not fully understood. VEGF has been found in surgically excised CNV membranes in patients with age-related macular degeneration (Frank et al. 1996). The primary contributor to the production of VEGF is the RPE as a response to heterogeneous stressors (Ambati & Fowler 2012). The complement components C3a and C5a induce VEGF expression in vitro and in vivo (Nozaki et al. 2006), and cultured human RPE cells (ARPE-19) secrete VEGF after oxidative stress and subsequently reduced regulation of the complement cascade (Thurman et al. 2009). The role of macrophages in the formation of CNV is unclear, and studies on animal models have found both pro-angiogenic and protective effects of macrophages (Skeie & Mullins 2009). However, macrophages have been found in human CNV membranes (Lopez et al. 1991), and they have also been found to express VEGF (Grossniklaus et al. 2002).

The RPE cells ontop of drusen progress towards atrophy, and the drusenoid material in turn regress. The tension of oxygen is reduced by 30-50% at the apex of drusen, depending on drusen height and distance to choriocapillaris (Stefánsson et al. 2011). RPE atop drusen might migrate anteriorly to seek oxygen from retinal capillaries, apparent as intraretinal hyperreflective foci on SD-OCT (Curcio et al. 2017), or these hyperreflective foci might represent dead or dying RPE.

Drusen have been shown to have a cubic growth rate over time (Schlanitz et al. 2017), and some drusen can regress without visible progression to advanced AMD (Complications of Age-Related Macular Degeneration Prevention Trial Research Group 2006; Schlanitz et al. 2017). However, there is convincing evidence that soft drusen and DPEDs facilitates RPE and photoreceptor atrophy, with rods being the most vulnerable in the early phases of the disease. This process is affected by distance to choriocapillaris, lipotoxicity, hypoxia, immunoreactivity, and a loss of nutrients (Curcio 2018b).

1.2.4 Drusenoid pigment epithelial detachments

DPEDs are a high-risk manifestation of AMD but a relatively uncommon presentation with only 3.2 % of AMD patients in the AREDS trial presenting with DPEDs ≥ 350 μm (Cukras et al. 2010). DPEDs are thought to be caused by the confluence of soft drusen (Casswell et al. 1985; Abdelsalam et al. 1999), and in part by the accumulation of fluid caused by the hydrophobicity of Bruch's membrane (Bird 1991; Arnold et al. 1997), and are often found in the central macula (Casswell et al. 1985). The size-criterion of DPEDs varies in the literature from 350 μm to 1 disc diameter (Roquet et al. 2004; Cukras et al. 2010; Alexandre de Amorim Garcia Filho et al. 2013).

The retrospective study of DPEDs in the prospective AREDS trial showed that within five years, 42% progressed to advanced AMD, with 19% developing central geographic atrophy and 23% CNV (Cukras et al. 2010). A retrospective study with DPEDs found that in 12 eyes with a follow-up of more than ten years, 25% developed CNV, and 75% developed geographic atrophy (Roquet et al. 2004). In contrast, patients in the AREDS trial with only small drusen, some intermediate drusen or pigment abnormalities had only a 1.3% probability of developing advanced AMD over five years (Age-Related Eye Disease Study Research Group 2001).

DPEDs appear yellow on clinical examination, often with a stellate pattern of brown pigment, and are often indistinguishable from nearby drusen (Mrejen et al. 2013). On fluorescein angiography (FA), the fluorescence is markedly reduced in areas with drusen probably because of the low fluid content in the sub-RPE space and the blocking effect of drusen material of the choriocapillaris (Casswell et al. 1985). The fluorescence increases over time without late leakage called "staining." There can be focal areas of hypofluoresence caused by pigment epithelium abnormalities called "blocking," and areas of hyperfluoresence caused by atrophy of the RPE called "window defects." On ICGA, the choroidal vessels are hypofluorescent in the presence of drusen and can be markedly obscured in the presence of DPEDs (Arnold et al. 1997). ICGA has better visualization of the choroidal circulation since the RPE does not so readily block the signal, and because indocyanine green is mainly protein bound and does not diffuse out

of the fenestrated choriocapillaris, which would obscure visualization of CNV. ICGA is better than FA in diagnosing occult CNV (Type 1 CNV, under the RPE) in the presence of serous PEDs (Yannuzzi et al. 1992; Gass 1994). In DPEDs with no CNV, ICGA will appear hypofluorescent in the early and late phases, with no "hotspot" or "plaque" within or at the border of the DPED (Mrejen et al. 2013).

The exclusion of CNV on multimodal angiography in DPEDs can be challenging, and treatment is controversial (Baba et al. 2012). DPEDs can have no findings on FA, ICGA, and SD-OCT angiography that indicates CNV, despite rather extensive changes seen on SD-OCT, including subretinal fluid and intraretinal cysts (Roquet et al. 2004). However, subretinal fluid might also be degenerative and associated with acquired vitelliform lesions (Mrejen et al. 2013). Case series and case reports have suggested a potential treatment benefit of anti-VEGF or PDT. Ritter et al. treated twelve avascular drusenoid and serous PEDs with anti-VEGF and reported stabilization of BCVA after one year, but with heterogeneous anatomical outcomes (Ritter et al. 2010). Another prospective case series treated six patients with anti-VEGF, which led to the stabilization of BCVA and improvement in two patients (Gallego-Pinazo et al. 2011). Another case report showed regression of DPED and improvement of BCVA after PDT (Lee & Kim 2008). Drusen regression and improvement or stabilization of vision have also been reported following argon laser photocoagulation of extensive soft drusen and DPEDs (Sarks et al. 1996).

1.2.5 Geographic atrophy

In the AREDS study, drusen were present in 100% of later diagnosed areas of geographic atrophy, implicating drusen as the origin of this endpoint (Klein et al. 2008). Geographic atrophy is defined in color fundus photography as a sharply demarcated round hypopigmented area (Figure 4A), with visible choroidal vasculature, of at least ≥ 175 µm in diameter (Bird et al. 1995). In fundus autofluorescence imaging, the same areas are hypofluorescent because of the loss of RPE cells and lipofuscin (Figure 4B) (von Ruckmann et al. 1997).

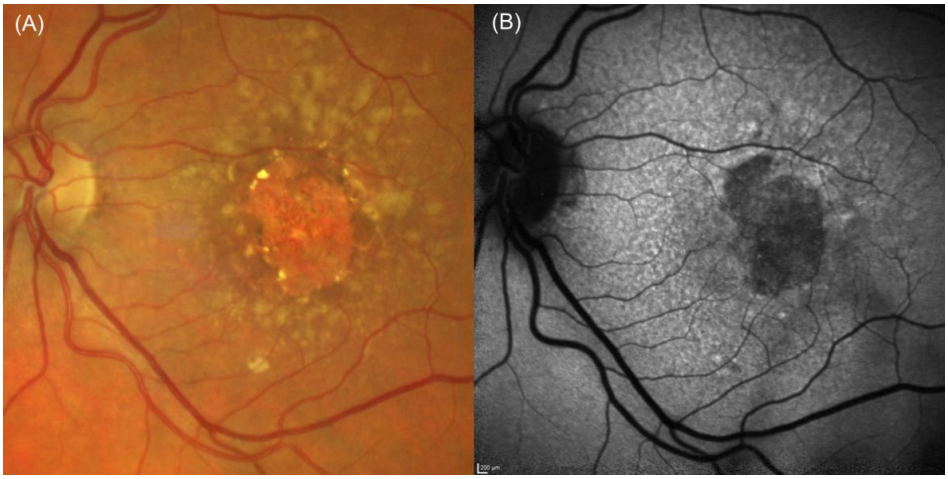

Figure 4 Central geographic atrophy on (A) color fundus photography showing a sharply demarcated oval hypopigmented area in the fovea with visible choroidal vasculature. (B) The corresponding area on fundus autofluorescence with hypofluoresence because of the loss of retinal pigment epithelium and lipofuscin.

Geographic atrophy in AMD usually starts in the perifovea, and patients may maintain good visual acuity until the fovea is affected (Sarks et al. 1988). The growth of geographic atrophy on color fundus photography and fundus autofluorescence is typically faster towards the periphery of the macula than towards the fovea and varies considerably between patients (Holz et al. 2014).

In the Beaver Eye Dam and Geographic Atrophy Progression Studies, eyes with multifocal lesions had a higher growth rate and involvement of the fovea compared to those with just one area of geographic atrophy (Klein et al. 2008; Schmitz-Valckenberg et al. 2016). Lesions with banded or diffuse fundus autofluorescence patterns grow more rapidly than those with focal or no pattern (Schmitz-Valckenberg et al. 2016).

The high-resolution SD-OCT findings of geographic atrophy and the perilesional loss of the photoreceptor lines, outer nuclear layer, and descent of the outer plexiform layer had also been described (Fleckenstein et al. 2010). Drusen height was found to be associated with an increased risk of focal atrophy (Ouyang et al. 2013), and drusen height was associated with a focal loss of the overlying photoreceptor layer (Schuman et al. 2009).

1.2.6 Treatment

Non-neovascular AMD

There is currently no available treatment for non-neovascular AMD. However, the AREDS study showed, for AMD patients in AREDS category 3 and 4, that treatment with oral supplements of anti-oxidants and zinc reduced the probability of progression to advanced AMD from 28% for the placebo group to 20% for the treatment group (Age-Related Eye Disease Study Research Group 2001). Five years after the trial ended, there was still a beneficial effect of the AREDS formulation; however, only for the development of CNV and not geographic atrophy (Chew et al. 2013). The AREDS2 trial did not show an added benefit of adding lutein + zeaxanthin, docosahexaenoic acid + eicosapentaenoic acid, or both to the original AREDS formulation (The Age-Related Eye Disease Study 2 Research Group 2013). However, smokers could substitute the carotenoid in the original AREDS formulation with lutein and zeaxanthin, because of the increased risk of lung cancer with beta-carotene (The Age-Related Eye Disease Study 2 Research Group 2013).

The regression of drusen has been reported to follow thermal laser macular photocoagulation. A retrospective study of 27 patients and 42 eyes with progressive visual loss, extensive drusen, and no CNV on angiography were treated with thermal laser photocoagulation. 52% had stabilization of vision and regression of drusen after an average of 3 years of follow-up (Wetzig 1988). Another study treated 12 patients (10 with extensive drusen) with thermal laser photocoagulation that had a high-risk of progressing to advanced AMD. After 12 months, one patient improved by one line in visual acuity, seven patients were stable and one worsened by four lines due to CNV, and nine of the patients had drusen regression (Guymer et al. 1997). Nine patients with a follow-up of more than 12 months retained 20/30 vision or better, except one that developed geographic atrophy. A small randomized controlled trial of 30 patients with bilateral extensive confluent drusen and pigment abnormalities have shown that thermal laser photocoagulation of temporal drusen facilitates macular drusen regression in 29 of the 30 treated eyes, compared to only 2 of the 30 control eyes (Figueroa et al. 1997). In

the same study, after three years, 17% of the treated eyes improved in visual acuity, and 33% remained stable compared to no improvement and 50% remaining stable in the untreated control group. Another small randomized controlled trial of 38 patients showed that drusen were significantly reduced in eyes with thermal laser photocoagulation compared to an increase in the control group (Frennesson & Nilsson 1998). However, a large randomized controlled trial that included 1052 participants evaluated thermal laser photocoagulation of patients with ≥ 10 large drusen ≥ 125 μm failed to demonstrate a difference in BCVA and progression to advanced AMD between groups (Complications of Age-Related Macular Degeneration Prevention Trial Research Group 2006).

Rheopheresis (extracorporeal plasma filtration) has also been tried to treat non-neovascular AMD. The plasmapheresis treatment eliminates high-molecular-weight plasma proteins and aims to reduce plasma viscosity, resulting in improvement in the microcirculation (Pulido et al. 2005). In an interim analysis of the MIRA-1 randomized controlled study, there were favorable visual outcomes in the treatment group (Pulido et al. 2005). However, analysis of the 1-year results did not show a difference between groups in the intention to treat analysis, but only in the modified per-protocol analysis (Pulido et al. 2006). The validity of the results was questioned as 37% of the treated, and 29% of the placebo cases did not meet inclusion criteria; in addition, SD-OCT or multimodal angiography was not routinely obtained to exclude CNV. Small randomized controlled trials have since found a benefit with reduction of the DPED area and increase of BCVA for the treatment groups (Koss et al. 2009; Rencova et al. 2011; Blaha et al. 2013). However, there have been no large randomized controlled trials since the MIRA-1 study to determine the efficacy of the somewhat invasive treatment with Rheopheresis.

Treatment with cholesterol-lowering drugs has also been evaluated in non-neovascular AMD. One study suggests that human-derived ARPE-19 cells synthesize and secrete apoB100 lipoproteins and that cultures treated with statins have inhibited secretion by reducing cellular cholesterol (Wu et al. 2010). In a double-masked randomized placebo-controlled trial, 114 AMD patients received either simvastatin 40mg/day or

placebo, and those with intermediate AMD showed a two-fold decrease in the risk of progression compared to controls (Guymer et al. 2014).

Neovascular AMD

Laser photocoagulation was the first available treatment for CNV associated with AMD, but only for well-defined lesions that spared the center of the macula (Virgili & Bini 2007). In the randomized controlled TAP trial evaluating the treatment of predominantly classic CNV (type 2 CNV on SD-OCT above the RPE) with PDT, the treatment group had a lower percentage of ≥ 15 early treatment diabetic retinopathy study (ETDRS) letters loss compared to the placebo group after 1 and 2 years of follow-up (Gass 1994; Bressler 1999; Bressler 2001). The randomized controlled VIP trial evaluated the treatment of type 1 CNV with PDT showed that the treatment group had a significantly lower percentage of patients losing ≥ 15 ETDRS letters compared to the placebo group after two years of follow-up (Verteporfin In Photodynamic Therapy Study Group 2001). However, PDT treatment carried a risk of severe visual loss, with 4.4% of patients in the VIP trial losing > 20 ETDRS letters compared to pre-treatment.

Even though treatment with laser and PDT could reduce the risk of losing visual acuity in neovascular AMD, it was not until after the introduction of anti-VEGF therapy that patients started gaining some of their lost visual function. The first study that evaluated treatment with anti-VEGF (bevacizumab) was a study by Michels et al. in 2005 that successfully treated nine patients with systemic anti-VEGF for subfoveal CNV with improvement in visual function, SD-OCT, and disappearance of leakage on angiography (Michels et al. 2005). The randomized controlled phase 3 trial called Minimally classic/occult trial of the anti-VEGF antibody Ranibizumab in the Treatment of Neovascular Age-Related Macular Degeneration (MARINA), showed the superiority of intravitreal injections with 0.3mg and 0.5mg of Ranibizumab with a gain of 6.3 and 7.2 ETDRS letters, respectively, compared to the loss of 10.3 ETDRS letters in the placebo group (Rosenfeld et al. 2006). Another randomized controlled trial (ANCHOR) compared monthly Ranibizumab 0.3 mg or 0.5 mg with sham PDT therapy to sham injections with PDT therapy for predominantly classic CNV. The anti-VEGF treatment

groups had an increase of 8.5 and 11.3 ETDRS letters compared to a loss of 9.5 ETDRS letters in the PDT group (Brown et al. 2006). Because of the high cost of Ranibizumab injections, the randomized controlled trials, CATT and LUCAS, have shown that Bevacizumab is non-inferior to Ranibizumab, which has made Bevacizumab the first-line of treatment in many countries (Martin et al. 2011; Berg et al. 2015). Additional anti-VEGF agents have become available, and Aflibercept has shown to be non-inferior to Ranibizumab with bi-monthly intravitreal injections, after a loading dose (Heier et al. 2012).

The long term effect of anti-VEGF treatment has been evaluated in the SEVEN-UP study. This study showed that after a mean of 7.3 years since the MARINA and ANCHOR studies, there was geographic atrophy present in 98% of eyes, and its progression and size were significantly associated with a decrease in visual acuity (Bhisitkul et al. 2015). The Fight Retinal Blindness Study group observed 1212 eyes with neovascular AMD using the treat and extend regimen with a mean follow-up time of 53.5 months. Mean visual acuity was higher than baseline mean visual acuity for six years, and by year seven, it was 2.6 ETDRS letters lower than baseline for the 131 eyes (11%) still being followed. During the first five years, 53% discontinued therapy due to deterioration of vision because of geographic atrophy or subretinal fibrosis (Gillies et al. 2015).

1.3 Artificial Intelligence

In many disciplines of medicine, imaging has become increasingly important for the diagnosis and management of diseases. The sheer amount of images and information available makes every patient a big-data challenge and opportunity (Obermeyer & Lee 2017). The image-heavy disciplines of radiology, pathology, dermatology, and ophthalmology are especially suited for the application of artificial intelligence (Jiang et al. 2017).

1.3.1 History and Definitions

Artificial intelligence is a branch of computer science, originating from a workshop by John McCarthy in 1956. The idea behind artificial intelligence is that humans can describe any form of information in such a precise way that computers can do it. Arthur Samuel created in 1959 machine learning, where computer algorithms can extract generalized principles from data, resulting in mathematical models with detailed rules of a given dataset.

Artificial neural networks are an evolution of machine learning, where layers of neurons process information from an input to an output layer. It was not until after the development of deep neural networks in 2012 that the performance truly increased (Krizhevsky et al. 2012). In deep neural networks, multiple intermediate layers are positioned between the input and output layer, and each layer can transform the signal input to a more abstract and higher-level representation. Deep neural networks were the beginning of a new subfield in artificial intelligence called deep learning (LeCun et al. 2015). In deep learning, the neural network can extract the differentiating features of the conditions in the dataset and use them for classification (Figure 5). The most suitable deep learning architecture for imaging data is convolutional neural networks (CNN) (Lecun et al. 1998). CNNs resemble the organization of the visual cortex, where each neuron process data only from its receptive subfield.

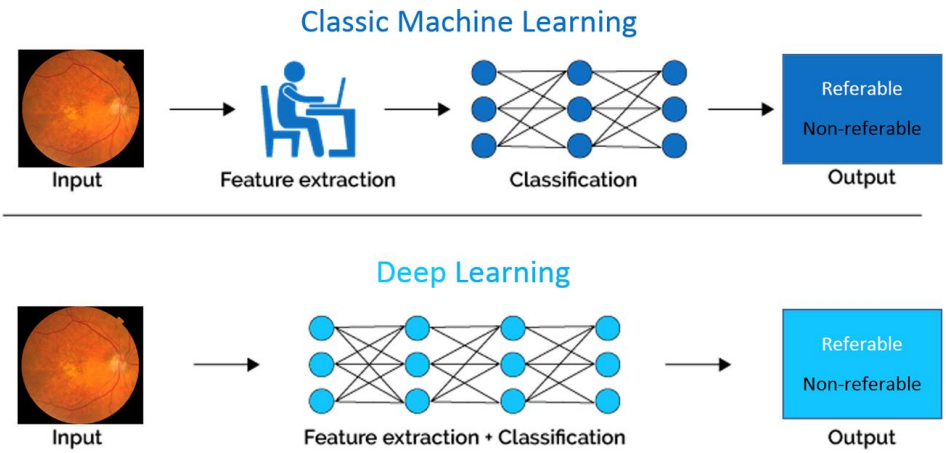

Figure 5 Illustration of the principal difference between the classic machine learning models and the deep learning ones. Instead of learning to classify an input image from hand-engineered features deep learning models are learning to both extract features and classify from the input directly, hence allowing for fully "end-to-end" learning. (Schmidt-Erfurth et al. 2018). *CC BY-NC-ND 4.0*.

The convolutional layers are a set of mathematical filters that extract features from an image that are successively stacked to create progressively more sophisticated and descriptive features (from simple lines and edges to an intricate image). Deep learning models trained with sufficiently large datasets can, in this way, recognize visual patterns. In 2015, deep learning models exceeded human-level performance at 2D image classification of 1.2 million images into 1000 categories in the annual ImageNet Large Scale Visual Recognition Competition (He et al. 2015; Russakovsky et al. 2015).

1.3.2 Deep learning and age-related macular degeneration

In ophthalmology, high-resolution color fundus photography in the 1990s and SD-OCT images in the 2000s have been used for the diagnosis and follow-up of disease, resulting in large image-databases. SD-OCT has become the gold standard in the management of most macular diseases, including AMD (Schmidt-Erfurth et al. 2017). An SD-OCT

image is obtained with 20.000-52.000 axial-scans per second, with a resolution of 5-7 µm, enabling a detailed assessment of pathology (de Boer et al. 2003). The ever-increasing number of SD-OCT images is an untapped pool of information, with about 60 million voxels per volume that can train deep learning models for classification, segmentation, and prediction tasks (Schmidt-Erfurth et al. 2018).

Most studies using deep learning models in ophthalmology utilize pre-trained architectures (AlexNet, Inception, VGGnet, ResNet) from past ImageNet competition winners with transfer learning (Apostolopoulos et al. 2016; Lee et al. 2017; Kermany et al. 2018; Lu et al. 2018; Motozawa et al. 2019; Perdomo et al. 2019). Transfer learning has the advantage of increasing performance on smaller datasets, but it limits them to 2D image classification. One study has trained two deep learning models from scratch to segment 3D SD-OCT images that were utilized by a second model for the classification of multiple macular diseases (De Fauw et al. 2018).

1.3.3 Performance

Deep learning models have, during the recent years, shown high performance in classifying retinal disease on both fundus photography and SD-OCT-images, comparable to or better than experts in the field.

A study trained and validated a deep learning model on nearly 500.000 color fundus photographs and obtained area under the receiver operator curves (AUC) of 93.6%, 94.2%, and 93.1% for detecting referable diabetic retinopathy, glaucoma suspects, and AMD, respectively (Ting et al. 2017). Another study trained on 2D SD-OCT images and had similar performance as six ophthalmologists in diagnosing CNV, diabetic macular edema, drusen, and normal with an AUC of 99.9% (Kermany et al. 2018). Another deep learning model trained on over 100.000 central 2D SD-OCT images that distinguished AMD from control cases with AUC of 97.5% when all SD-OCT scans from the same patient were used (Lee et al. 2017). De Fauw et al. trained two deep learning models on a wide range of macular disease from 14.884 3D SD-OCT volumes. The first of the two models segmented 3D SD-OCT images that were classified by the

second model. The AUC from the validation dataset of 997 patients was 99.2%, and the deep learning model (5.5% error rate) performed comparable to the two best retina specialists (6.7% and 6.8% error rates) and significantly outperformed the other six experts (>7.3% error rate) (De Fauw et al. 2018). Another deep learning model trained on 25.134 2D SD-OCT images to detect macular holes, subretinal fluid, cystoid macular edema, and epiretinal membranes obtained an AUC of 98.4% and performed equivalently to or better than two retina specialists (Lu et al. 2018).

1.3.3 Visualization of the "black box" in deep learning

Several authors have highlighted the need for visualization methods to understand the results of the deep learning models (Lu et al. 2018; Ting et al. 2019). Even though deep learning models have a performance comparable to or better than experts in the field, the clinicians must understand which image features were used in the diagnosis. Through visualization methods, it is possible to gain some insight into which parts of an image that were important for the diagnosis. Visualization methods currently used display low-resolution heat maps (Lee et al. 2017; Kermany et al. 2018), or alter the CNN architecture (Perdomo et al. 2019), potentially limiting its performance (Mopuri et al. 2019). A new visualization method called CNN fixations was adapted for our study. This method is capable of displaying high-resolution points of interest that were important for the diagnosis (Mopuri et al. 2019) in addition to lower resolution heat maps. The CNN fixations method does not alter the CNN architecture and has not previously been utilized to visualize the points of interest important for the diagnosis of retinal disease.

2. Aims

The aims of this thesis were to evaluate treatment, observe the natural history with today's new technology, and find possible disease features of AMD and DPED. These aims resulted in three different studies of AMD patients with DPEDs.

1. To test treatment with anti-VEGF, PDT, and triamcinolone acetonide in AMD patients with AMD and serous or drusenoid PEDs without identifiable CNV on angiography.

2. To study the natural history of DPEDs with multimodal imaging and investigate the association of DPED volume on visual function and retinal atrophy.

3. To train and validate a deep learning model on SD-OCT volumes from AMD cases and controls, and through the adaptation of a novel visualization method, learn the precise image regions used in the identification of AMD.

3. Material and methods

3.1 Study designs

Paper I

The first study, "Treatment of large avascular retinal pigment epithelium detachments in age-related macular degeneration with aflibercept, photodynamic therapy, and triamcinolone acetonide," was a randomized controlled trial that started in April 2014 with a planned follow-up period of two years. The study was registered at Clinicaltrials.gov: NCT01746875.

Paper II

The second study, "Drusenoid pigment epithelial detachment volume is associated with a decrease in best-corrected visual acuity and central retinal thickness. The Norwegian Pigment Epithelial Detachment Study (NORPED) report no.1", reports the one-year results from a prospective, observational, multicentre study that included patients from March 2016 to December 2017, with a planned follow-up period of five years. The study is an ongoing research collaboration with the University hospitals of Bergen and Stavanger.

Paper III

The third study, "Retinal nerve fibre and choroid layers are signified as age-related macular degeneration by deep learning in classification of spectral-domain optical coherence tomography macular volumes," evaluated the performance of a deep learning model to detect AMD on two different datasets, and through the adaptation of a novel visualization method learn the image features used in the identification of the disease. The study was a collaboration with the Department of Computer Science, Norwegian University of Science and Technology.

3.2 Study populations

Paper I

Patients with large serous PEDs or DPEDs without suspicion of CNV were referred from other eye departments and ophthalmologists in the Central Norway Health Region to the eye department at St.Olavs Hospital.

The included patients were older than 50 years with treatment-naïve AMD, subfoveal PED ≥ 1500 μm, BCVA from ≤20/32 to ≥20/400, and no visible CNV on fluorescein angiography (FA) or indocyanine green angiography (ICGA). Patients with subfoveal fibrosis, central geographic atrophy, or concurrent eye disease that could affect BCVA were excluded.

PEDs that did not show leakage on FA or "hotspots" or "plaques" on ICGA were defined as avascular. The PEDs that appeared yellow on clinical examination, with primarily hyperreflective contents on SD-OCT (Cirrus HD-OCT, Carl Zeiss Meditec AG, Jena, Germany), staining on FA, and hypofluoresence on ICGA, were defined as DPEDs. PEDs with hyporeflective contents on SD-OCT, pooling on FA, and hypofluoresence on ICGA were defined as serous PEDs.

The fundus and angiographic images (Zeiss FF 450 plus, Carl Zeiss Meditec AG, Jena, Germany) were reviewed and graded by two retina specialists, and pseudonymized images were sent to an external retina specialist to ensure a correct diagnosis of avascular PED.

Paper II

Patients with large DPEDs were referred to the University Hospital of Trondheim, Bergen, and Stavanger. Patients examined with the Spectralis HRA-OCT (Heidelberg Engineering GmbH, Heidelberg, Germany) in Trondheim and Bergen were included in

this study. This was done because the semi-automatic segmentation program Rev Analyzer (ADCIS SA, Saint-Contest, France) that was used for calculation of DPED volume only was compatible with the Spectralis HRA-OCT.

Included patients were ≥ 50 years of age, had a DPED ≥ 1000 µm, and BCVA ≥ 20/400. Eyes with previous vitrectomy, concurrent corticosteroid therapy, previous intravitreal anti-VEGF injections or PDT, subfoveal fibrosis, central geographic atrophy, CNV on FA or ICGA, glaucoma with central visual field defects, diabetic macular edema, proliferative diabetic retinopathy, and uveitis were excluded.

PEDs that appeared yellow on clinical examination, predominantly hyperreflective contents on SD-OCT, staining on FA, and hypofluoresence on ICGA were defined as DPEDs (Casswell et al. 1985; Arnold et al. 1997). SD-OCT angiography (Cirrus HD-OCT, Carl Zeiss Meditec AG, Jena, Germany) was also obtained at every study visit to exclude CNV.

Baseline FA and ICGA images obtained with Spectralis HRA-OCT were pseudonymized and sent to an external reading center to ensure a correct diagnosis of avascular DPED.

Paper III

The study was conducted on the Age-Related Eye Disease 2 (AREDS2) Ancillary SD-OCT (A2A SD-OCT) study and NORPED datasets. These datasets contained images from patients with intermediate or advanced AMD in the A2A SD-OCT study and early, intermediate (DPEDs), or advanced AMD in the NORPED dataset.

The A2A SD-OCT study dataset (http://people.duke.edu/~sf59/RPEDC_Ophth_2013_dataset.htm) included patients 50-85 years of age with intermediate AMD and drusen ≥ 125 µm in both eyes, or one eligible eye and advanced AMD in the fellow eye. Exclusion criteria were previous vitreoretinal surgery and other ophthalmological diseases. In the dataset, there was an age-matched control group with no signs of AMD (Farsiu et al. 2014). The SD-OCT

system used in the A2A-study was from Bioptigen, inc (Morrisville, NC, USA), with 1000 A-scans per B-scan and 100 B-scans per volume.

The NORPED dataset is described for paper II. However, the fellow eyes were included regardless of previous therapy and stage of AMD. An unmatched control group of hospital staff recruited from the eye department at St.Olavs Hospital was also included. The SD-OCT system used was from the Spectralis HRA-OCT, with the follow-up mode, a dense scan pattern of 49 B-scans, and eye-tracking enabled. Each line in the B-scan consisted of 18-30 averaged scans with the automatic real-time function.

3.3 Randomization and masking (Paper I)

Stratified randomization on the presence of drusenoid PED was performed by a web-based randomization system developed and administered by Unit of Applied Clinical Research, The Faculty of Medicine, Norwegian University of Science and Technology, Trondheim, Norway. The nurses measuring the primary outcome BCVA were blinded to group allocation; other forms of masking were not used.

3.4 Intervention (Paper I)

The intervention consisted of 3 monthly intravitreal injections of aflibercept 2mg/0.05mL (Eylea; Regeneron Inc., Tarrytown, NY, USA), and three additional monthly injections if the PED persisted at three months. At the six and nine months study visits, patients were treated with triple-therapy that consisted of half-fluence PDT in combination with aflibercept 2mg/0.05mL and triamcinolone acetonide 4mg/0.1ml (Triesence; Alcon lab Inc., Forthworth, TX, USA) if the PED had not completely resolved. Half-fluence PDT was chosen to reduce the risk of chorioretinal atrophy (Newman 2016).

3.5 Outcome measures (Paper I and II)

3.5.1 Best-corrected visual acuity

BCVA was measured using ETDRS charts in an illuminated cabinet (ESV3000; Good-Lite, Elgin, IL, USA) at 4 m, with an automatic adjustment of 85 cd/m^2. Room lighting was dimmed until 90-110 lux was measured in front of the cabinet. Refraction was done at baseline and yearly by a physician or optician. A trained nurse in Paper I measured BCVA, and for paper II the same physician carried out all measurements of BCVA during follow-up.

3.5.2 Spectral-domain optical coherence tomography measurements

Paper I: Maximum DPED-height and diameter were measured on five different scans centered in the fovea, and the mean of the three highest measurements was used. The automatic segmentation of the RPE and Bruch's membrane and calculation of volume is inaccurate with the software in Cirrus HD-OCT (Ho et al. 2015), and other segmentation programs were not readily available. However, after manual segmentation and subtracting of total retinal and PED volume, measured from the internal limiting membrane to Bruch's membrane, with retinal volume, measured from the internal limiting membrane to the RPE, the DPED-volume could be calculated (Figure 6). Central retinal thickness was automatically obtained after the manual segmentation of the RPE and the internal limiting membrane layers.

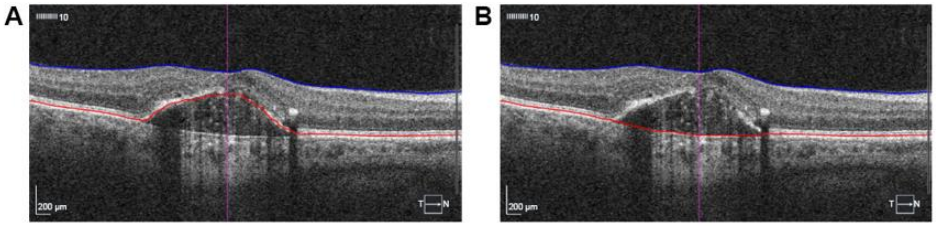

Figure 6 Manual segmentation and volume measurement of retinal pigment epithelium detachment from macular cube 512x128 scans. (A) Segmentation of internal limiting membrane and retinal pigment epithelium. (B) Segmentation of the internal limiting membrane to the fit line of the retinal pigment epithelium. (Tvenning et al. 2019). CC BY-NC 3.0.

Paper II: The volumes of DPED and intraretinal hyperreflective foci were calculated with a semi-automatic segmentation program (ReV Analyzer version 3.0.5; ADCIS SA, Saint-Contest, France) (Figure 7). For each scan, the DPED and intraretinal hyperreflective foci were semi-automatically delineated, which enabled calculation of their volumes.

Subfoveal DPED height, diameter, and central retinal thickness were measured with the caliper available in the Spectralis HRA-OCT viewing software (Spectralis Viewing Module version 6.0.9.0; Heidelberg Engineering GmbH, Heidelberg, Germany). The mean of the three centremost scans, centered in the middle of the fovea guided by SD-OCT, was used for statistical analysis. The DPEDs were classified as subfoveal if they were within the innermost guiding circle of the ETDRS grid available in the Spectralis Viewing module. Central retinal thickness was measured from the internal limiting membrane to, but not including, the RPE. DPED height was measured from the outer aspect of the RPE to Bruch's membrane. The SD-OCT images were in the 1:1 µm format during measurements.

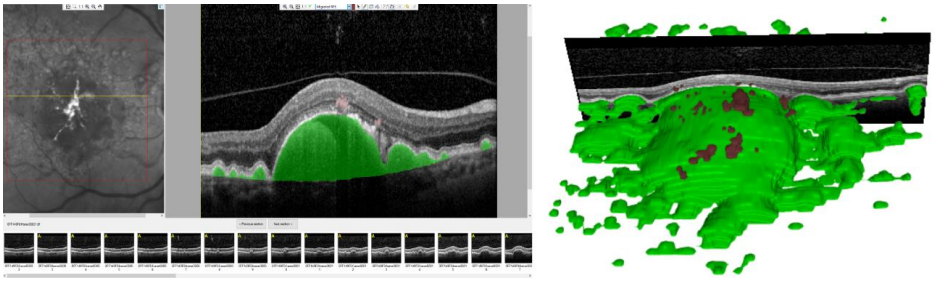

Figure 7 Semi-automatic segmentation and calculation of drusenoid pigment epithelial detachment and intraretinal hyperreflective foci volumes on spectral-domain optical coherence tomography scans. The green areas represent a drusenoid pigment epithelial detachment and drusen, and the brown areas represent intraretinal hyperreflective foci.

3.5.3 Grading of atrophy on spectral-domain optical coherence tomography

The consensus of atrophy meeting (CAM) group defined complete RPE and outer retinal atrophy (cRORA) as; 1) region of hypertransmission of at least 250 µm in diameter in any lateral dimension, 2) zone of attenuation or disruption of the RPE of at least 250 µm diameter, 3) evidence of overlying photoreceptor degeneration (Sadda et al. 2018). Features of photoreceptor degeneration included all of the following: loss of interdigitation zone, ellipsoid zone, and external limiting membrane, and thinning of the outer nuclear layer, which also could be identified by a descending outer plexiform layer. The criteria for incomplete RPE and outer retinal atrophy (iRORA) were not established, but for Paper I, we defined iRORA as 1) criteria for cRORA not met, 2) hypertransmission and a discontinuous RPE band, and 3) evidence of some photoreceptor degeneration. Guymer et al. published the next CAM report describing iRORA as a pre-print in 2019, and it was evident that the photoreceptor degeneration for the iRORA definition was the same as for cRORA, but the size of < 250 µm distinguished it from cRORA (Guymer et al. 2020). Thus, the CAM defined criteria for iRORA were used for Paper II. For paper II, we also defined complete outer retinal atrophy (cORA) as 1) evidence of photoreceptor degeneration and 2) intact or discontinuous RPE (Figure 8).

Figure 8 Pathological findings and classification of atrophy in drusenoid pigment epithelial detachments on optical coherence tomography scans.

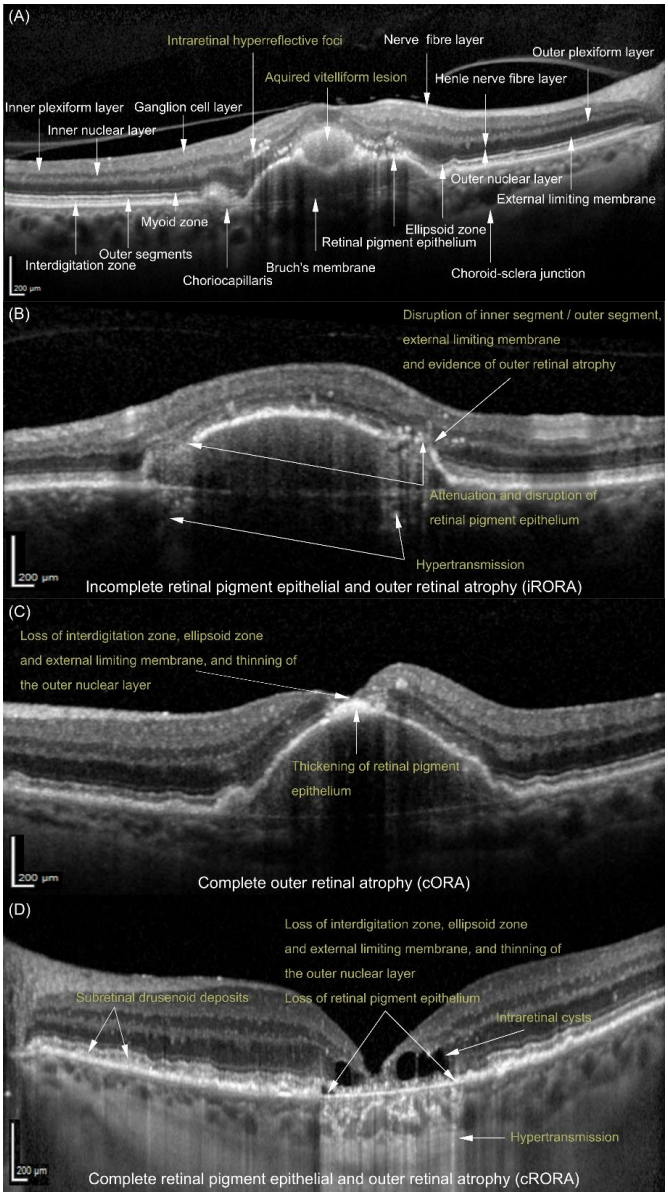

(A) Retinal layers, intraretinal hyperreflective foci, and acquired vitelliform lesion.

(B) Incomplete retinal pigment epithelium and outer retinal atrophy (iRORA).

(C) Complete outer retinal atrophy (cORA) and thickening of the retinal pigment epithelium.

(D) Complete retinal pigment epithelium and outer retinal atrophy (cRORA), intraretinal cysts, and subretinal drusenoid deposits.

Scale bar = 200 µm.

(Tvenning et al. 2020). CC BY-NC-ND 4.0.

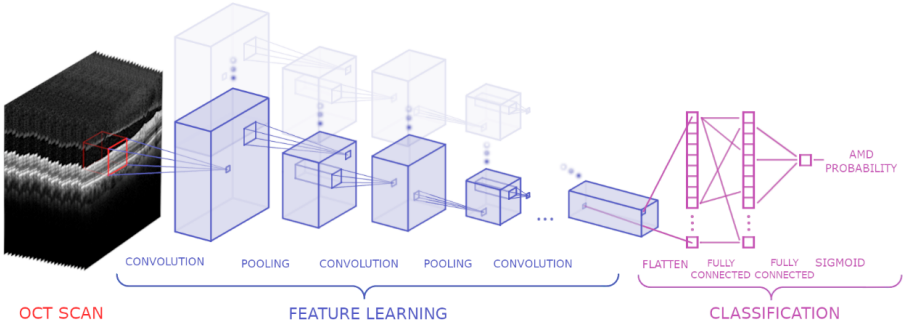

Figure 9 Simplified illustration of a 3D deep learning model. The spectral-domain optical coherence tomography (SD-OCT) volume seen to the left is the input to the deep learning model. Under feature learning, the model learns to extract specific features in the SD-OCT volume through convolutional and pooling layers. The blue boxes represent filtered versions of the SD-OCT volume. The faded blue boxes deeper into the image represents all the filtered version of the SD-OCT volume created from the learned filters of each convolutional layer. The compact set of features coming out of the feature learning section is flattened out and given to a final neural network performing the classification. The classification section of the deep learning model can be viewed as clusters of neurons where all neurons in one layer are connected to all neurons in the next. The final output of the network is put through a sigmoid function that makes the output a probability between 0 and 1.

3.6 The deep learning model (Paper III)

OptiNet is a (2+1)D deep learning model (LeCun et al. 2012; Tran et al. 2018), a variant of 3D, and was trained from scratch without transfer learning. Transfer learning is the use of pre-trained parts from other deep learning architectures. The deep learning model learns the image features that differentiate AMD from controls by itself and uses these features to make a classification (Figure 9). Each convolutional layer learns filters that extract specific information from the SD-OCT volumes. The first layers learn simple features such as lines and edges, and consecutive layers build upon simple features to find more complex features deeper into the CNN. The CNN reduces the information it

needs to handle by reducing the size of the filtered SD-OCT volumes, also known as max-pooling (Scherer et al. 2010). The model ends up with a decimal number between 0 and 1, where 1 indicates 100% certainty of AMD.

Ten independent OptiNet models were trained and validated on the A2A and NORPED datasets, respectively. For calculation of OptiNet's performance, the output value was thresholded such that 0.5 and higher was AMD, and a value lower than 0.5 was a control.

Visualization was performed through computing points of interest and heat maps. The technique called CNN fixations reveals what the model signifies as AMD in the SD-OCT volume (Mopuri et al. 2019). (2+1)D convolution was handled by expanding the general concept from Mopuri et al. The points of interest were calculated for 1D convolution and then for 2D convolution while transforming the locations' dimensionality according to the implementation of (2+1)D convolution. Heat maps were created that illustrates the densities of the points of interest in the SD-OCT scan. A retina specialist evaluated the location of the points of interest in the SD-OCT scans, and their presence in each retinal layer and feature of AMD selected by OptiNet was registered.

3.7 Statistical methods

Paper I

The sample size for statistical analysis with ANCOVA was calculated with a pre-post correlation of 0.8, 90 % power, $\alpha = 5$ %, and an expected difference of 50% between groups in pigment epithelium detachment volume. The data used for this calculation was based on a previous study (Ritter et al. 2010). The required sample size was estimated to be 22 in each group, 48 in total with a 10 % dropout. However, the sample size was not calculated on the primary outcome BCVA, but on a DPED volume reduction of 50%, that we expected would lead to stabilization or improvement in BCVA. After a discussion in the research group, it was decided that a sample size of 60 patients would be enough to detect a clinically meaningful difference and account for

some of the uncertainty in the standard deviation and pre-post correlation used in the calculation.

A marginal model with restricted maximum likelihood estimation was used to account for the correlated data with multiple measurements over time. Unstructured or exponential covariance structures were used. All statistical models had age, baseline value, group, time, and the interaction of group and time as predictors. The p-values were Sidak adjusted because of multiple comparisons. Model fit was evaluated with Akaike's information criterion and likelihood ratio tests. Residuals were checked for normality with histograms and Q-Q plots. Fischer's exact test was used to compare categorical outcomes. Two-tailed P-values <0.05 were considered statistically significant.

Paper II

Linear mixed models were used for statistical analysis. The eyes of patients were nested within patients with repeated measurements to account for the correlated eye data (Ying et al. 2017). Fixed effects were calculated with restricted likelihood estimation. As described by Nakagawa and Schielzeth, R^2 for the fixed effect(s) and the full models, including random effects, were calculated and named R^2 marginal and R^2 conditional, respectively (Nakagawa & Schielzeth 2013). The normal distribution of the residuals was evaluated with histograms and Q-Q plots. Only observations of DPEDs in the growth phase were included in the statistical models, which excluded 3 of 188 observations, due to foveal cRORA or cORA. Akaike's information criterion was used to evaluate model fit.

Paper III

The scientific computing package (SciPy), in the programming language Python 3, was used to calculate mean AUC, accuracy, sensitivity, specificity, negative predictive value, and positive predictive value for the ten independent models trained and

validated on the A2A and NORPED datasets. Descriptive statistics were also obtained with Stata 15.1.

3.8 Ethics

Paper I and II

These studies were approved by the Regional Committee for Medical and Health Research Ethics Central Norway (2012/1743). The ethical basis for randomized controlled trials is the individual or preferably collective uncertainty about the therapeutic effects of each arm in a trial (Freedman 1987). Endophthalmitis and retinal detachment are rare, but potential sight-threatening complications following intravitreal injections. Anti-VEGF injections might also accelerate the formation of geographic atrophy (Gemenetzi et al. 2017) and increase the risk of RPE-tears, resulting in sudden vision loss (Chang et al. 2007). PDT therapy can result in acute severe vision loss (Verteporfin In Photodynamic Therapy Study Group 2001) or RPE-tears (Goldstein et al. 2005), and it can increase the risk of chorioretinal atrophy (Newman 2016). A rise in intraocular pressure and cataract formation are potential complications following intravitreal injections with steroids, but these can be managed with medications or cataract surgery. Despite these risks, these patients did not have any treatment options, and the disease is relentless, with a high risk of loss of visual function. No previous randomized controlled trials had been conducted, and there was not enough previous evidence to conclude if treatment would have been beneficial. Another ethical consideration was the decision to stop further inclusion and treatment of patients when the study was underpowered to detect a potential treatment benefit. However, in light of the new knowledge about the SD-OCT findings preceding geographic atrophy, and that our study participants appeared to be on this route, our research group found it unethical to continue the study. The prospective observational study of DPEDs had few ethical considerations and was approved after alterations made on the first application.

Informed consent was obtained from all study participants, and the studies followed the tenets of the Declaration of Helsinki.

Paper III

The use of anonymized SD-OCT images from the study participants in the NORPED study was approved after a new application to the Regional Committee for Medical and Health Research Ethics Central Norway (2012/1743), and a new informed consent was obtained from all study participants. The anonymized A2A SD-OCT study dataset had been made freely available online by Farsiu et al. (Farsiu et al. 2014), and four institutional review boards approved their use of the SD-OCT images from the A2A SD-OCT study. Informed consent had been obtained from all subjects in that study.

3.9 Financial support

The studies and thesis have been made possible by the Dam Foundation (2016/FO80635). The authors have no financial disclosures.

4. Results

4.1 Paper I

Fourteen patients with AMD and PED ≥1500 μm in diameter were referred from April 2014 to February 2015. Four out of these patients were ineligible because of CNV and serous PED (2), fibrovascular PED (1), and DPED (1). One patient was ineligible because of adult-onset foveomacular vitelliform dystrophy. Nine patients were included in the study, with five randomized to the treatment group. However, one of the patients in the treatment group was excluded from statistical analysis because of the disappearance of bilateral serous PEDs after tapering of systemic corticosteroid therapy and likely central serous chorioretinopathy. The remaining eight study participants had DPED. Furthermore, after an interim analysis of 6 months' data, the inclusion and treatment of patients were stopped because SD-OCT images showed that 75% of the study participants were in the progression of atrophy (Figure 10). The patients in the treatment group received six monthly injections with Aflibercept. Two patients received both treatments of triple-therapy (Figure 10, ID: 2 and 3), one patient received one treatment (Figure 10, ID: 7), and one patient did not (Figure 10, ID: 5). The patients were followed for 12 months, and three in each group had a follow-up of 24 months.

4.1.1 Primary outcome

After 24 months of follow-up, estimated means of BCVA decreased by 4.2 ETDRS letters and 20.8 ETDRS letters in the treatment and observation groups, respectively (Figure 11A). The difference between groups during follow-up was not statistically significant (P=0.140, 95% CI -5.3, 38.6).

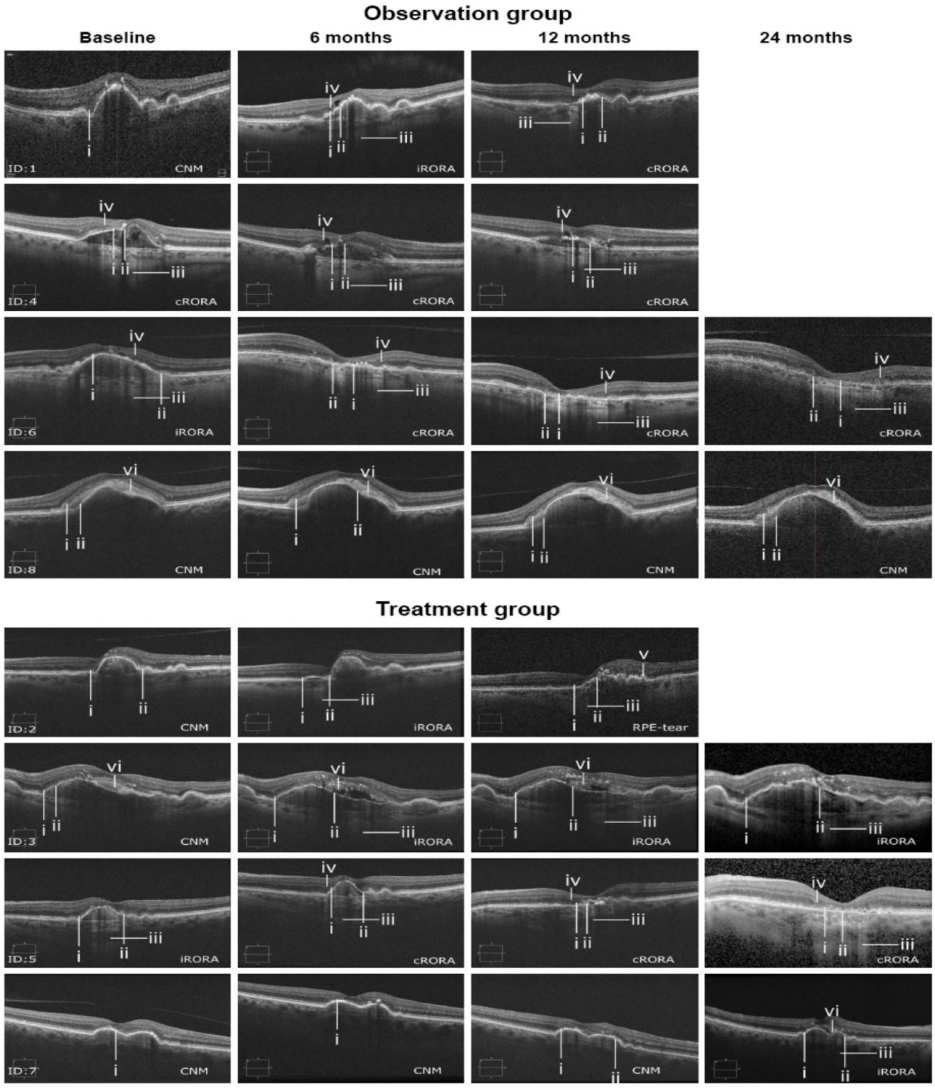

Figure 10 Grading of GA by OCT.

Notes: (i) Photoreceptor degeneration. (ii) Attenuation or disruption of RPE. (iii) Hypertransmission. (iv) Descending outer plexiform layer. (v) Scrolled up RPE. (vi) Subretinal drusenoid material. **Abbreviations:** CNM, criteria for iRORA/cRORA not met; cRORA, complete RPE and outer retinal atrophy; ID, patient number; iRORA, incomplete RPE and outer retinal atrophy; RPE, retinal pigment epithelium; OCT, optical coherence tomography; GA, geographic atrophy. (Tvenning et al. 2019). CC BY-NC 3.0.

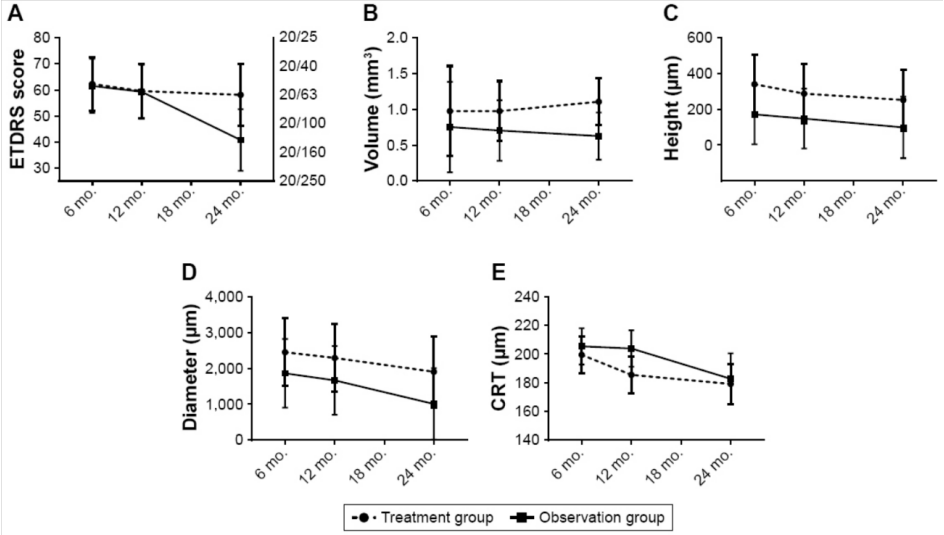

Figure 11 Estimated means of BCVA, PED volume, height and diameter, and CRT from 6 to 24 months.

Notes: (**A**) BCVA; the rightmost y-axis corresponds to Snellen equivalent. (**B**) PED volume. (**C**) PED height. (**D**) PED diameter. (**E**) CRT. The error bars represent 95% CIs (n=22 observations on eight patients).

Abbreviations: BCVA, best-corrected visual acuity; CRT, central retinal thickness; ETDRS, Early Treatment Diabetic Retinopathy Study; mo., months; PED, pigment epithelium detachment. (Tvenning et al. 2019). CC BY-NC 3.0.

4.1.2 Secondary outcomes

After 24 months of follow-up, the estimated means of DPED volume increased by 0.13 mm^3 and decreased by 0.13 mm^3 in the treatment and observation groups, respectively (Figure 11B). The difference between groups during follow-up was not statistically significant (P=0.433, 95% CI -0.40, 0.91). The increasing age of patients predicted a decrease in DPED volume (P=0.043, 95% CI -0.07, -0.001). A large DPED at baseline predicted a larger follow-up DPED volume (P<0.001, 95% CI 1.53, 2.20).

DPED height decreased by 88 µm and 73 µm in the treatment and observation groups, respectively (Figure 11C). The difference between groups during follow-up months was not statistically significant (P=0.842, 95% CI -169, 138).

DPED diameter decreased by 544 µm and 856 µm in the treatment and observation groups, respectively (Figure 11D). The difference between groups during follow-up was not statistically significant (P=0.603, 95% CI -863, 1487). A larger baseline DPED diameter and follow-up time predicted a decrease in DPED diameter (P=0.022 and P=0.044, respectively).

Central retinal thickness decreased by 20 µm and 23 µm in the treatment and observation group, respectively (Figure 11E). The difference between groups during follow-up was not statistically significant (P=0.852, 95% CI -23, 28). The increasing age of patients and follow-up duration were significant predictors of decreasing central retinal thickness (P<0.001 and P=0.019, respectively). A larger baseline central retinal thickness value predicted a larger follow-up value (p<0.001).

4.1.3 Progression of atrophy

At baseline, 38% of patients had atrophy (defined as iRORA or cRORA) that increased to 75%, 71% (one excluded because of RPE-tear), and 86% after 6, 12, and 24 months of follow-up. One patient in the treatment group and two patients in the observation group progressed to cRORA after 24 months of follow-up. A decrease in DPED volume was significantly associated with the development of cRORA (Fisher's exact test, P=0.029).

4.1.4 Safety outcomes

None of the patients in the treatment group developed endophthalmitis or retinal detachment following intravitreal injections. The intraocular pressure following intravitreal injections with triamcinolone acetonide did not need treatment. One patient

was diagnosed with CNV after the first triple therapy and subsequently developed an RPE-tear after the second triple therapy with full-fluence PDT. The standard full-fluence PDT has shown a reduced risk of moderate and severe vision loss in treatment of type 1 CNV in AMD (Verteporfin In Photodynamic Therapy Study Group 2001), which was the reason the abovementioned patient received this treatment after development of CNV after half-fluence PDT.

4.2 Paper II

Forty-four patients and 66 eyes with DPED were included in the study. During the first year, three patients and four eyes were lost to follow-up. Two eyes (3%) had a reduction in DPED volume. One of these eyes progressed to subfoveal cRORA, and the other progressed to complete outer retinal atrophy with subfoveal thickening of the RPE layer on SD-OCT. At baseline, three eyes (5%) had extrafoveal iRORA, which increased to six (10%) by 12 months. None of the eyes developed CNV.

4.2.1 Best-corrected visual acuity

BCVA and DPED volume

In the linear mixed model, BCVA decreased by 4.0 ETDRS letters for every increase in DPED volume by 1.0 mm^3 (95% CI, -7.0 to -1.0, p = 0.008) (Figure 12A). BCVA decreased by 0.4 ETDRS letters for every patient-year (95% CI, -0.6 to -0.2, p <0.001). The subfoveal location reduced BCVA by 5.5 ETDRS letters (95% CI, -10.6 to -0.3, p = 0.036), and presence of acquired vitelliform lesions reduced BCVA by 5.6 ETDRS letters (95% CI, -8.1 to -3.1, p <0.001). The volume of intraretinal hyperreflective foci, the presence of foveal subretinal fluid and intraretinal cysts, subretinal drusenoid deposits, and follow-up duration were not significant predictors of BCVA. The fixed effects in the statistical model predicted 40% of the variance in BCVA (R^2 marginal), and the whole model, including random effects, predicted 83% (R^2 conditional).

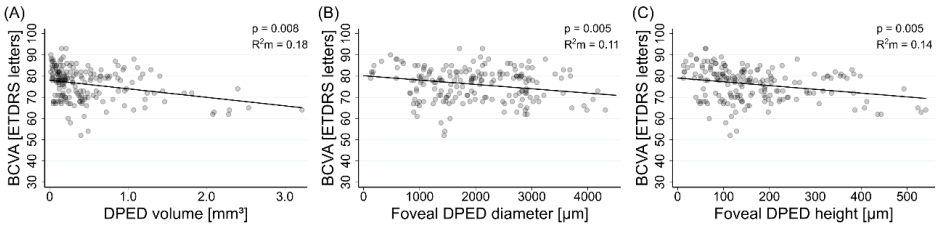

Figure 12 The associated decrease in best-corrected visual acuity (BCVA) with increasing drusenoid pigment epithelial detachment (DPED) volume, foveal diameter, and height.

(A) BCVA and DPED volume. (B) BCVA and foveal DPED diameter. (C) BCVA and foveal DPED height. Statistical analysis; linear mixed models. The lines represent linear predictions. Scatterplots of BCVA and DPED volume, diameter, and height. The marginal coefficient of determination (R^2m) is the proportion of the variance in BCVA predicted by the fixed effects of DPED volume, diameter, and height. N = 185 observations, 66 eyes and 44 patients. A p-value <0.05 was considered statistically significant. (Tvenning et al. 2020). .

BCVA and DPED diameter

BCVA decreased by 2.1 ETDRS letters for every increase in foveal DPED diameter by 1000 µm (95% CI, -3.5 to -0.6, p = 0.005) (Figure 12B). BCVA decreased by 0.4 ETDRS letters for every patient-year (95% CI, -0.6 to -0.1, p = 0.003). The presence of acquired vitelliform lesions reduced BCVA by 5.6 ETDRS letters (95% CI, -8.1 to -3.1, p <0.001), and the presence of subretinal drusenoid deposits increased BCVA by 3.5 ETDRS letters (95% CI, 0.4 to 6.6, p = 0.027). The volume of intraretinal hyperreflective foci, the presence of foveal subretinal fluid and intraretinal cysts, and follow-up duration were not significant predictors of BCVA. The fixed effects in the statistical model predicted 35% of the variance in BCVA (R^2 marginal), and the whole model, including random effects, predicted 84% (R^2 conditional).

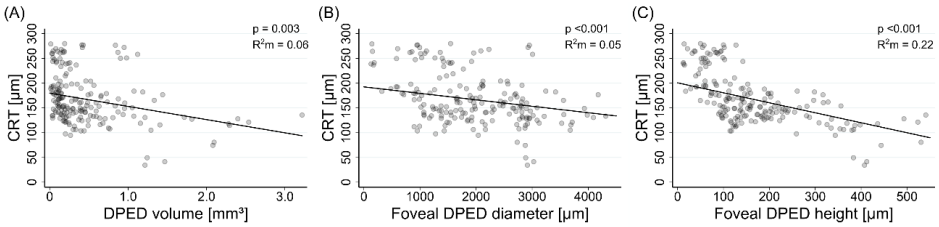

Figure 13 The associated decrease in central retinal thickness (CRT) with increasing drusenoid pigment epithelial detachment (DPED) volume, foveal DPED diameter, and height. (A) CRT and DPED volume. (B) CRT and foveal DPED diameter. (C) CRT and foveal DPED height. Statistical analysis; linear mixed models. The lines represent linear predictions. Scatterplots of CRT and DPED volume, diameter, and height. The marginal coefficient of determination (R^2m) is the proportion of the variance in CRT predicted by the fixed effects of DPED volume, diameter, and height. N = 185 observations, 66 eyes and 44 patients. A p-value <0.05 was considered statistically significant. (Tvenning et al. 2020). .

BCVA and DPED height

BCVA decreased by 1.8 ETDRS letters for every increase in foveal DPED height by 100 µm (95% CI, -3.0 to -0.5, p = 0.005) (Figure 12C). BCVA decreased with 0.3 ETDRS letters for every patient-year (95% CI, -0.6 to -0.1, p = 0.005). The presence of acquired vitelliform lesions reduced BCVA by 6.1 ETDRS letters (95% CI, -8.6 to -3.6, p <0.001). The volume of intraretinal hyperreflective foci, the presence of foveal subretinal fluid and intraretinal cysts, subretinal drusenoid deposits, and follow-up duration were not significant predictors of BCVA. The fixed effects in the statistical model predicted 36% of the variance in BCVA (R^2 marginal), and the whole model, including random effects, predicted 82% (R^2 conditional).

4.2.4 Central retinal thickness

Central retinal thickness and DPED volume

Central retinal thickness decreased by 26.7 µm for every increase in DPED volume by 1.0 mm^3 (95% CI, -44.4 to -9.0, p = 0.003) (Figure 13A). Patient age, subfoveal location of DPEDs, the volume of intraretinal hyperreflective foci, the presence of acquired vitelliform lesions, foveal subretinal fluid, and intraretinal cysts, subretinal drusenoid deposits, and follow-up duration were not significant predictors of central retinal thickness. The fixed effects in the statistical model predicted 10% of the variance in central retinal thickness (R^2 marginal), and the whole model, including random effects, predicted 95% (R^2 conditional).

Central retinal thickness and DPED diameter

Central retinal thickness decreased by 13.1 µm for every increase in foveal DPED diameter by 1000 µm (95% CI, -19.5 to -6.6, p <0.001) (Figure 13B), and the presence of subretinal fluid in the fovea led to an increase in central retinal thickness of 8.8 µm (95% CI, 0.4 to 17.3, p = 0.042). Patient age, the volume of intraretinal hyperreflective foci, the presence of acquired vitelliform lesions, intraretinal cysts, subretinal drusenoid deposits, and follow-up duration were not significant predictors of central retinal thickness. The fixed effects in the statistical model predicted 8% of the variance in central retinal thickness (R^2 marginal), and the whole model, including random effects, predicted 95% (R^2 conditional).

Central retinal thickness and DPED height

Central retinal thickness decreased by 20.2 µm for every increase in foveal DPED height by 100 µm (95% CI, -26.6 to -13.7, p <0.001) (Figure 13C). Patient age, the volume of intraretinal hyperreflective foci, the presence of acquired vitelliform lesions, foveal subretinal fluid, intraretinal cysts, subretinal drusenoid deposits, and follow-up duration were not significant predictors of central retinal thickness. The fixed effects in

the statistical model predicted 23% of the variance in central retinal thickness (R^2 marginal), and the whole model, including random effects, predicted 95% (R^2 conditional).

4.3 Paper III

269 AMD patients and 115 controls were included from the A2A dataset, with one SD-OCT volume from the same participant. 40 AMD patients (62 eyes) and 23 controls were included from the NORPED dataset with 337 and 46 SD-OCT volumes, respectively.

4.3.1 Performance of OptiNet

The mean AUC of OptiNet was 99.7% and 99.9% on the A2A and NORPED datasets, respectively, additional results are presented in Table 2. The AUC was calculated from the mean receiver operator characteristics curves of ten independent models on each dataset (Figure 14). Table 3 shows the AUC of previous studies conducted on the A2A dataset.

Metric	**A2A dataset**	**NORPED dataset**
Accuracy	96.5 ± 2.1 %	98.9 ± 0.8 %
Positive Predictive Value	97.6 ± 3.2 %	99.5 ± 0.9 %
Sensitivity	97.6 ± 2.3 %	99.2 ± 0.6 %
Negative Predictive Value	94.8 ± 5.1 %	93.9 ± 4.6 %
Specificity	93.8 ± 8.3 %	95.8 ± 7.7 %
AUC	99.7 ± 0.4 %	99.9 ± 0.1 %

Table 2 The performance of OptiNet on the validation partition of the A2A and NORPED datasets. The results are of the format mean ± standard deviation based on ten trained models from the OptiNet architecture for each of the two datasets.
A2A; Age-Related Eye Disease 2 Ancillary SD-OCT study, AUC; area under the receiver operator curve, NORPED; Norwegian Pigment Epithelial Detachment Study

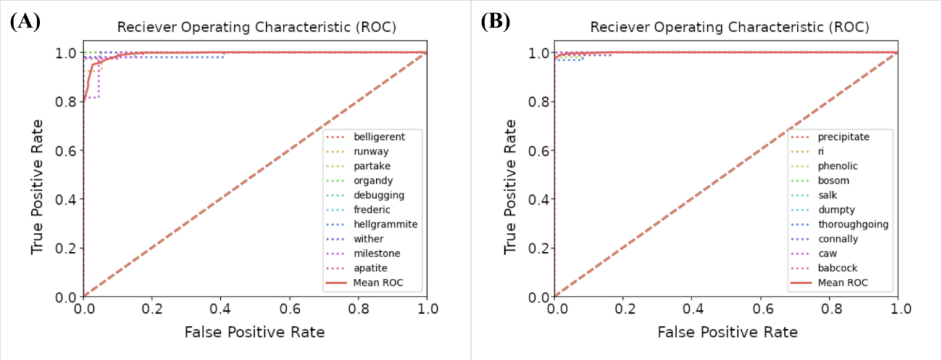

Figure 14 Receiver operating characteristic curves computed from the models of OptiNet trained on the A2A and NORPED datasets**.**

(A) ROC curves calculated for all ten models of OptiNet trained on the A2A dataset. (B) ROC curves calculated for all ten models of OptiNet trained on the NORPED dataset. Each model has a randomly generated name, which is shown in the lower-right corner of both figures. The mean ROC curve is identified as the solid line in the graph.

Abbreviations: A2A; Age-Related Eye Disease 2 Ancillary SD-OCT study, ROC; receiver operating characteristic curves, NORPED; Norwegian Pigment Epithelial Detachment Study.

Study	Method	Results
(Apostolopoulos et al. 2016)	Convolutional neural network	AUC: 99.7%
(Santos et al. 2018)	Support vector machine	AUC: 98.9%
(Venhuizen et al. 2015)	Unsupervised feature learning, bag of words	AUC: 98.4%
(Farsiu et al. 2014)	Generalized linear regression	AUC: 99.2%

Table 3 Previous studies and performance on the A2A dataset.
AUC = area under the receiver operator curve, A2A = Age-Related Eye Disease 2 Ancillary spectral domain-optical coherence tomography study.

4.3.2 Visualization

The points of interest were calculated from the validation partitions on both datasets. The displayed images can be magnified, and the exact location of the points of interest can be seen and registered (Figure 15). The percentage of SD-OCT volumes to have at least one point of interest and their distribution in retinal layers, zones, and structures are presented in Table 4. When combining the results from both datasets, the retinal layers and structures that most often had one point of interest were the RPE (98%), ellipsoid (88%) and interdigitation (84%) zone, outer segment (78%), retinal nerve fiber (82%) and choroid layer (70%), and in drusen (97%). Figure 16 shows how three AMD cases are displayed to the user, and Figure 17 shows a control case.

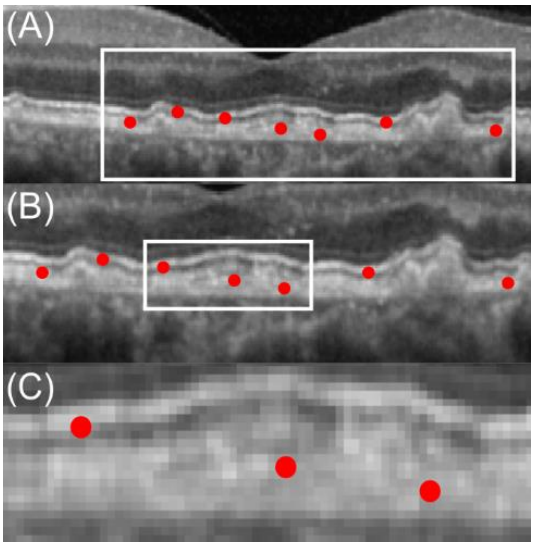

Figure 15 The high-resolution visualization of points of interest from a patient with age-related macular degeneration on spectral-domain optical coherence tomography scans. (A) The normal presentation of points of interest (red dots). (B) - (C) Increasing magnification showing the high-resolution visualization of points of interest in specific retinal layers and structures.

	NORPED (n=102*)		A2A (n=48*)		Combined (n=150*)	
	n	(%)	n	(%)	n	(%)
Retinal pigment epithelium	99	(97 %)	48	(100 %)	147	(98 %)
Interdigitation zone	87	(85 %)	39	(81 %)	126	(84 %)
Ellipsoid zone	86	(85 %)	46	(96 %)	132	(88 %)
Outer segment	83	(81 %)	34	(73 %)	117	(78 %)
Retinal nerve fiber	81	(79 %)	42	(88 %)	123	(82 %)
Choroid	59	(58 %)	46	(96 %)	105	(70 %)
Inner plexiform	45	(44 %)	30	(63 %)	75	(50 %)
Outer plexiform	43	(42 %)	29	(61 %)	72	(48 %)
Ganglion cell	41	(40 %)	33	(69 %)	74	(49 %)
Henle nerve fiber	37	(36 %)	24	(50 %)	61	(41 %)
Vitreous	36	(35 %)	22	(46 %)	58	(39 %)
Inner nuclear	29	(28 %)	21	(44 %)	50	(33 %)
Outer nuclear	16	(16 %)	22	(45 %)	38	(25 %)
External limiting membrane	15	(15 %)	7	(15 %)	22	(15 %)
Bruch's membrane	8	(8 %)	7	(15 %)	15	(10 %)
Myoid zone	7	(7 %)	9	(19 %)	16	(11 %)
Drusen	99	(97 %)	47	(98 %)	146	(**97 %**)
Subretinal drusenoid deposits	42	(41 %)	11	(23 %)	53	(35 %)
Intraretinal hyperreflective foci	32	(31 %)	4	(8 %)	36	(24 %)
Acquired vitelliform lesion	24	(24 %)	-	-	24	(16 %)
Hypertransmission	13	(13 %)	5	(10 %)	18	(12 %)
Subretinal fluid	3	(3 %)	1	(2 %)	4	(3 %)
Intraretinal cysts	1	(1 %)	-	-	1	(1 %)

Table 4 The percentage of SD-OCT volumes to have at least one point of interest and their distribution in retinal layers, zones and features of AMD. AMD; age-related macular degeneration, A2A; Age-Related Eye Disease 2 Ancillary SD-OCT study, SD-OCT; spectral-domain optical coherence tomography, n=number. * SD-OCT images from the validation partitions.

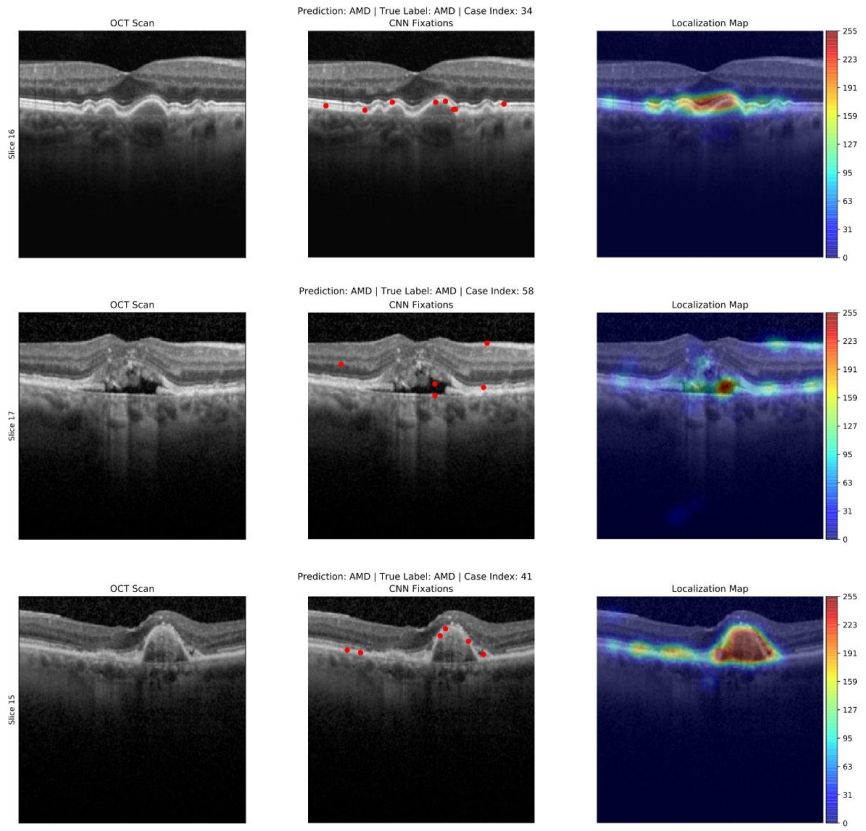

Figure 16 Visualization of points of interest in three cases with age-related macular degeneration (AMD). The figure shows how the deep learning model, OptiNet, displays results to the user on three AMD cases. Three images are given for each AMD case, displaying the regular spectral-domain optical coherence tomography (SD-OCT) scan, points of interest, and a localization heat map. Each row shows one of the cross-sections of a SD-OCT scan from different patients. Convolutional neural network (CNN) fixations show the points of interest (red dots) that were important for the classification. The localization map shows the density as a Gaussian blur of the points of interest. A high value on the color bar, displayed in red, implies high interest from the deep learning model.

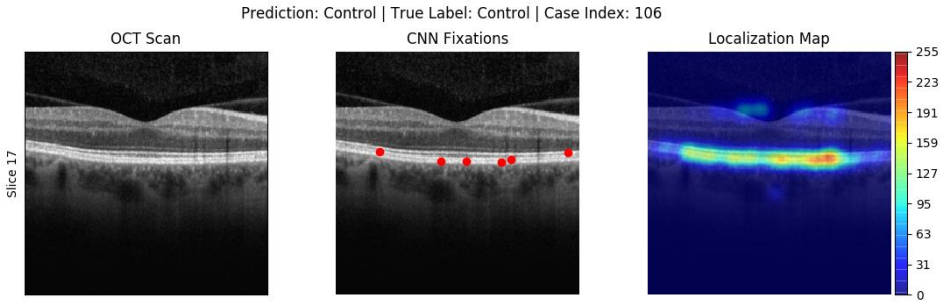

Figure 17 Visualization of points of interest in a control case. The points of interest (red dots) are mainly located in the layer of the retinal pigment epithelium and photoreceptors. The deep learning model was trained to output a probability of age-related macular degeneration, and an output probability ≥ 0.5 indicates a case with age-related macular degeneration, and <0.5 indicates a control case.

5. Discussion

The main findings of this thesis are that large foveal DPEDs are associated with a decrease in BCVA and central retinal thickness, probably because of the progressive RPE and photoreceptor atrophy. The sample size in paper I was too small to draw any conclusions about the treatment effect of anti-VEGF or in combination with PDT and triamcinolone acetonide in patients with DPED and no CNV on angiography. After 2 years of follow-up, the treatment and observation group had a decrease in BCVA and progression of atrophy. Furthermore, SD-OCT images can be utilized by artificial intelligence to identify AMD, and with the adaptation of a novel visualization method, provide precise feedback and reveal potential new disease features.

5.1 Rationale for the interventions in Paper I

There were no previous studies that had tested if treatment with anti-VEGF alone, or in combination with PDT and triamcinolone acetonide, would be beneficial for patients with avascular serous PEDs or DPEDs in a randomized controlled trial. However, uncontrolled intervention studies indicated that anti-VEGF treatment might stabilize disease progression (Ritter et al. 2010; Gallego-Pinazo et al. 2011). The prospective uncontrolled study of Ritter et al. that evaluated anti-VEGF treatment of 7 serous PEDs and 5 DPEDS was one of the studies that inspired our randomized controlled trial (Ritter et al. 2010). They suggested that anti-VEGF therapy may have an effect on decreasing the volume of PEDs without identifiable CNV. In their study, 2 of 5 DPEDs and 4 of 7 serous PEDs had a reduction in PED volume of 56%, and 2 PEDs resolved entirely, none developed CNV or central geographic atrophy, and BCVA remained stable during the first 12 months. However, four patients had an increase in PED volume by 33%. In another prospective uncontrolled trial, six patients with DPED, without CNV on FA, were treated with anti-VEGF (Gallego-Pinazo et al. 2011). 2 of 6 patients had an increase of 19 and 21 ETDRS letters, and the other remained stable with a mean follow-up of 17 months. However, ICGA was not used in that study, and some

of the patients might have had CNV. In addition, a case report has reported regression of drusen following PDT treatment of DPED without CNV (Lee & Kim 2008). Triamcinolone acetonide was included as a treatment because it had shown an additive effect with PDT, mainly in reducing the need for re-treatment with PDT in neovascular AMD (Spaide et al. 2003; Maberley & Canadian Retinal Trials Group 2009). Further arguments for this intensive and controversial therapy was the relentless natural history of the disease (Casswell et al. 1985; Cukras et al. 2010), and the possibility that the drusen material could block visualization of CNV (Arnold et al. 1997).

Both serous and drusenoid PEDs have a high risk of developing CNV. Retrospective studies have shown that 34% of serous PEDs developed CNV after a mean of 25 months follow-up, and 9% of DPEDs develop CNV after 41 months of follow-up (Casswell et al. 1985; Hartnett et al. 1992). A prospective study found that 32% of serous PEDs developed CNV after a median of 12 months of follow-up (Elman et al. 1986). ICGA is better than FA to detect type 1 CNV in serous PEDs (Yannuzzi et al. 1992), which was not used in the abovementioned studies and could explain why we did not find any serous PEDs without CNV in our study. However, serous PEDs without CNV exists in macular diseases and might be present because of the increased hydrophobicity in Bruch's membrane in AMD (Bird 1991) and increased choroidal permeability in central serous chorioretinopathy (Fujimoto et al. 2008).

5.2 Treatment efficacy (Paper I)

The first study was designed as a randomized controlled trial to test treatment with anti-VEGF, PDT, and triamcinolone acetonide of large serous and drusenoid PEDs, without identifiable CNV on FA and ICGA. However, most of the patients with serous PEDs evaluated for inclusion in our study were ineligible because of CNV. One included patient without CNV and serous PED had a misdiagnosis and was excluded from statistical analysis because of central serous chorioretinopathy. The remaining patients had DPEDs. Also, further inclusion and treatment were stopped after studies describing nascent geographic atrophy on SD-OCT that preceded the development of central geographic atrophy on color fundus photography were published (Wu et al. 2014), even

though there was no difference in BCVA. Nascent geographic atrophy is defined on SD-OCT by the subsidence of the outer plexiform and inner nuclear layer, and a hyporeflective wedge-shaped band within the limits of the outer plexiform layer. At the six month follow-up, we identified that 75% of our patients were in the progression of atrophy (Tvenning et al. 2019), later defined on SD-OCT as either iRORA or cRORA (Sadda et al. 2018; Guymer et al. 2020). One patient had cRORA at baseline, and the number of patients increased to three and four after 6 and 12 (24) months of follow-up, respectively. The results of the study by Ritter et al. were different from ours with BCVA remaining stable and no development of geographic atrophy or CNV. However, their follow-up time was only 12 months, and their DPEDs were considerable smaller (mean 0.38 mm^3) than ours (0.98 mm^3).

5.3 Geographic atrophy (Paper I and II)

Color fundus photography and fundus autofluorescence have been the primary imaging modalities in the studies of geographic atrophy. However, evaluation with SD-OCT has become essential, since the health of the neurosensory retina can be directly assessed, and early precursors can be found years before progression to advanced AMD (Schmidt-Erfurth et al. 2017). We believed that treatments reducing the volume of PEDs would improve the prognosis because of the reduced distance from the RPE to the choriocapillaris. However, a study by Balaratnasingam et al. described the lifecycle of DPEDs and showed that a reduction in DPED volume led to geographic atrophy (Balaratnasingam et al. 2016). Geographic atrophy in AMD is usually located perifoveal, and patients retain good vision for many years until foveal involvement (Sarks et al. 1988). However, drusen were in one study present in 100% of following areas with geographic atrophy (Klein et al. 2008), and DPEDs are usually located in the center of the macula, which suggest that geographic atrophy in DPEDs would involve the fovea in many patients (Sarks et al. 1988). Not all drusen that regress develop visible geographic atrophy or CNV. One prospective study of drusen found that 15% had a decrease in volume over 12 months, and 64% of these progressed to geographic atrophy, 23% to CNV, and 14% regressed without evidence of outer retinal alterations

on SD-OCT, fundus autofluorescence, and color fundus photography (Yehoshua et al. 2011). Prior to the development of geographic atrophy, it is in histopathology seen that the photoreceptor outer segments are absent on top of drusen (Sarks et al. 1988) with thinning of the photoreceptor layer seen on SD-OCT (Schuman et al. 2009). Thus, the location of drusen and DPEDs, and likely progression of geographic atrophy becomes essential for visual function. The few DPEDs (6%) in our second paper that were located perifoveal had markedly better BCVA (Tvenning et al. 2020). Regression of DPED volume might improve or stabilize visual function if there is no development of geographic atrophy or it occurs perifoveal, and preferentially early in the disease process, by re-establishing the close contact of the choriocapillaris to the RPE. However, for patients progressing to geographic atrophy, the fovea is likely to be involved since the lesions increase over time.

5.4 Best-corrected visual acuity and central retinal thickness

As indicated by our second paper, it is probably not only during the regression phase that visual function declines and atrophy progress in patients with DPED. It appears that this is a gradual process, with a decrease in BCVA and central retinal thickness, also during the growth phase of DPEDs (Tvenning et al. 2020). It has been suggested that the increasing distance of the RPE to the choriocapillaris in drusen and DPEDs leads to RPE and outer retinal atrophy because of reduced oxygen diffusion and nutrient transport (Friedman et al. 1995; Stefánsson et al. 2011; Mrejen et al. 2013). Oxygen diffusion decreases linearly from the RPE to the outer retina. According to Fick's law of diffusion, an increase of DPED height by 100 μm would result in an oxygen flux decrease by 50% (Stefánsson et al. 2011). Furthermore, oxygen permeability is decreased 3-5 fold in membranes containing water or lipids (Subczynski et al. 1989), which are the main components of DPEDs. The statistical model in our second paper on central retinal thickness and foveal DPED height supports the notion that the distance between the RPE to the photoreceptors is important for the outer retina. This model had the most explained variance (22%) compared to foveal DPED diameter (5%) and DPED volume (6%) in predicting central retinal thickness (Tvenning et al. 2020).

BCVA is usually affected late in the progression of AMD, because of the relative sparing of cones that are supported by the Müller cells, compared to the rods that rely more on the RPE (Curcio et al. 1996; Owsley et al. 2000). AMD patients typically have good visual acuity in the earlier stages of the disease, and it decreases substantially with the progression to advanced AMD (Chew et al. 2014). Dark adaptation time increases with AMD severity stage and can be used to detect earlier changes in visual function (Flamendorf et al. 2015), especially in the presence of subretinal drusenoid deposits (Chen et al. 2019). Despite this, we did find that the increasing size of DPEDs was associated with a decrease in BCVA. However, DPEDs are arguably not early or intermediate AMD, but somewhere in between intermediate and advanced AMD, because of its size, foveal location, and the high risk of progression to advanced AMD (Cukras et al. 2010). A cross-sectional study found reduced visual acuity, microperimetry, and multifocal electroretinography in patients with ≥ ½ disc diameter DPEDs compared to healthy controls (Ogino et al. 2014). The same study did not find a decrease in visual acuity or multifocal electroretinography in intermediate AMD patients with only multiple large drusen ≥125 µm compared to controls.

DPED volume as a predictor in statistical models of BCVA can be challenging because of its potential opposite effect. As we have shown in paper II, an increase in DPED volume is associated with a reduction in BCVA (Tvenning et al. 2020). However, during the progression towards geographic atrophy there is a reduction in DPED volume and a decrease in BCVA (Balaratnasingam et al. 2016). To complicate this even further, a reduction in drusen volume does not necessarily lead to visible geographic atrophy or CNV (Yehoshua et al. 2011), and in some cases even improvement in visual function (Csaky & Christie 2020). The many different and potential opposite meanings of a change in DPED volume shows the importance of reviewing the SD-OCT images for progression and location of atrophy. In a statistical model, the multitude of effects that DPED volume can have on BCVA can be accounted for with an interaction term with DPED volume. For instance, DPED volume can in this way have one meaning with no identified atrophy on SD-OCT, another meaning in the presence of iRORA and cRORA, and another in the more rare occasions of DPED volume reduction and no

visible atrophy or CNV. The statistical model should also account for foveal involvement of the atrophic process.

5.5 Spectral-domain optical coherence tomography predictors

The presence of acquired vitelliform lesions in patients with DPED was associated with a decrease in BCVA. This is plausible since these lesions are thought to be accumulations of RPE organelles (lipofuscin, melanolipofuscin, melanosomes) and outer segment debris because of RPE cell dysfunction (Arnold et al. 2003; Chen et al. 2016; Balaratnasingam et al. 2017).

Intraretinal hyperreflective foci on SD-OCT are probably activated RPE that migrates towards the inner retina (Christenbury et al. 2013), and they are a known risk factor for progression to advanced AMD (Nassisi et al. 2018). 85% of the patients in paper II had intraretinal hyperreflective foci at baseline, and their volume was varied, and most patients had small amounts. This corresponds well to the atrophic stage of the DPEDs in our study, with only 5% having iRORA or cRORA at baseline. The amount of intraretinal hyperreflective foci increases during the progression of geographic atrophy (Christenbury et al. 2013). With a longer follow-up of the patients in the NORPED study, we suspect that intraretinal hyperreflective foci will be a predictor of a decrease in BCVA and central retinal thickness.

Subretinal drusenoid deposits are associated with thinner choroids, reduced BCVA (Garg et al. 2013), advanced AMD (Zweifel et al. 2010a), and an increased rate of geographic atrophy progression (Pumariega et al. 2011; Marsiglia et al. 2013). However, we did not find that the presence of subretinal drusenoid deposits predicted a change in BCVA or central retinal thickness, even though 64% of eyes had these deposits. The individual effect of subretinal drusenoid deposits could have been overshadowed by the effect of DPED size in the multivariate statistical model. Also, BCVA is primarily a measure of cone-mediated vision, and subretinal drusenoid deposits appear to be associated with rod pathophysiology in AMD (Curcio et al. 2013).

A better outcome measure of the negative effect of subretinal drusenoid deposits on visual function in AMD could be to measure dark adaptation time (Chen et al. 2019).

5.6 Performance of the deep learning model

Previous deep learning models have diagnosed multiple retinal diseases on SD-OCT scans with AUCs ranging from to 97.5-99.9% on large datasets with 16884 SD-OCT volumes to > 100.000 SD-OCT scans and performed equivalent to or better than experts in the field (Lee et al. 2017; De Fauw et al. 2018; Kermany et al. 2018; Lu et al. 2018). OptiNet was trained from scratch and able to identify AMD and control cases with high performance on two relatively small datasets. CNNs typically need thousands of images in order to achieve high performance, but when two conditions are quite different (drusen and no drusen), not many cases might be needed. One study has shown that a CNN trained with only 200 computer tomography scans to classify different body regions on 6000 computer tomography scans were enough to achieve high accuracy, which illustrates that fewer training cases might be enough if the difference between images is sufficiently large (Cho et al. 2015). OptiNet used 3D SD-OCT volumes during learning and classification, in contrast to most studies using 2D SD-OCT scans (Apostolopoulos et al. 2016; Lee et al. 2017; Kermany et al. 2018; Lu et al. 2018; Motozawa et al. 2019). Few studies have used 3D SD-OCT volumes to classify retinal disease, and one of them used two deep learning models, one to segment the raw 3D SD-OCT volume, and another to classify the results of segmentation (De Fauw et al. 2018). Deep learning models trained on 3D images outperform those trained with 2D in lung nodule detection for lung cancer (Dou et al. 2017), and the use of 3D might also improve the classification of retinal disease.

5.7 Visualization

OptiNet learned disease features from the 3D SD-OCT volumes by itself. We did not annotate, or highlight image regions that we know are associated with AMD, and

consequently, the points of interest found by OptiNet are unbiased and might represent new disease features of AMD. OptiNet utilized known features of AMD in its classification, such as the photoreceptor layers, the RPE layer, and drusen (Fleckenstein et al. 2008). This visual feedback of points of interest used in the identification of AMD indicates that OptiNet learned disease features of AMD. In addition, our study showed that the retinal nerve fiber and choroid layer were frequent points of interest in the detection of AMD.

The association of the retinal nerve fiber layer to AMD remains to be determined. One prospective study with two years of follow-up did not find a difference in retinal nerve fiber layer volume between patients with AMD and unmatched controls (Lamin et al. 2019). A cross-sectional study found lower retinal nerve fiber layer thickness in treatment-naivè AMD patients with CNV compared to controls, but not for AREDS category 2-3 or those with central geographic atrophy (Zucchiatti et al. 2015). Furthermore, another study found a decrease in the ganglion cell layer + inner plexiform layer and inner nuclear layer + outer plexiform in AMD patients compared to controls, but not for the retinal nerve fiber layer (Savastano et al. 2014). Another large cross-sectional study found an increase in retinal nerve fiber layer thickness between early AMD and age-matched controls, but this finding was not present for moderate or severe early AMD (Brandl et al. 2019). It is known that the retinal nerve fiber layer thickness decreases with age (Budenz et al. 2007), and this could have explained the frequent points of interest in this layer in the NORPED dataset. However, the points of interest were also frequent in the retinal nerve fiber layer in the A2A dataset that had an age-matched control group.

The association of the choroid layer to AMD is also not determined. Age, refractive error and axial length influence choroidal thickness, and most studies adjusting for these factors find little evidence of an association to AMD (Jonas et al. 2014; Yiu et al. 2015; Ho et al. 2018). Neovascular AMD and polypoidal choroidal vasculopathy might have an increased choroidal thickness (Ting et al. 2016), and patients with AMD and subretinal drusenoid deposits might have decreased choroidal thickness (Keenan et al. 2020). Choroidal thickness has also been found to decrease following DPED regression and progression to geographic atrophy (Dolz-Marco et al. 2018).

Even though the observation of points of interest in the retinal nerve fiber and choroid layer in our study is interesting, deep learning models do not see images as we do. They extract simple features out of the images and builds upon these to create abstract representations used for classification (Yosinski et al. 2015). Despite this, the points of interest created by OptiNet were primarily located in regions known to be associated with AMD, indicating that the use of the visualization method CNN-fixations can produce interpretable findings to the clinician.

5.8 Limitations

We are all biased, and both patients, doctors, and study personnel want new treatments to have a beneficial effect or new hypotheses to be true. Studies need to be well-designed and ideally randomized to minimize bias, with the use of as much masking as possible.

Bias occurs in research when "systematic error [is] introduced into sampling or testing by selecting or encouraging one outcome or answer over others". Bias can occur in any stage of research from study planning, implementation, data analysis, and during publication (Pannucci & Wilkins 2010). Bias can broadly be classified into selection and information bias (Delgado-Rodriguez & Llorca 2004). Even though the first study was a randomized controlled trial, some biases are still present.

The main limitation of the randomized controlled trial in Paper I was the small cohort that limits any conclusions to be made.

Confounding is a type of bias, where known and unknown factors influence the outcomes (Greenland et al. 1999), and this can be present in all of our studies.

Selection bias is present in all of our studies, mostly because of the small sample sizes and the rather narrow inclusion criteria. This type of bias occurs when the study population does not represent the target population. The DPED size criteria of ≥1500 µm in the randomized controlled trial and ≥1000 µm in the observational study might exclude those with a different risk of progression to advanced AMD.

The researchers and patients were not blinded for group allocation in paper I, and there is a possibility of performance bias because of differences in the follow-up. The treatment group had more frequent visits to the hospital because of treatments compared to the control group. Even though the nurses were blinded for study allocation, there is a chance that the group allocation was discovered, potentially influencing BCVA measurements.

Paper I and II had pre-specified primary outcomes that reduced detection bias. However, the results from Paper I could indicate that large DPEDs are unhealthy for the overlying retina, and we developed a preconception that this could be true, which leads to confirmation bias in our following observational study.

Observational studies are also prone to post hoc analysis bias, as most of these studies collect a large amount of data that potentially can produce unexpected and significant results by chance. However, for paper II we had a hypothesis that the increasing DPED volume would reduce BCVA and central retinal thickness, which reduced the chance of post hoc analysis bias.

The prospective designs decreased some types of bias in that there was little missing information. Furthermore, the prospective design reduced the chance of recall bias that occurs when patients need to remember previous exposures that might be related to the disease.

There is also a chance of misclassification bias, in that some of the DPEDs could have had CNV not identified on angiography in Paper I and II.

There is a chance of patient bias in that some of the included patients in Paper I and II would want to perform exceedingly well on BCVA measurements. However, functional measurements are probably not as likely to have this type of bias compared to questionnaires.

Paper I and II could potentially have regression to the mean bias**,** where the first observations of an outcome are far above the average response, and this value normalizes without intervention by the next follow-up and could lead to erroneous conclusions about the effect of exposure (Barnett et al. 2004). However, Paper I

randomized the patients, and there were multiple measurements over time in both paper I and II. In addition, the baseline value was a predictor in the statistical model in Paper I, thereby adjusting for regression to the mean.

The AMD datasets in paper III has spectrum bias in that most of the cases were intermediate or advanced AMD. Another limitation of paper III is that the deep learning model has not been tested on a general population cohort where most subjects are normal. Furthermore, the SD-OCT images used by the deep learning model were of high quality, in contrast to the scans obtained in an everyday clinical setting.

In Paper I, there is a chance that we made both type I and II errors because of the small sample sizes. Type I errors occur when significant results are a product of chance, and Type 2 errors occur when a difference or association is present but not found. In the building of the statistical models in Paper II many predictors were added and removed in order to get the best model fit. During this process, it is possible for type I errors to occur. We could have corrected for multiple comparisons by using another threshold of significance, i.e., $p<0.01$ or lower, but this could have increased the chance of a type II error. However, the sample size was reasonably large, with repeated measurements over time, and the highly significant results in our paper are probably not a product of chance.

5.9 Implications of current findings and future research

The small sample size of paper I limits any conclusion to be made about treatment with anti-VEGF or in combination with PDT and triamcinolone acetonide of DPEDs without identifiable CNV on angiography. Large DPEDs are probably not intermediate or advanced AMD, but somewhere in between, and this is an important consideration for future clinical trials. The foveal location and high drusen load represent a high risk of progressive outer retinal atrophy, ultimately leading to central geographic atrophy. If the DPED volume could be reduced early in the disease process, the risk of losing BCVA would probably also be reduced. It has previously been reported that thermal laser photocoagulation in patients with extensive drusen can reduce drusen load with the

stabilization of visual acuity (Wetzig 1988; Sarks et al. 1996; Figueroa et al. 1997; Guymer et al. 1997). However, a meta-analysis of 11 randomized controlled trials, including 2159 participants and 3580 eyes, did not find that thermal photocoagulation with xenon, krypton, or argon lasers or sub threshold diode lasers of non-neovascular AMD slowed or accelerated progression to advanced AMD or visual acuity loss, despite the reduction of drusen area (Virgili et al. 2015). Thermal laser might increase the risk of CNV, but mostly in fellow eyes of those with CNV in the other eye (The Choroidal Neovascularization Prevention Trial Research Group 2003).

A recent large multi-center randomized clinical trial, the Laser Intervention in Early Age-Related Macular Degeneration Study (LEAD), has investigated possible treatment benefit of sub threshold nanosecond laser therapy for patients with at least one drusen ≥ 125 µm within 1500 µm from the fovea in both eyes with three years of follow-up. They found no difference in progression to advanced AMD between groups, but post-hoc analyses showed that in patients without subretinal drusenoid deposits, nanosecond laser may slow progression, and might increase progression in those with these deposits (Guymer et al. 2019). DPEDs >1000 µm were excluded from the LEAD trial because DPEDs in a pilot study treated with sub threshold nanosecond laser therapy progressed to central geographic atrophy after 12 months of follow-up (Guymer et al. 2014). It is thought that laser-induced damage by a nanosecond laser below visual threshold activates nearby RPE, which migrate to repair the damage and, in the process, release matrix metalloproteinase that potentially could be one mechanism in drusen regression (Zhang et al. 2012).

A recent case report showed that BCVA remained stable, and low luminance visual function improved 24 months after spontaneous DPED regression without progression to central geographic atrophy or CNV (Csaky & Christie 2020). If it is possible to reduce the amount of drusen or induce drusen regression in patients with DPED, before signs of atrophy on SD-OCT, patients would probably benefit from treatment. For decades it has been speculated if modifiable cardiovascular risk factors also alter AMD development and progression. Statins, or HMG Co-A reductase inhibitors, have been of interest because drusen are in part composed of lipoproteins and cholesterol. Statins reduce the production of low-density lipoprotein cholesterol, increase the expression of

low-density lipoprotein cholesterol receptors, and reduce the amount of triglycerides (Wierzbicki et al. 2003). The different statins have different effects on high-density lipoproteins, whereas Simvastatin can increase high-density lipoproteins, Atorvastatin can reduce the amount at a higher dosage (Wierzbicki & Mikhailidis 2002). Evidence also suggests that statins inhibit vascular inflammation, are immune modulators, and have an effect on endothelial progenitor stem cells (Wierzbicki et al. 2003; Blum & Shamburek 2009). The plethora of effects that statins exert appear to be relevant in the current understanding of AMD as a vascular-metabolic-inflammatory disease. However, available studies on statin treatment and AMD report conflicting results. Several studies report a protective effect of statins on AMD (McCarty et al. 2001; McGwin et al. 2003; McGwin et al. 2005; Tan et al. 2007), whilst others report none (Klein et al. 2001; van Leeuwen et al. 2003; Smeeth et al. 2005; McGwin et al. 2006; Klein et al. 2007; Maguire et al. 2009), and even increased risk of CNV (VanderBeek et al. 2013). A recent meta-analysis of case-control, cohort and cross-sectional studies (Ma et al. 2015) found that patients treated with statins had a reduced risk in developing early AMD and CNV, but not for geographic atrophy or if all stages of AMD were combined. A randomized-controlled trial was conducted and showed the treatment benefit of statins (40 mg Simvastatin) in reducing the progression of AMD, which was most evident for patients with the at-risk CFH genotype CC (Y402H) (Guymer et al. 2013). More recently, an uncontrolled prospective trial showed that treatment with 80 mg of Atorvastatin in patients with large soft drusen and DPEDs had a positive treatment effect with drusen regression in 44% of patients without the development of geographic atrophy or CNV after one year of follow-up (Vavvas et al. 2016). AMD is a heterogeneous disease, and it is possible that only a subset of AMD patients with certain genotypes, drusen type, or disease stage would benefit from statin treatment. A recent Cochrane review found only two randomized controlled trials that tested treatment with statins for AMD, and the evidence from those two was insufficient to conclude on the role of statin therapy and AMD (Gehlbach et al. 2016). A new and larger randomized controlled trial testing treatment with statins on AMD, including DPEDs, is warranted. This study would need a large sample with sufficient power to detect a treatment benefit, longer follow-up, and probably stratified on AMD genotype, drusen type, and AMD stage. Those with signs of nascent geographic atrophy on SD-OCT or CNV

should be excluded. A major challenge to conduct such a study would be recruitment since most of these patients are asymptomatic, and that many elderly patients already use lipid-lowering medications.

Few patients met the new SD-OCT criteria for foveal iRORA in paper II, but cRORA were present after one year of follow-up. This was despite extensive changes in SD-OCT scans, decreased central retinal thickness, and BCVA. The new definition for iRORA is probably best suited for evaluating perifoveal atrophy since the outer plexiform layer is absent subfoveal, and the evaluation of thinning of the outer nuclear layer is subjective. Maybe it is enough to define foveal iRORA with loss of the interdigitation zone, ellipsoid zone, and external limiting membrane, and a loss of the RPE <250μm. The new definitions of atrophy on SD-OCT will be evaluated when more patients in the NORPED study develop these end-points after additional follow-up time.

It is already known that deep learning models perform at the same high level as experts in the field in diagnosing retinal disease. However, we have shown the potential of a novel visualization method in identifying disease features. If a deep learning model is trained on a prospective dataset of those that progress to geographic atrophy, maybe it will be possible to find the first disease features of this process, which can be used for future clinical trials. If the same concept is applied for CNV, it might be possible to identify the patients that are at the highest risk for this treatable complication.

5.10 Conclusions

The sample size in paper I was too small to draw any conclusions about the treatment effect of anti-VEGF or in combination with PDT and triamcinolone acetonide in patients with DPED and no CNV on angiography. After 2 years of follow-up, the treatment and observation group had a decrease in BCVA and progression of atrophy on SD-OCT.

In paper II, the increasing size of DPEDs during their growth phase was associated with a decrease in BCVA and central retinal thickness. Furthermore, the subfoveal location of DPEDs and the presence of acquired vitelliform lesions were associated with an additional decrease in BCVA.

OptiNet identified AMD and control cases with high performance using SD-OCT volumes from two relatively small datasets. The visualization method revealed that areas known to be affected by AMD, such as the photoreceptor layers, the RPE layer, and drusen, were associated with the disease. Interestingly, the retinal nerve fibre and choroid layer were frequently used points of interest, and their association with AMD remains to be determined. By utilizing high-resolution visualization methods, the clinician can gain insight into which image areas the deep learning model identifies as AMD, and thereby possibly gain new knowledge of the disease.

5.11 Final significance and future direction

DPEDs is a presentation of AMD, often leading to central geographic atrophy with a loss of visual function, and the prognosis is poor. Currently, there are none proven treatments for these patients. This thesis adds to the understanding that large accumulations of lipoproteins and fluid beneath the RPE during the growth phase of DPEDs probably contributes to the death of RPE and photoreceptors. Future treatment trials should probably aim to reduce the drusen burden that increases the risk of visual acuity loss and progression to advanced AMD. Maybe it will be possible to halt the progression by reducing the materials needed in the formation of drusen by statins or other lipid-lowering drugs. However, there is still a lot we do not understand about the pathophysiology of AMD and which type of intervention future research should focus on.

The visualization method applied in our deep learning model indicates that the retinal nerve fibre and choroid layer might be altered in AMD, which previously has not been thoroughly explored, and future studies could investigate this further. A future direction for our deep learning model is to test it on a general population cohort to see if it can identify AMD when most people are normal.

6. References

Abdelsalam A, Del Priore L & Zarbin MA (1999): Drusen in Age-Related Macular Degeneration: Pathogenesis, Natural Course, and Laser Photocoagulation–Induced Regression. Surv Ophthalmol **44**: 1-29.

Age-Related Eye Disease Study Research Group (2001): A Randomized, Placebo-Controlled, Clinical Trial of High-Dose Supplementation With Vitamins C and E, Beta Carotene, and Zinc for Age-Related Macular Degeneration and Vision Loss: AREDS Report No. 8. Arch Ophthalmol **119**: 1417-1436.

Ahmad KM, Klug K, Herr S, Sterling P & Schein S (2003): Cell density ratios in a foveal patch in macaque retina. Vis Neurosci **20**: 189-209.

Alexandre de Amorim Garcia Filho C, Yehoshua Z, Gregori G, Farah ME, Feuer W & Rosenfeld PJ (2013): Spectral-domain optical coherence tomography imaging of drusenoid pigment epithelial detachments. Retina **33**: 1558-1566.

Ambati J, Atkinson JP & Gelfand BD (2013): Immunology of age-related macular degeneration. Nat Rev Immunol **13**: 438-451.

Ambati J & Fowler BJ (2012): Mechanisms of age-related macular degeneration. Neuron **75**: 26-39.

Anderson DH, Mullins RF, Hageman GS & Johnson LV (2002): A role for local inflammation in the formation of drusen in the aging eye. Am J Ophthalmol **134**: 411-431.

Anderson DH, Radeke MJ, Gallo NB, et al. (2010): The pivotal role of the complement system in aging and age-related macular degeneration: hypothesis re-visited. Prog Retin Eye Res **29**: 95-112.

Apostolopoulos S, Ciller C, De Zanet SI, Wolf S & Sznitman R (2016): RetiNet: Automatic AMD identification in OCT volumetric data. arXiv preprint arXiv:1610.03628.

Arnold JJ, Quaranta M, Soubrane G, Sarks SH & Coscas G (1997): Indocyanine Green Angiography of Drusen. Am J Ophthalmol **124**: 344-356.

Arnold JJ, Sarks JP, Killingsworth MC, Kettle EK & Sarks SH (2003): Adult vitelliform macular degeneration: a clinicopathological study. Eye (Lond) **17**: 717-726.

Baba T, Kitahashi M, Kubota-Taniai M, Oshitari T & Yamamoto S (2012): Two-year course of subfoveal pigment epithelial detachment in eyes with age-related macular degeneration and visual acuity better than 20/40. Ophthalmologica **228**: 102-109.

Balaratnasingam C, Messinger JD, Sloan KR, Yannuzzi LA, Freund KB & Curcio CA (2017): Histologic and Optical Coherence Tomographic Correlates in Drusenoid Pigment Epithelium Detachment in Age-Related Macular Degeneration. Ophthalmology **124**: 644-656.

Balaratnasingam C, Yannuzzi LA, Curcio CA, et al. (2016): Associations Between Retinal Pigment Epithelium and Drusen Volume Changes During the Lifecycle of Large Drusenoid Pigment Epithelial Detachments. Invest Ophthalmol Vis Sci **57**: 5479-5489.

Barnett AG, van der Pols JC & Dobson AJ (2004): Regression to the mean: what it is and how to deal with it. Int J Epidemiol **34**: 215-220.

Bazan NG, Gordon WC & Rodriguez de Turco EB (1992): Docosahexaenoic acid uptake and metabolism in photoreceptors: retinal conservation by an efficient retinal pigment epithelial cell-mediated recycling process. Adv Exp Med Biol **318**: 295-306.

Berg K, Pedersen TR, Sandvik L & Bragadóttir R (2015): Comparison of Ranibizumab and Bevacizumab for Neovascular Age-Related Macular Degeneration According to LUCAS Treat-and-Extend Protocol. Ophthalmology **122**: 146-152.

Bhisitkul RB, Mendes TS, Rofagha S, Enanoria W, Boyer DS, Sadda SR & Zhang K (2015): Macular atrophy progression and 7-year vision outcomes in subjects from the

ANCHOR, MARINA, and HORIZON studies: The SEVEN-UP study. Am J Ophthalmol **159**: 915-924.e912.
Bird AC (1991): Doyne Lecture. Pathogenesis of retinal pigment epithelial detachment in the elderly; the relevance of Bruch's membrane change. Eye (Lond) **5 (Pt 1)**: 1-12.
Bird AC, Bressler NM, Bressler SB, et al. (1995): An international classification and grading system for age-related maculopathy and age-related macular degeneration. The International ARM Epidemiological Study Group. Surv Ophthalmol **39**: 367-374.
Blaha M, Rencova E, Langrova H, Studnicka J, Blaha V, Rozsival P, Lanska M & Sobotka L (2013): Rheohaemapheresis in the treatment of nonvascular age-related macular degeneration. Atheroscler Suppl **14**: 179-184.
Bloch SB, Larsen M & Munch IC (2012): Incidence of legal blindness from age-related macular degeneration in denmark: year 2000 to 2010. Am J Ophthalmol **153**: 209-213 e202.
Blum A & Shamburek R (2009): The pleiotropic effects of statins on endothelial function, vascular inflammation, immunomodulation and thrombogenesis. Atherosclerosis **203**: 325-330.
Bok D (1993): The retinal pigment epithelium: a versatile partner in vision. J Cell Sci Suppl **17**: 189-195.
Boulton M & Dayhaw-Barker P (2001): The role of the retinal pigment epithelium: topographical variation and ageing changes. Eye (Lond) **15**: 384-389.
Bourne RR, Jonas JB, Flaxman SR, et al. (2014): Prevalence and causes of vision loss in high-income countries and in Eastern and Central Europe: 1990-2010. Br J Ophthalmol **98**: 629-638.
Brandl C, Brücklmayer C, Günther F, et al. (2019): Retinal Layer Thicknesses in Early Age-Related Macular Degeneration: Results From the German AugUR Study. Invest Ophthalmol Vis Sci **60**: 1581-1594.
Bressler NM (1999): Photodynamic therapy of subfoveal choroidal veovascularization in age-related macular degeneration with verteporfin: one-year results of 2 randomized clinical trials—TAP Report 1. Arch Ophthalmol **117**: 1329-1345.
Bressler NM (2001): Photodynamic therapy of subfoveal choroidal neovascularization in age-related macular degeneration with verteporfin: two-year results of 2 randomized clinical trials—TAP Report 2. Arch Ophthalmol **119**: 198-207.
Bringmann A, Iandiev I, Pannicke T, Wurm A, Hollborn M, Wiedemann P, Osborne NN & Reichenbach A (2009): Cellular signaling and factors involved in Müller cell gliosis: neuroprotective and detrimental effects. Prog Retin Eye Res **28**: 423-451.
Bringmann A, Pannicke T, Grosche J, Francke M, Wiedemann P, Skatchkov SN, Osborne NN & Reichenbach A (2006): Müller cells in the healthy and diseased retina. Prog Retin Eye Res **25**: 397-424.
Brown DM, Kaiser PK, Michels M, Soubrane G, Heier JS, Kim RY, Sy JP & Schneider S (2006): Ranibizumab versus Verteporfin for Neovascular Age-Related Macular Degeneration. N Engl J Med **355**: 1432-1444.
Budenz DL, Anderson DR, Varma R, et al. (2007): Determinants of Normal Retinal Nerve Fiber Layer Thickness Measured by Stratus OCT. Ophthalmology **114**: 1046-1052.
Casswell AG, Kohen D & Bird AC (1985): Retinal pigment epithelial detachments in the elderly: classification and outcome. Br J Ophthalmol **69**: 397-403.
Chakravarthy U, Wong TY, Fletcher A, et al. (2010): Clinical risk factors for age-related macular degeneration: a systematic review and meta-analysis. BMC Ophthalmol **10**: 31.
Chang LK, Flaxel CJ, Lauer AK & Sarraf D (2007): RPE tears after pegaptanib treatment in age-related macular degeneration. Retina **27**: 857-863.

Chen KC, Jung JJ, Curcio CA, Balaratnasingam C, Gallego-Pinazo R, Dolz-Marco R, Freund KB & Yannuzzi LA (2016): Intraretinal Hyperreflective Foci in Acquired Vitelliform Lesions of the Macula: Clinical and Histologic Study. Am J Ophthalmol **164**: 89-98.
Chen KG, Alvarez JA, Yazdanie M, et al. (2019): Longitudinal Study of Dark Adaptation as a Functional Outcome Measure for Age-Related Macular Degeneration. Ophthalmology **126**: 856-865.
Chen M & Xu H (2015): Parainflammation, chronic inflammation, and age-related macular degeneration. J Leukoc Biol **98**: 713-725.
Chen W, Stambolian D, Edwards AO, et al. (2010): Genetic variants near TIMP3 and high-density lipoprotein-associated loci influence susceptibility to age-related macular degeneration. Proc Natl Acad Sci U S A **107**: 7401-7406.
Chew EY, Clemons TE, Agrón E, Sperduto RD, Sangiovanni JP, Davis MD, Ferris FL & Age-Related Eye Disease Study Research Group (2014): Ten-year follow-up of age-related macular degeneration in the age-related eye disease study: AREDS report no. 36. JAMA Ophthalmol **132**: 272-277.
Chew EY, Clemons TE, Agrón E, Sperduto RD, SanGiovanni JP, Kurinij N & Davis MD (2013): Long-Term Effects of Vitamins C and E, β-Carotene, and Zinc on Age-related Macular Degeneration: AREDS Report No. 35. Ophthalmology **120**: 1604-1611.e1604.
Cho J, Lee K, Shin E, Choy G & Do S (2015): How much data is needed to train a medical image deep learning system to achieve necessary high accuracy? arXiv preprint arXiv:1511.06348.
Christenbury JG, Folgar FA, O'Connell RV, Chiu SJ, Farsiu S & Toth CA (2013): Progression of Intermediate Age-related Macular Degeneration with Proliferation and Inner Retinal Migration of Hyperreflective Foci. Ophthalmology **120**: 1038-1045.
Complications of Age-Related Macular Degeneration Prevention Trial Research Group (2006): Laser treatment in patients with bilateral large drusen: the complications of age-related macular degeneration prevention trial. Ophthalmology **113**: 1974-1986.
Copland DA, Theodoropoulou S, Liu J & Dick AD (2018): A Perspective of AMD Through the Eyes of Immunology. Invest Ophthalmol Vis Sci **59**: AMD83-AMD92.
Csaky KG & Christie AH (2020): Anatomic and Functional Improvement of a Drusenoid Pigment Epithelial Detachment: A Case Report. Retin Cases Brief Rep doi:10.1097/ICB.0000000000000964.
Cukras C, Agron E, Klein ML, Ferris FL, Chew EY, Gensler G, Wong WT & Age-Related Eye Disease Study Research Group (2010): Natural history of drusenoid pigment epithelial detachment in age-related macular degeneration: Age-Related Eye Disease Study Report No. 28. Ophthalmology **117**: 489-499.
Curcio CA (2018a): Antecedents of Soft Drusen, the Specific Deposits of Age-Related Macular Degeneration, in the Biology of Human Macula. Invest Ophthalmol Vis Sci **59**: AMD182-AMD194.
Curcio CA (2018b): Soft Drusen in Age-Related Macular Degeneration: Biology and Targeting Via the Oil Spill Strategies. Invest Ophthalmol Vis Sci **59**: AMD160-AMD181.
Curcio CA, Medeiros NE & Millican CL (1996): Photoreceptor loss in age-related macular degeneration. Invest Ophthalmol Vis Sci **37**: 1236-1249.
Curcio CA, Messinger JD, Sloan KR, McGwin G, Medeiros NE & Spaide RF (2013): Subretinal drusenoid deposits in non-neovascular age-related macular degeneration: morphology, prevalence, topography, and biogenesis model. Retina **33**: 265-276.
Curcio CA, Millican CL, Bailey T & Kruth HS (2001): Accumulation of cholesterol with age in human Bruch's membrane. Invest Ophthalmol Vis Sci **42**: 265-274.
Curcio CA, Sloan KR, Kalina RE & Hendrickson AE (1990): Human photoreceptor topography. J Comp Neurol **292**: 497-523.

Curcio CA, Zanzottera EC, Ach T, Balaratnasingam C & Freund KB (2017): Activated Retinal Pigment Epithelium, an Optical Coherence Tomography Biomarker for Progression in Age-Related Macular Degeneration. Invest Ophthalmol Vis Sci **58**: BIO211-BIO226.
de Boer JF, Cense B, Park BH, Pierce MC, Tearney GJ & Bouma BE (2003): Improved signal-to-noise ratio in spectral-domain compared with time-domain optical coherence tomography. Opt Lett **28**: 2067-2069.
De Fauw J, Ledsam JR, Romera-Paredes B, et al. (2018): Clinically applicable deep learning for diagnosis and referral in retinal disease. Nat Med **24**: 1342-1350.
Delgado-Rodriguez M & Llorca J (2004): Bias. J Epidemiol Community Health **58**: 635-641.
Dolz-Marco R, Balaratnasingam C, Gattoussi S, Ahn S, Yannuzzi LA & Freund KB (2018): Long-term Choroidal Thickness Changes in Eyes With Drusenoid Pigment Epithelium Detachment. Am J Ophthalmol **191**: 23-33.
Dou Q, Chen H, Yu L, Qin J & Heng PA (2017): Multilevel Contextual 3-D CNNs for False Positive Reduction in Pulmonary Nodule Detection. IEEE Trans Biomed Eng **64**: 1558-1567.
Elman MJ, Fine SL, Murphy RP, Patz A & Auer C (1986): The natural history of serous retinal pigment epithelium detachment in patients with age-related macular degeneration. Ophthalmology **93**: 224-230.
Ethier CR, Johnson M & Ruberti J (2004): Ocular biomechanics and biotransport. Annu Rev Biomed Eng **6**: 249-273.
Faber C, Singh A, Kruger Falk M, Juel HB, Sorensen TL & Nissen MH (2013): Age-related macular degeneration is associated with increased proportion of CD56(+) T cells in peripheral blood. Ophthalmology **120**: 2310-2316.
Farsiu S, Chiu SJ, O'Connell RV, Folgar FA, Yuan E, Izatt JA & Toth CA (2014): Quantitative classification of eyes with and without intermediate age-related macular degeneration using optical coherence tomography. Ophthalmology **121**: 162-172.
Ferris FL, Wilkinson CP, Bird A, Chakravarthy U, Chew E, Csaky K & Sadda SR (2013): Clinical Classification of Age-related Macular Degeneration. Ophthalmology **120**: 844-851.
Figueroa MS, Regueras A, Bertrand J, Aparicio MJ & Manrique MG (1997): Laser photocoagulation for macular soft drusen. Updated results. Retina **17**: 378-384.
Flamendorf J, Agrón E, Wong WT, et al. (2015): Impairments in Dark Adaptation Are Associated with Age-Related Macular Degeneration Severity and Reticular Pseudodrusen. Ophthalmology **122**: 2053-2062.
Flaxman SR, Bourne RRA, Resnikoff S, et al. (2017): Global causes of blindness and distance vision impairment 1990–2020: a systematic review and meta-analysis. Lancet Glob Health **5**: e1221-e1234.
Fleckenstein M, Charbel Issa P, Helb HM, Schmitz-Valckenberg S, Finger RP, Scholl HP, Loeffler KU & Holz FG (2008): High-resolution spectral domain-OCT imaging in geographic atrophy associated with age-related macular degeneration. Invest Ophthalmol Vis Sci **49**: 4137-4144.
Fleckenstein M, Schmitz-Valckenberg S, Adrion C, et al. (2010): Tracking Progression with Spectral-Domain Optical Coherence Tomography in Geographic Atrophy Caused by Age-Related Macular Degeneration. Invest Ophthalmol Vis Sci **51**: 3846-3852.
Frank RN, Amin RH, Eliott D, Puklin JE & Abrams GW (1996): Basic fibroblast growth factor and vascular endothelial growth factor are present in epiretinal and choroidal neovascular membranes. Am J Ophthalmol **122**: 393-403.
Freedman B (1987): Equipoise and the Ethics of Clinical Research. N Engl J Med **317**: 141-145.
Frennesson C & Nilsson SE (1998): Prophylactic laser treatment in early age related maculopathy reduced the incidence of exudative complications. Br J Ophthalmol **82**: 1169-1174.

Friedman E, Krupsky S, Lane AM, Oak SS, Friedman ES, Egan K & Gragoudas ES (1995): Ocular Blood Flow Velocity in Age-related Macular Degeneration. Ophthalmology **102**: 640-646.

Fritsche LG, Fariss RN, Stambolian D, Abecasis GR, Curcio CA & Swaroop A (2014): Age-related macular degeneration: genetics and biology coming together. Annu Rev Genomics Hum Genet **15**: 151-171.

Fujimoto H, Gomi F, Wakabayashi T, Sawa M, Tsujikawa M & Tano Y (2008): Morphologic changes in acute central serous chorioretinopathy evaluated by fourier-domain optical coherence tomography. Ophthalmology **115**: 1494-1500, 1500.e1491-1492.

Gallego-Pinazo R, Marina A, Suelves C, Frances-Munoz E, Millan JM, Arevalo JF, Mullor JL & Diaz-Llopis M (2011): Intravitreal ranibizumab for symptomatic drusenoid pigment epithelial detachment without choroidal neovascularization in age-related macular degeneration. Clin Ophthalmol **5**: 161-165.

Gao H & Hollyfield JG (1992): Aging of the human retina. Differential loss of neurons and retinal pigment epithelial cells. Invest Ophthalmol Vis Sci **33**: 1-17.

Garg A, Oll M, Yzer S, Chang S, Barile GR, Merriam JC, Tsang SH & Bearelly S (2013): Reticular Pseudodrusen in Early Age-Related Macular Degeneration Are Associated With Choroidal Thinning. Invest Ophthalmol Vis Sci **54**: 7075-7081.

Gass JD (1994): Biomicroscopic and histopathologic considerations regarding the feasibility of surgical excision of subfoveal neovascular membranes. Trans Am Ophthalmol Soc **92**: 91-116.

Gehlbach P, Li T & Hatef E (2016): Statins for age-related macular degeneration. Cochrane Database Syst Rev: CD006927.

Gemenetzi M, Lotery AJ & Patel PJ (2017): Risk of geographic atrophy in age-related macular degeneration patients treated with intravitreal anti-VEGF agents. Eye (Lond) **31**: 1-9.

Gillies MC, Campain A, Barthelmes D, et al. (2015): Long-Term Outcomes of Treatment of Neovascular Age-Related Macular Degeneration: Data from an Observational Study. Ophthalmology **122**: 1837-1845.

Goldstein M, Heilweil G, Barak A & Loewenstein A (2005): Retinal pigment epithelial tear following photodynamic therapy for choroidal neovascularization secondary to AMD. Eye (Lond) **19**: 1315-1324.

Grassmann F, Heid IM & Weber BH (2017): Recombinant Haplotypes Narrow the ARMS2/HTRA1 Association Signal for Age-Related Macular Degeneration. Genetics **205**: 919-924.

Greenland S, Robins JM & Pearl J (1999): Confounding and collapsibility in causal inference. Stat Sci **14**: 29-46.

Grossniklaus HE, Ling JX, Wallace TM, et al. (2002): Macrophage and retinal pigment epithelium expression of angiogenic cytokines in choroidal neovascularization. Mol Vis **8**: 119-126.

Gupta N, Brown KE & Milam AH (2003): Activated microglia in human retinitis pigmentosa, late-onset retinal degeneration, and age-related macular degeneration. Exp Eye Res **76**: 463-471.

Guymer RH, Baird PN, Varsamidis M, et al. (2013): Proof of concept, randomized, placebo-controlled study of the effect of simvastatin on the course of age-related macular degeneration. PLoS One **8**: e83759.

Guymer RH, Baird PN, Varsamidis M, et al. (2014): Proof of Concept, Randomized, Placebo-Controlled Study of the Effect of Simvastatin on the Course of Age-Related Macular Degeneration. PLoS One **8**: e83759.

Guymer RH, Brassington KH, Dimitrov P, et al. (2014): Nanosecond-laser application in intermediate AMD: 12-month results of fundus appearance and macular function. Clin Experiment Ophthalmol **42**: 466-479.

Guymer RH, Gross-Jendroska M, Owens SL, Bird AC & Fitzke FW (1997): Laser treatment in subjects with high-risk clinical features of age-related macular degeneration. Posterior pole appearance and retinal function. Arch Ophthalmol **115**: 595-603.

Guymer RH, Rosenfeld PJ, Curcio CA, et al. (2020): Incomplete Retinal Pigment Epithelial and Outer Retinal Atrophy in Age-Related Macular Degeneration: Classification of Atrophy Meeting Report 4. Ophthalmology **127**: 394-409.

Guymer RH, Wu Z, Hodgson LAB, et al. (2019): Subthreshold Nanosecond Laser Intervention in Age-Related Macular Degeneration: The LEAD Randomized Controlled Clinical Trial. Ophthalmology **126**: 829-838.

Hartnett ME, Weiter JJ, Garsd A & Jalkh AE (1992): Classification of retinal pigment epithelial detachments associated with drusen. Graefes Arch Clin Exp Ophthalmol **230**: 11-19.

He K, Zhang X, Ren S & Sun J (2015): Delving deep into rectifiers: Surpassing human-level performance on imagenet classification. 2015 IEEE International Conference on Computer Vision (ICCV). Santiago, Chile. 1026-1034.

Heier JS, Brown DM, Chong V, et al. (2012): Intravitreal Aflibercept (VEGF Trap-Eye) in Wet Age-related Macular Degeneration. Ophthalmology **119**: 2537-2548.

Ho CY, Lek JJ, Aung KZ, McGuinness MB, Luu CD & Guymer RH (2018): Relationship between reticular pseudodrusen and choroidal thickness in intermediate age-related macular degeneration. Clin Exp Ophthalmol **46**: 485-494.

Ho J, Adhi M, Baumal C, Liu J, Fujimoto JG, Duker JS & Waheed NK (2015): Agreement and reproducibility of retinal pigment epithelial detachment volumetric measurements through optical coherence tomography. Retina **35**: 467-472.

Holz FG, Strauss EC, Schmitz-Valckenberg S & van Lookeren Campagne M (2014): Geographic Atrophy: Clinical Features and Potential Therapeutic Approaches. Ophthalmology **121**: 1079-1091.

Jastrzebska B, Debinski A, Filipek S & Palczewski K (2011): Role of membrane integrity on G protein-coupled receptors: Rhodopsin stability and function. Prog Lipid Res **50**: 267-277.

Jiang F, Jiang Y, Zhi H, et al. (2017): Artificial intelligence in healthcare: past, present and future. Stroke Vasc Neurol **2**: 230-243.

Joachim N, Mitchell P, Burlutsky G, Kifley A & Wang JJ (2015): The Incidence and Progression of Age-Related Macular Degeneration over 15 Years: The Blue Mountains Eye Study. Ophthalmology **122**: 2482-2489.

Johnson PT, Betts KE, Radeke MJ, Hageman GS, Anderson DH & Johnson LV (2006): Individuals homozygous for the age-related macular degeneration risk-conferring variant of complement factor H have elevated levels of CRP in the choroid. Proc Natl Acad Sci U S A **103**: 17456-17461.

Jonas JB, Forster TM, Steinmetz P, Schlichtenbrede FC & Harder BC (2014): Choroidal thickness in age-related macular degeneration. Retina **34**: 1149-1155.

Keenan TD, Klein B, Agron E, Chew EY, Cukras CA & Wong WT (2020): Choroidal Thickness and Vascularity Vary with Disease Severity and Subretinal Drusenoid Deposit Presence in Nonadvanced Age-Related Macular Degeneration. Retina **40**: 632-642.

Kermany DS, Goldbaum M, Cai W, et al. (2018): Identifying Medical Diagnoses and Treatable Diseases by Image-Based Deep Learning. Cell **172**: 1122-1131.e1129.

Klein ML, Ferris FL, Armstrong J, Hwang TS, Chew EY, Bressler SB & Chandra SR (2008): Retinal Precursors and the Development of Geographic Atrophy in Age-Related Macular Degeneration. Ophthalmology **115**: 1026-1031.

Klein R, Klein BE, Jensen SC, Cruickshanks KJ, Lee KE, Danforth LG & Tomany SC (2001): Medication use and the 5-year incidence of early age-related maculopathy: the Beaver Dam Eye Study. Arch Ophthalmol **119**: 1354-1359.
Klein R, Knudtson MD & Klein BE (2007): Statin use and the five-year incidence and progression of age-related macular degeneration. Am J Ophthalmol **144**: 1-6.
Klein R, Meuer SM, Knudtson MD & Klein BE (2008): The epidemiology of progression of pure geographic atrophy: the Beaver Dam Eye Study. Am J Ophthalmol **146**: 692-699.
Klein RJ, Zeiss C, Chew EY, et al. (2005): Complement factor H polymorphism in age-related macular degeneration. Science **308**: 385-389.
Koss MJ, Kurz P, Tsobanelis T, Lehmacher W, Fassbender C, Klingel R & Koch FH (2009): Prospective, randomized, controlled clinical study evaluating the efficacy of Rheopheresis for dry age-related macular degeneration. Dry AMD treatment with Rheopheresis Trial-ART. Graefes Arch Clin Exp Ophthalmol **247**: 1297-1306.
Krizhevsky A, Sutskever I & Hinton GE (2012): ImageNet classification with deep convolutional neural networks. Advances in Neural Information Processing Systems. Lake Tahoe, NV, USA. **2**: 1097-1105.
Lamin A, Oakley JD, Dubis AM, Russakoff DB & Sivaprasad S (2019): Changes in volume of various retinal layers over time in early and intermediate age-related macular degeneration. Eye (Lond) **33**: 428-434.
LeCun Y, Bengio Y & Hinton G (2015): Deep learning. Nature **521**: 436-444.
Lecun Y, Bottou L, Bengio Y & Haffner P (1998): Gradient-based learning applied to document recognition. Proc IEEE Inst Electr Electron Eng **86**: 2278-2324.
LeCun YA, Bottou L, Orr GB & Müller KR (2012): Efficient BackProp. In: Montavon G, Orr GB and Müller K(eds.) Neural Networks: Tricks of the Trade. Berlin, Heidelberg: Springer 9-48.
Lee CS, Baughman DM & Lee AY (2017): Deep Learning Is Effective for Classifying Normal versus Age-Related Macular Degeneration OCT Images. Ophthalmol Retina **1**: 322-327.
Lee NY & Kim KS (2008): Photodynamic therapy treatment for eyes with drusenoid pigment epithelium detachment. Korean J Ophthalmol **22**: 194-196.
Litts KM, Ach T, Hammack KM, Sloan KR, Zhang Y, Freund KB & Curcio CA (2016): Quantitative Analysis of Outer Retinal Tubulation in Age-Related Macular Degeneration From Spectral-Domain Optical Coherence Tomography and Histology. Invest Ophthalmol Vis Sci **57**: 2647-2656.
Long KO, Fisher SK, Fariss RN & Anderson DH (1986): Disc shedding and autophagy in the cone-dominant ground squirrel retina. Exp Eye Res **43**: 193-205.
Lopez PF, Grossniklaus HE, Lambert HM, Aaberg TM, Capone A, Jr., Sternberg P, Jr. & L'Hernault N (1991): Pathologic features of surgically excised subretinal neovascular membranes in age-related macular degeneration. Am J Ophthalmol **112**: 647-656.
Lu W, Tong Y, Yu Y, Xing Y, Chen C & Shen Y (2018): Deep Learning-Based Automated Classification of Multi-Categorical Abnormalities From Optical Coherence Tomography Images. Transl Vis Sci Technol **7**: 41-41.
Ma L, Wang Y, Du J, Wang M, Zhang R & Fu Y (2015): The association between statin use and risk of age-related macular degeneration. Sci Rep **5**: 18280.
Maberley D & Canadian Retinal Trials Group (2009): Photodynamic therapy and intravitreal triamcinolone for neovascular age-related macular degeneration: a randomized clinical trial. Ophthalmology **116**: 2149-2157.e2141.
Maguire MG, Ying GS, McCannel CA, Liu C, Dai Y & Complications of Age-related Macular Degeneration Prevention Trial Research Group (2009): Statin use and the incidence of advanced age-related macular degeneration in the Complications of Age-related Macular Degeneration Prevention Trial. Ophthalmology **116**: 2381-2385.

Marsiglia M, Boddu S, Bearelly S, Xu L, Breaux BE, Jr., Freund KB, Yannuzzi LA & Smith RT (2013): Association between geographic atrophy progression and reticular pseudodrusen in eyes with dry age-related macular degeneration. Invest Ophthalmol Vis Sci **54**: 7362-7369.

Martin DF, Maguire MG, Ying GS, Grunwald JE, Fine SL & Jaffe GJ (2011): Ranibizumab and bevacizumab for neovascular age-related macular degeneration. N Engl J Med **364**: 1897-1908.

McCarty CA, Mukesh BN, Guymer RH, Baird PN & Taylor HR (2001): Cholesterol-lowering medications reduce the risk of age-related maculopathy progression. Med J Aust **175**: 340.

McGwin G, Jr., Modjarrad K, Hall TA, Xie A & Owsley C (2006): 3-hydroxy-3-methylglutaryl coenzyme a reductase inhibitors and the presence of age-related macular degeneration in the Cardiovascular Health Study. Arch Ophthalmol **124**: 33-37.

McGwin G, Jr., Owsley C, Curcio CA & Crain RJ (2003): The association between statin use and age related maculopathy. Br J Ophthalmol **87**: 1121-1125.

McGwin G, Jr., Xie A & Owsley C (2005): The use of cholesterol-lowering medications and age-related macular degeneration. Ophthalmology **112**: 488-494.

Michels S, Rosenfeld PJ, Puliafito CA, Marcus EN & Venkatraman AS (2005): Systemic Bevacizumab (Avastin) Therapy for Neovascular Age-Related Macular Degeneration: Twelve-Week Results of an Uncontrolled Open-Label Clinical Study. Ophthalmology **112**: 1035-1047.e1039.

Moore DJ & Clover GM (2001): The Effect of Age on the Macromolecular Permeability of Human Bruch's Membrane. Invest Ophthalmol Vis Sci **42**: 2970-2975.

Mopuri KR, Garg U & Venkatesh Babu R (2019): CNN Fixations: An Unraveling Approach to Visualize the Discriminative Image Regions. IEEE Trans Image Process **28**: 2116-2125.

Motozawa N, An G, Takagi S, et al. (2019): Optical Coherence Tomography-Based Deep-Learning Models for Classifying Normal and Age-Related Macular Degeneration and Exudative and Non-Exudative Age-Related Macular Degeneration Changes. Ophthalmol Ther **8**: 527-539.

Mrejen S, Sarraf D, Mukkamala SK & Freund KB (2013): Multimodal imaging of pigment epithelial detachment: a guide to evaluation. Retina **33**: 1735-1762.

Muniz A, Villazana-Espinoza ET, Hatch AL, Trevino SG, Allen DM & Tsin ATC (2007): A novel cone visual cycle in the cone-dominated retina. Exp Eye Res **85**: 175-184.

Nakagawa S & Schielzeth H (2013): A general and simple method for obtaining R2 from generalized linear mixed-effects models. Methods Ecol Evol **4**: 133-142.

Nassisi M, Fan W, Shi Y, Lei J, Borrelli E, Ip M & Sadda SR (2018): Quantity of Intraretinal Hyperreflective Foci in Patients With Intermediate Age-Related Macular Degeneration Correlates With 1-Year Progression. Invest Ophthalmol Vis Sci **59**: 3431-3439.

Newman DK (2016): Photodynamic therapy: current role in the treatment of chorioretinal conditions. Eye (Lond) **30**: 202-210.

Nozaki M, Raisler BJ, Sakurai E, et al. (2006): Drusen complement components C3a and C5a promote choroidal neovascularization. Proc Natl Acad Sci U S A **103**: 2328-2333.

Obermeyer Z & Lee TH (2017): Lost in Thought — The Limits of the Human Mind and the Future of Medicine. N Engl J Med **377**: 1209-1211.

Ogino K, Tsujikawa A, Yamashiro K, et al. (2014): Multimodal evaluation of macular function in age-related macular degeneration. Jpn J Ophthalmol **58**: 155-165.

Ouyang Y, Heussen FM, Hariri A, Keane PA & Sadda SR (2013): Optical coherence tomography-based observation of the natural history of drusenoid lesion in eyes with dry age-related macular degeneration. Ophthalmology **120**: 2656-2665.

Owsley C, Jackson GR, Cideciyan AV, et al. (2000): Psychophysical evidence for rod vulnerability in age-related macular degeneration. Invest Ophthalmol Vis Sci **41**: 267-273.
Pannucci CJ & Wilkins EG (2010): Identifying and avoiding bias in research. Plast Reconstr Surg **126**: 619-625.
Pauleikhoff D, Harper CA, Marshall J & Bird AC (1990): Aging changes in Bruch's membrane. A histochemical and morphologic study. Ophthalmology **97**: 171-178.
Perdomo O, Rios H, Rodriguez FJ, Otalora S, Meriaudeau F, Muller H & Gonzalez FA (2019): Classification of diabetes-related retinal diseases using a deep learning approach in optical coherence tomography. Comput Methods Programs Biomed **178**: 181-189.
Peyman GA & Bok D (1972): Peroxidase diffusion in the normal and laser-coagulated primate retina. Invest Ophthalmol Vis Sci **11**: 35-45.
Politi L, Rotstein N & Carri N (2001): Effects of docosahexaenoic acid on retinal development: cellular and molecular aspects. Lipids **36**: 927-935.
Powner MB, Gillies MC, Tretiach M, Scott A, Guymer RH, Hageman GS & Fruttiger M (2010): Perifoveal müller cell depletion in a case of macular telangiectasia type 2. Ophthalmology **117**: 2407-2416.
Pulido J, Sanders D, Winters JL & Klingel R (2005): Clinical outcomes and mechanism of action for rheopheresis treatment of age-related macular degeneration (AMD). J Clin Apher **20**: 185-194.
Pulido JS, Winters JL & Boyer D (2006): Preliminary analysis of the final multicenter investigation of rheopheresis for age related macular degeneration (AMD) trial (MIRA-1) results. Trans Am Ophthalmol Soc **104**: 221-231.
Pumariega NM, Smith RT, Sohrab MA, Letien V & Souied EH (2011): A prospective study of reticular macular disease. Ophthalmology **118**: 1619-1625.
Reichenbach A & Bringmann A (2013): New functions of Müller cells. Glia **61**: 651-678.
Rencova E, Blaha M, Studnicka J, et al. (2011): Haemorheopheresis could block the progression of the dry form of age-related macular degeneration with soft drusen to the neovascular form. Acta Ophthalmol **89**: 463-471.
Ritter M, Bolz M, Sacu S, Deak GG, Kiss C, Pruente C & Schmidt-Erfurth UM (2010): Effect of intravitreal ranibizumab in avascular pigment epithelial detachment. Eye (Lond) **24**: 962-968.
Rodriguez de Cordoba S, Esparza-Gordillo J, Goicoechea de Jorge E, Lopez-Trascasa M & Sanchez-Corral P (2004): The human complement factor H: functional roles, genetic variations and disease associations. Mol Immunol **41**: 355-367.
Roquet W, Roudot-Thoraval F, Coscas G & Soubrane G (2004): Clinical features of drusenoid pigment epithelial detachment in age related macular degeneration. Br J Ophthalmol **88**: 638-642.
Rosenfeld PJ, Brown DM, Heier JS, Boyer DS, Kaiser PK, Chung CY & Kim RY (2006): Ranibizumab for neovascular age-related macular degeneration. N Engl J Med **355**: 1419-1431.
Russakovsky O, Deng J, Su H, et al. (2015): ImageNet Large Scale Visual Recognition Challenge. Int J Comput Vis **115**: 211-252.
Sadda SR, Guymer R, Holz FG, et al. (2018): Consensus Definition for Atrophy Associated with Age-Related Macular Degeneration on OCT: Classification of Atrophy Report 3. Ophthalmology **125**: 537-548.
Santos AM, Paiva AC, Santos APM, et al. (2018): Semivariogram and Semimadogram functions as descriptors for AMD diagnosis on SD-OCT topographic maps using Support Vector Machine. Biomed Eng Online **17**: 160.
Sarks JP, Sarks SH & Killingsworth MC (1988): Evolution of geographic atrophy of the retinal pigment epithelium. Eye (Lond) **2 (Pt 5)**: 552-577.

Sarks S, Cherepanoff S, Killingsworth M & Sarks J (2007): Relationship of Basal Laminar Deposit and Membranous Debris to the Clinical Presentation of Early Age-Related Macular Degeneration. Invest Ophthalmol Vis Sci **48**: 968-977.
Sarks SH (1980): Council Lecture. Drusen and their relationship to senile macular degeneration. Aust J Ophthalmol **8**: 117-130.
Sarks SH, Arnold JJ, Sarks JP, Gilles MC & Walter CJ (1996): Prophylactic perifoveal laser treatment of soft drusen. Aust N Z J Ophthalmol **24**: 15-26.
Savastano MC, Minnella AM, Tamburrino A, Giovinco G, Ventre S & Falsini B (2014): Differential Vulnerability of Retinal Layers to Early Age-Related Macular Degeneration: Evidence by SD-OCT Segmentation Analysis. Invest Ophthalmol Vis Sci **55**: 560-566.
Scherer D, Müller A & Behnke S (2010): Evaluation of Pooling Operations in Convolutional Architectures for Object Recognition. In: Diamantaras K, Duch W and Iliadis LS(eds.) Artificial Neural Networks - ICANN 2010. Berlin, Heidelberg: Springer 92-101.
Schlanitz FG, Baumann B, Kundi M, et al. (2017): Drusen volume development over time and its relevance to the course of age-related macular degeneration. Br J Ophthalmol **101**: 198-203.
Schmidt-Erfurth U, Klimscha S, Waldstein SM & Bogunovic H (2017): A view of the current and future role of optical coherence tomography in the management of age-related macular degeneration. Eye (Lond) **31**: 26-44.
Schmidt-Erfurth U, Sadeghipour A, Gerendas BS, Waldstein SM & Bogunovic H (2018): Artificial intelligence in retina. Prog Retin Eye Res **67**: 1-29.
Schmitz-Valckenberg S, Sahel J-A, Danis R, Fleckenstein M, Jaffe GJ, Wolf S, Pruente C & Holz FG (2016): Natural History of Geographic Atrophy Progression Secondary to Age-Related Macular Degeneration (Geographic Atrophy Progression Study). Ophthalmology **123**: 361-368.
Schuman SG, Koreishi AF, Farsiu S, Jung SH, Izatt JA & Toth CA (2009): Photoreceptor layer thinning over drusen in eyes with age-related macular degeneration imaged in vivo with spectral-domain optical coherence tomography. Ophthalmology **116**: 488-496.
Seddon JM, McLeod DS, Bhutto IA, Villalonga MB, Silver RE, Wenick AS, Edwards MM & Lutty GA (2016): Histopathological Insights Into Choroidal Vascular Loss in Clinically Documented Cases of Age-Related Macular Degeneration. JAMA Ophthalmol **134**: 1272-1280.
Shaw PX, Zhang L, Zhang M, et al. (2012): Complement factor H genotypes impact risk of age-related macular degeneration by interaction with oxidized phospholipids. Proc Natl Acad Sci U S A **109**: 13757-13762.
Shindou H, Koso H, Sasaki J, et al. (2017): Docosahexaenoic acid preserves visual function by maintaining correct disc morphology in retinal photoreceptor cells. J Biol Chem **292**: 12054-12064.
Skeie JM & Mullins RF (2009): Macrophages in neovascular age-related macular degeneration: friends or foes? Eye (Lond) **23**: 747-755.
Smeeth L, Cook C, Chakravarthy U, Hubbard R & Fletcher AE (2005): A case control study of age related macular degeneration and use of statins. Br J Ophthalmol **89**: 1171-1175.
Spaide RF, Sorenson J & Maranan L (2003): Combined photodynamic therapy with verteporfin and intravitreal triamcinolone acetonide for choroidal neovascularization. Ophthalmology **110**: 1517-1525.
Stefánsson E, Geirsdóttir Á & Sigurdsson H (2011): Metabolic physiology in age related macular degeneration. Prog Retin Eye Res **30**: 72-80.
Subczynski WK, Hyde JS & Kusumi A (1989): Oxygen permeability of phosphatidylcholine--cholesterol membranes. Proc Natl Acad Sci U S A **86**: 4474-4478.

Tan JS, Mitchell P, Rochtchina E & Wang JJ (2007): Statins and the long-term risk of incident age-related macular degeneration: the Blue Mountains Eye Study. Am J Ophthalmol **143**: 685-687.

The Age-Related Eye Disease Study 2 Research Group (2013): Lutein + zeaxanthin and omega-3 fatty acids for age-related macular degeneration: the Age-Related Eye Disease Study 2 (AREDS2) randomized clinical trial. JAMA **309**: 2005-2015.

The Choroidal Neovascularization Prevention Trial Research Group (2003): Laser treatment in fellow eyes with large drusen: updated findings from a pilot randomized clinical trial. Ophthalmology **110**: 971-978.

Thornton J, Edwards R, Mitchell P, Harrison RA, Buchan I & Kelly SP (2005): Smoking and age-related macular degeneration: a review of association. Eye **19**: 935-944.

Thurman JM, Renner B, Kunchithapautham K, et al. (2009): Oxidative stress renders retinal pigment epithelial cells susceptible to complement-mediated injury. J Biol Chem **284**: 16939-16947.

Ting DS, Ng WY, Ng SR, et al. (2016): Choroidal Thickness Changes in Age-Related Macular Degeneration and Polypoidal Choroidal Vasculopathy: A 12-Month Prospective Study. Am J Ophthalmol **164**: 128-136 e121.

Ting DSW, Cheung CY-L, Lim G, et al. (2017): Development and Validation of a Deep Learning System for Diabetic Retinopathy and Related Eye Diseases Using Retinal Images From Multiethnic Populations With Diabetes. JAMA **318**: 2211-2223.

Ting DSW, Peng L, Varadarajan AV, et al. (2019): Deep learning in ophthalmology: The technical and clinical considerations. Prog Retin Eye Res **72**: 100759.

Toomey CB, Johnson LV & Bowes Rickman C (2018): Complement factor H in AMD: Bridging genetic associations and pathobiology. Prog Retin Eye Res **62**: 38-57.

Tran D, Wang H, Torresani L, Ray J, LeCun Y & Paluri M (2018): A Closer Look at Spatiotemporal Convolutions for Action Recognition. Proc IEEE Comput Soc Conf Comput Vis Pattern Recognit. Salt Lake City, UT, USA. 6450-6459.

Tvenning A-O, Krohn J, Forsaa V, Malmin A, Hedels C & Austeng D (2020): Drusenoid pigment epithelial detachment volume is associated with a decrease in best-corrected visual acuity and central retinal thickness: the Norwegian Pigment Epithelial Detachment Study (NORPED) report no. 1 Acta Ophthalmol doi:10.1111/aos.14423.

Tvenning AO, Hedels C, Krohn J & Austeng D (2019): Treatment of large avascular retinal pigment epithelium detachments in age-related macular degeneration with aflibercept, photodynamic therapy, and triamcinolone acetonide. Clin Ophthalmol **13**: 233-241.

van Leeuwen R, Vingerling JR, Hofman A, de Jong PT & Stricker BH (2003): Cholesterol lowering drugs and risk of age related maculopathy: prospective cohort study with cumulative exposure measurement. BMJ **326**: 255-256.

VanderBeek BL, Zacks DN, Talwar N, Nan B & Stein JD (2013): Role of statins in the development and progression of age-related macular degeneration. Retina **33**: 414-422.

Vavvas DG, Daniels AB, Kapsala ZG, et al. (2016): Regression of Some High-risk Features of Age-related Macular Degeneration (AMD) in Patients Receiving Intensive Statin Treatment. EBioMedicine **5**: 198-203.

Venhuizen F, van Ginneken B, Bloemen B, van Grinsven M, Philipsen R, Hoyng C, Theelen T & Sánchez C (2015): Automated age-related macular degeneration classification in OCT using unsupervised feature learning. Proceedings SPIE Medical Imaging. Orlando, USA. **9414**.

Verteporfin In Photodynamic Therapy Study Group (2001): Verteporfin therapy of subfoveal choroidal neovascularization in age-related macular degeneration: two-year results of a randomized clinical trial including lesions with occult with no classic choroidal neovascularization—verteporfin in photodynamic therapy report 2. Am J Ophthalmol **131**: 541-560.

Virgili G & Bini A (2007): Laser photocoagulation for neovascular age-related macular degeneration. Cochrane Database Syst Rev: CD004763.
Virgili G, Michelessi M, Parodi MB, Bacherini D & Evans JR (2015): Laser treatment of drusen to prevent progression to advanced age-related macular degeneration. Cochrane Database Syst Rev: CD006537.
von Ruckmann A, Fitzke FW & Bird AC (1997): Fundus autofluorescence in age-related macular disease imaged with a laser scanning ophthalmoscope. Invest Ophthalmol Vis Sci **38**: 478-486.
Wang L, Clark ME, Crossman DK, Kojima K, Messinger JD, Mobley JA & Curcio CA (2010): Abundant Lipid and Protein Components of Drusen. PLoS One **5**: e10329.
Wang L, Li CM, Rudolf M, Belyaeva OV, Chung BH, Messinger JD, Kedishvili NY & Curcio CA (2009): Lipoprotein particles of intraocular origin in human Bruch membrane: an unusual lipid profile. Invest Ophthalmol Vis Sci **50**: 870-877.
Wetzig PC (1988): Treatment of drusen-related aging macular degeneration by photocoagulation. Trans Am Ophthalmol Soc **86**: 276-290.
Wierzbicki AS & Mikhailidis DP (2002): Dose–response effects of atorvastatin and simvastatin on high-density lipoprotein cholesterol in hypercholesterolaemic patients: a review of five comparative studies. Int J Cardiol **84**: 53-57.
Wierzbicki AS, Poston R & Ferro A (2003): The lipid and non-lipid effects of statins. Pharmacol Ther **99**: 95-112.
Wong WL, Su X, Li X, Cheung CM, Klein R, Cheng CY & Wong TY (2014): Global prevalence of age-related macular degeneration and disease burden projection for 2020 and 2040: a systematic review and meta-analysis. Lancet Glob Health **2**: e106-116.
Wu T, Fujihara M, Tian J, et al. (2010): Apolipoprotein B100 secretion by cultured ARPE-19 cells is modulated by alteration of cholesterol levels. J Neurochem **114**: 1734-1744.
Wu Z, Luu CD, Ayton LN, et al. (2014): Optical coherence tomography-defined changes preceding the development of drusen-associated atrophy in age-related macular degeneration. Ophthalmology **121**: 2415-2422.
Yannuzzi LA, Slakter JS, Sorenson JA, Guyer DR & Orlock DA (1992): Digital indocyanine green videoangiography and choroidal neovascularization. Retina **12**: 191-223.
Yehoshua Z, Wang F, Rosenfeld PJ, Penha FM, Feuer WJ & Gregori G (2011): Natural history of drusen morphology in age-related macular degeneration using spectral domain optical coherence tomography. Ophthalmology **118**: 2434-2441.
Ying GS, Maguire MG, Glynn R & Rosner B (2017): Tutorial on Biostatistics: Linear Regression Analysis of Continuous Correlated Eye Data. Ophthalmic Epidemiol **24**: 130-140.
Yiu G, Chiu SJ, Petrou PA, et al. (2015): Relationship of central choroidal thickness with age-related macular degeneration status. Am J Ophthalmol **159**: 617-626.
Yosinski J, Clune J, Nguyen A, Fuchs T & Lipson H (2015): Understanding neural networks through deep visualization. arXiv preprint arXiv:1506.06579.
Zarubina AV, Neely DC, Clark ME, et al. (2016): Prevalence of Subretinal Drusenoid Deposits in Older Persons with and without Age-Related Macular Degeneration, by Multimodal Imaging. Ophthalmology **123**: 1090-1100.
Zhang JJ, Sun Y, Hussain AA & Marshall J (2012): Laser-mediated activation of human retinal pigment epithelial cells and concomitant release of matrix metalloproteinases. Invest Ophthalmol Vis Sci **53**: 2928-2937.
Zucchiatti I, Parodi MB, Pierro L, Cicinelli MV, Gagliardi M, Castellino N & Bandello F (2015): Macular ganglion cell complex and retinal nerve fiber layer comparison in different stages of age-related macular degeneration. Am J Ophthalmol **160**: 602-607.e601.

Zweifel SA, Imamura Y, Spaide TC, Fujiwara T & Spaide RF (2010a): Prevalence and Significance of Subretinal Drusenoid Deposits (Reticular Pseudodrusen) in Age-Related Macular Degeneration. Ophthalmology **117**: 1775-1781.
Zweifel SA, Spaide RF, Curcio CA, Malek G & Imamura Y (2010b): Reticular pseudodrusen are subretinal drusenoid deposits. Ophthalmology **117**: 303-312.e301.

7. Papers I-III

Paper I

Clinical Ophthalmology

Dovepress
open access to scientific and medical research

Open Access Full Text Article

ORIGINAL RESEARCH

Treatment of large avascular retinal pigment epithelium detachments in age-related macular degeneration with aflibercept, photodynamic therapy, and triamcinolone acetonide

This article was published in the following Dove Medical Press journal:
Clinical Ophthalmology

Arnt-Ole Tvenning[1,2]
Christian Hedels[3]
Jørgen Krohn[4,5]
Dordi Austeng[1,2]

[1]Department of Neuromedicine and Movement Science, Faculty of Medicine and Health Sciences, NTNU, Norwegian University of Science and Technology, 7491 Trondheim, Norway; [2]Department of Ophthalmology, St. Olavs Hospital, Trondheim University Hospital, 7006 Trondheim, Norway; [3]Hedels Eye Clinic, 6517 Kristiansund, Norway; [4]Department of Clinical Medicine, Section of Ophthalmology, University of Bergen, 5021 Bergen, Norway; [5]Department of Ophthalmology, Haukeland University Hospital, 5053 Bergen, Norway

Purpose: To evaluate the use of aflibercept, triamcinolone acetonide, and photodynamic therapy (PDT) in the treatment of avascular pigment epithelium detachments (aPEDs).

Patients and methods: Patients with treatment-naïve aPEDs ≥1,500 µm in diameter were randomized to treatment or observation. Treatment consisted of 6 monthly intravitreal injections of aflibercept. If the aPED persisted, the patients were treated with half-fluence PDT in combination with intravitreal triamcinolone acetonide and aflibercept. The primary outcome was change of best-corrected visual acuity (BCVA) after 24 months of follow-up. Secondary outcomes were changes in pigment epithelium volume, height and diameter, central retinal thickness, and number of patients developing choroidal neovascularization or geographic atrophy (GA).

Results: Treatment and inclusion of patients were stopped after an interim analysis of 6-month data because 75% of the aPEDs were in different stages of GA. Nine patients with aPED were included in the study, of these one patient was excluded because of bilateral central serous chorioretinopathy. The remaining eight had drusenoid aPEDs. After 24 months of follow-up, estimated means of BCVA decreased by 4.2 and 20.8 letters in the treatment and observation group, respectively. This decrease over time was not significantly different between groups (P=0.140, 95% CI 5.3, 38.6). Estimated means of PED volume, height, diameter, and central retinal thickness were not significantly different between groups. Choroidal neovascularization and retinal pigment epithelium tear developed in one patient in the treatment group. One patient in the treatment group and two patients in the observation group progressed to complete retinal pigment epithelium and outer retinal atrophy. A decrease in PED volume was associated with the development of complete retinal pigment epithelium and outer retinal atrophy (P=0.029).

Conclusion: This small trial indicates that multitargeted, primarily antiangiogenic therapy does not favorably alter the natural course of drusenoid aPEDs.

Keywords: drusenoid, geographic atrophy, anti-VEGF, PDT

Plain language summary

How to manage large accumulations of lipids and fluid in the part of your eye responsible for good vision, without associated leaking blood vessels, is not fully understood. Their presence is associated with a risk of visual impairment. Available treatments (anti-vascular endothelial growth factor and photodynamic therapy) have in small studies and case reports shown some beneficial effects.

We investigated if treatment could be beneficial by designing a study with patients randomly assigned to treatment or observation. Treatment consisted of injecting the eye with anti-vascular

Correspondence: Arnt-Ole Tvenning
Department of Neuromedicine and Movement Science, Faculty of Medicine and Health Sciences, NTNU, Norwegian University of Science and Technology, P.O. Box 8905, 7491 Trondheim, Norway
Tel +47 72 57 5012
Fax +47 72 57 4833
Email arnt.o.tvenning@ntnu.no

submit your manuscript | www.dovepress.com
Dovepress
http://dx.doi.org/10.2147/OPTH.S188315

endothelial growth factor monthly for 6 months, and then adding photodynamic therapy and injections of corticosteroids if the accumulation of lipids and fluid did not resolve. Our study was stopped early when 6 months data were available because 75% of the patients progressed to a more advanced form of the disease with no currently available treatment.

This small study indicates that treatment with a combination of anti-vascular endothelial growth factor, corticosteroid, and photodynamic therapy does not favorably alter the natural course of large accumulations of lipids and fluid in age-related macular degeneration without associated leaking blood vessels.

Introduction

Age-related macular degeneration (AMD) is the most common cause of permanent vision loss in the industrialized world.[1–3] With the introduction of anti-vascular endothelial growth factor (anti-VEGF) agents, treatment for neovascular AMD (nAMD) has undergone significant advances. There are still dilemmas to be solved, and research on biomarkers relevant for visual function, disease activity, and prognosis is desirable.[4] One such biomarker, pigment epithelium detachment (PED), is still a challenge, both in avascular PED (aPED) and when neovascularization is present (nPED). The pathophysiologic mechanisms underlying the development of PEDs are not fully understood, and probably represent a continuum of degenerative changes and formation of choroidal neovascularization (CNV).[5] Serous aPEDs are thought to arise from age-related formation of a hydrophobic barrier in Bruch's membrane preventing the free diffusion of fluid from retinal pigment epithelium (RPE) to choriocapillaris.[6] Drusenoid aPED formation is a result of the confluence of large drusen, and probably with increasing size the hydrophobic composition of the drusenoid deposits also creates a barrier in Bruch's membrane with accumulation of fluid.[7,8]

In some retrospective case series, nPEDs respond well to treatment with anti-VEGF.[9–11] In other studies, the results are not so promising,[12] and nPEDs might be more resistant to treatment.[4] Nonresponders to anti-VEGF treatment have the option of photodynamic therapy (PDT), which has been shown to stabilize disease progression,[13] but the treatment may lead to chorioretinal atrophy and decline in visual acuity.[14]

The natural course of aPED is unfavorable. In the Age-Related Eye Disease Study, it was found that 42% of 282 eyes with drusenoid aPEDs progressed to advanced AMD, with either central geographic atrophy (GA) (19%) or nAMD (23%).[15] In one study with long follow-up of 12 eyes with drusenoid aPED, all patients developed advanced AMD, with a 10-year occurrence rate of 75% for central GA and 25% for nAMD.[8] Patients presenting with aPEDs remain a diagnostic and therapeutic challenge, and treatment is controversial.[12] One prospective case series treated 12 drusenoid and serous aPEDs with anti-VEGF, which led to stabilization of best-corrected visual acuity (BCVA) after 1 year, but with heterogeneous anatomical outcomes.[16] In another prospective case series, six patients with drusenoid aPEDs were treated with anti-VEGF agents that led to stabilization of BCVA and improvement in 33% of patients.[17] Two case reports have reported regression of drusen and drusenoid PEDs following anti-VEGF treatment for associated CNV.[18,19] Other case reports have shown regression of drusenoid aPED and improvement of BCVA after PDT.[20,21]

In the present study, we planned to evaluate the treatment of serous and drusenoid aPEDs. Our original hypothesis was that some aPEDs may be caused by subtle CNV, undetectable with today's technology, and that early treatment could be beneficial. To our knowledge, this is the first randomized controlled trial evaluating treatment of aPEDs with aflibercept, PDT, and triamcinolone acetonide.

Patients and methods

The study was conducted at the Department of Ophthalmology, Trondheim University Hospital, and the inclusion of patients started in April 2014. Patients with AMD and large PEDs, that on clinical evaluation seemed to be avascular, were referred from other eye departments and ophthalmologists in the Central Norway Health Region. The study is registered at ClinicalTrials.gov: NCT01746875, and was approved by the Regional Committee for Medical and Health Research Ethics Central Norway (2012/1743). All study participants provided a written informed consent, and the study was conducted in accordance with the Declaration of Helsinki.

Inclusion criteria were patients older than 50 years with treatment-naïve AMD, fluorescein angiographic (FA)- and indocyanine green angiographic (ICG)-verified subfoveal aPED ≥1,500 µm in diameter, and BCVA ≤20/32 and ≥20/400. Exclusion criteria were subfoveal fibrosis, central GA, and concurrent eye diseases that could affect BCVA.

The diagnosis of aPED was made by FA, ICG, and spectral-domain optical coherence tomography (OCT). PEDs with no leakage on FA and an absence of plaques and hot spots on ICG were defined as aPEDs. The aPEDs were defined as drusenoid if they appeared yellow on clinical fundus examination with predominantly hyper-reflective contents on OCT, staining/pooling on FA, and hypofluorescence on ICG.

The aPEDs were defined as serous if they appeared as dome-shaped with predominantly hyporeflective contents on OCT, pooling on FA, and hypofluorescence on ICG. Central GA was defined as an area with window defects on FA and ICG, sharply delineated margins on fundus photography with visible choroidal vasculature, loss of a hyper-reflective RPE line, and increased choroidal reflectivity on OCT, hypofluorescence on fundus autofluoresence (FAF), and subfoveal localization.

Fundus and angiographic images (Zeiss FF 450 plus, Carl Zeiss Meditec AG, Jena, Germany) were reviewed and graded by two retina specialists (AT and DA). To ensure a correct diagnosis, all the images were also anonymized and sent for evaluation to an external retina specialist (CH) prior to randomization. Randomization was performed by a web-based randomization system developed and administered by Unit of Applied Clinical Research, The Faculty of Medicine, Norwegian University of Science and Technology, Trondheim, Norway. The patients were stratified on the presence of drusenoid aPED.

BCVA was measured using Early Treatment Diabetic Retinopathy Study (ETDRS) chart in an illuminated Cabinet (ESV3000; Good-Lite, Elgin, IL, USA) at 4 m, with automatic adjustment of 85 cd/m^2. Room lighting was dimmed so that 90–110 lux could be measured in front of the cabinet. The examiners were blinded for patient group. Refraction was performed by a physician or optician prior to BCVA measurement at baseline, 1 year, and 2 years. Maximum PED height and diameter were measured by OCT (Cirrus HD-OCT; Carl Zeiss Meditec AG) on five different slides on macular cube scans starting in the central fovea (512 128), and the mean of the three highest values was used. PED volume was calculated after manual segmentation and subtracting of total retinal and PED volume, measured from the internal limiting membrane (ILM) to the fit-RPE line, with retinal volume, measured from ILM to RPE line (Figure 1). Central retinal thickness (CRT) was obtained automatically after manual segmentation of RPE and ILM.

Patients randomized to the treatment group received three monthly intravitreal injections of aflibercept 2 mg/0.05 mL (Eylea; Regeneron Inc., Tarrytown, NY, USA), with 3 additional monthly injections if the PED persisted at 3 months. If the PED did not completely resolve as measured by OCT, the patients were treated with half-fluence PDT in combination with aflibercept 2 mg/0.05 mL and triamcinolone acetonide 4 mg/0.1 mL (Triesence; Alcon lab Inc., Forthworth, TX, USA) at 6 and 9 months (triple-therapy). The half-fluence PDT treatment protocol consisted of intravenous administration of 15 mg Verteporfin (Visudyne; Bausch and Lomb Inc., Bridgewater, NJ, USA) in a 30 mL solution over 10 minutes, and after a waiting period of 5 minutes, infrared light (689 nm) with a spot size of 3,000–4,000 µm was applied for 83 seconds with 25 J/cm^2 and 300 mW/cm^2 (Visulas 690s, Carl Zeiss Meditec AG). Intravitreal injections of aflibercept and triamcinolone acetonide were given on separate days 0–2 weeks after the PDT treatment. Additional follow-up examinations were performed at 6-month intervals in both groups and included BCVA measurements, OCT, fundus photography, FA, ICG, and FAF.

The primary outcome measure was changes in BCVA from baseline to 24 months. Secondary outcome measures were changes in PED height, diameter and volume, CRT, and number of patients with progression of GA or development of CNV. Progression of GA was graded as described by Sadda et al[22]: complete RPE and outer retinal atrophy (cRORA); 1) region of hypertransmission of at least 250 µm in diameter in any lateral dimension, 2) zone of attenuation or disruption of the RPE of at least 250 µm in diameter, 3) evidence of overlying photoreceptor degeneration. Features of photoreceptor degeneration include all of the following: loss of interdigitation zone, ellipsoid zone, and external limiting membrane, and thinning of the outer nuclear layer, which also can be identified by a descending outer plexiform layer. In case of incomplete RPE and outer retinal atrophy (iRORA), the criteria for cRORA are not met, but hypertransmission and

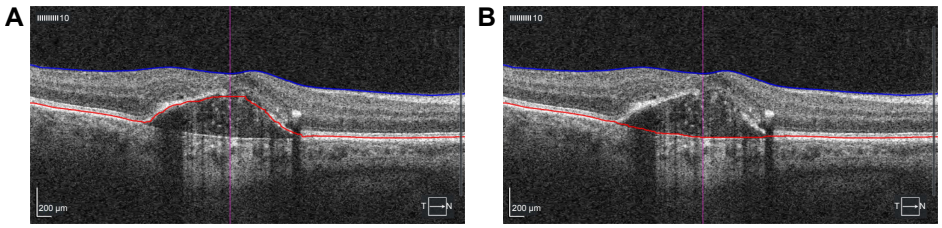

Figure 1 Manual segmentation and volume measurement of retinal pigment epithelium detachment from macular cube 512 128 scans.
Notes: (**A**) Segmentation of internal limiting membrane and retinal pigment epithelium. (**B**) Segmentation of internal limiting membrane to fit line of retinal pigment epithelium.

a discontinuous RPE band with evidence of photoreceptor degeneration are found. Exclusion criteria were presence of scrolled RPE or other signs of an RPE tear.

A sample size of 60 patients was decided to be sufficient to detect a clinically meaningful difference. Marginal models with restricted maximum likelihood estimation and unstructured or exponential covariance structure were used. All marginal models had age, baseline value, group, time, and the interaction between group and time as predictors. The *P*-values and 95% CIs of the comparisons of estimated means were Sidak adjusted because of multiple comparisons. Model fit was evaluated with Akaike's information criterion and likelihood ratio tests. The residuals were checked for normality compared to the normal distribution assessed with histograms, Q–Q plots, and Shapiro–Wilks test. Two-tailed *P*-values <0.05 were considered statistically significant. SPSS statistics 25 (IBM) and Stata 15.1 (StataCorp LLC) were used for statistical analysis.

Results

A total of 14 patients with AMD and aPED ≥1,500 µm in diameter were referred from April 2014 to February 2015. Of these, five patients did not meet the inclusion criteria. Two patients with serous PED, one with fibrovascular PED and one with drusenoid PED, had CNV. One patient had adult-onset foveomacular vitelliform dystrophy. Thus, nine patients with aPEDs were included in the study, with five randomized to the treatment group. One patient from the treatment group was excluded after 3 months of follow-up because of disappearance of bilateral serous aPEDs after tapering of systemic corticosteroid therapy on suspicion of central serous chorioretinopathy. Baseline characteristics of the eight drusenoid aPEDs are summarized in Table 1.

An interim analysis was performed after 6 months of follow-up. Because examination of the OCT images showed that the patients in both the treatment and observation groups were in different stages of GA formation and progression (Figure 2), it was decided to stop further inclusion and treatment of patients.

The four participants in the treatment group received 6 monthly injections of aflibercept, but further treatment differed. Two patients (Figure 2, ID: 2 and 3) received both treatments with triple-therapy, one patient had only one treatment (Figure 2, ID: 7) and one patient did not receive triple-therapy (Figure 2, ID: 5). All patients were followed for 12 months (mean 12.4, range 12–13), and three patients in each group had a follow-up of 24 months (mean 24.2, range 24–25).

Best-corrected visual acuity

After 24 months of follow-up, estimated means of BCVA decreased by 4.2 ETDRS letters and 20.8 ETDRS letters in the treatment and observation groups, respectively (Figure 3A). The loss of ETDRS letters from 6 to 24 months did not differ significantly between groups (*P*=0.140, 95% CI 5.3, 38.6). After 6, 12, and 24 months of follow-up, the difference of BCVA was 0.8 ETDRS letters (*P*=1.0, 95% CI 21.3, 22.8), 0.3 ETDRS letters (*P*=1.0, 95% CI 21.8, 22.3), and 17.4 ETDRS letters (*P*=0.478, 95% CI 7.7, 42.4) between the treatment and observation groups, respectively. Follow-up duration and age of patients were significant predictors of decreasing BCVA (*P*=0.048 and *P*=0.009, respectively). BCVA at baseline was not a significant predictor (*P*=0.593).

PED volume

After 24 months of follow-up, estimated means of PED volume increased by 0.13 mm^3 in the treatment group and decreased by 0.13 mm^3 in the observation group (Figure 3B). The change of PED volume from 6 to 24 months did not differ significantly between the groups (*P*=0.433, 95% CI 0.40, 0.91). After 6, 12, and 24 months of follow-up, differences in PED volume were 0.22 mm^3 (*P*=1.0, 95%

Table 1 Baseline characteristics of drusenoid aPEDs

	Treatment (n=4)					Observation (n=4)				
	Mean	**SD**	**Median**	**Min**	**Max**	**Mean**	**SD**	**Median**	**Min**	**Max**
Age, years	76.8	7.4	76	69	86	73.8	7.8	74	64	83
BCVA, ETDRS letters	65.0	7.0	65.0	58	72	66.8	6.5	70.0	57	70
PED										
Height, µm	279	106	284	160	387	345	53	338	298	406
Diameter, µm	2,657	1,124	2,243	1,848	4,293	2,275	258	2,276	2,012	2,535
Volume, mm^3	0.98	0.83	0.65	0.40	2.20	0.90	0.50	0.75	0.50	1.60
CRT, µm	218	3.7	219	213	222	199	12.7	204	180	208

Abbreviations: aPED, avascular pigment epithelium detachment; BCVA, best-corrected visual acuity; CRT, central retinal thickness; ETDRS, Early Treatment Diabetic Retinopathy Study; n, number of patients; PED, pigment epithelium detachment.

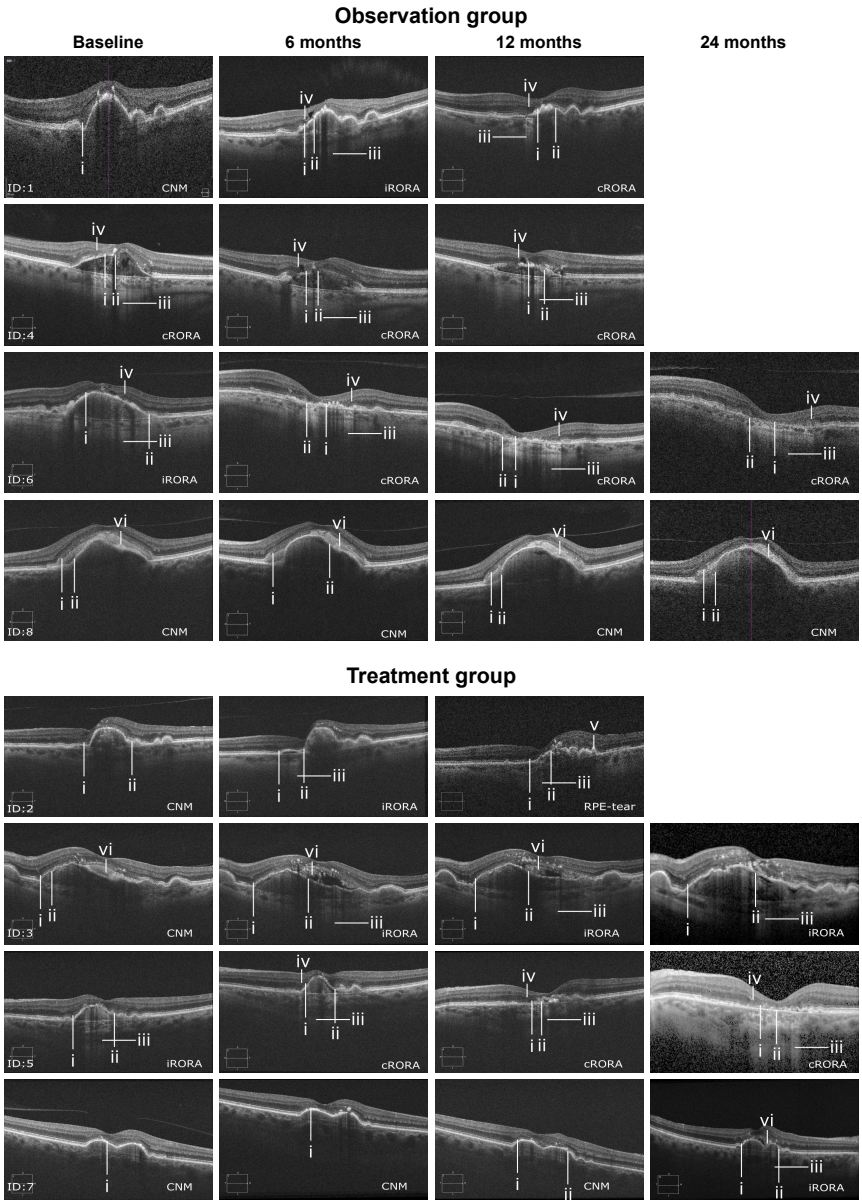

Figure 2 Grading of GA by OCT.
Notes: (i) Photoreceptor degeneration. (ii) Attenuation or disruption of RPE. (iii) Hypertransmission. (iv) Descending outer plexiform layer. (v) Scrolled up RPE. (vi) Subretinal drusenoid material.
Abbreviations: CNM, criteria for iRORA/cRORA not met; cRORA, complete RPE and outer retinal atrophy; ID, patient number; iRORA, incomplete RPE and outer retinal atrophy; RPE, retinal pigment epithelium; OCT, optical coherence tomography; GA, geographic atrophy.

CI 1.12, 1.56), 0.27 mm^3 (P=0.99, 95% CI 0.63, 1.17), and 0.48 mm^3 (P=0.487, 95% CI 0.22, 1.18) between the treatment and observation groups, respectively. Age of patients was a significant predictor of decreasing PED volume (P=0.043, 95% CI 0.07, 0.001). A larger baseline value significantly predicted a larger follow-up PED volume (P<0.001, 95% CI 1.53, 2.20). Follow-up duration was not a significant predictor (P=0.433).

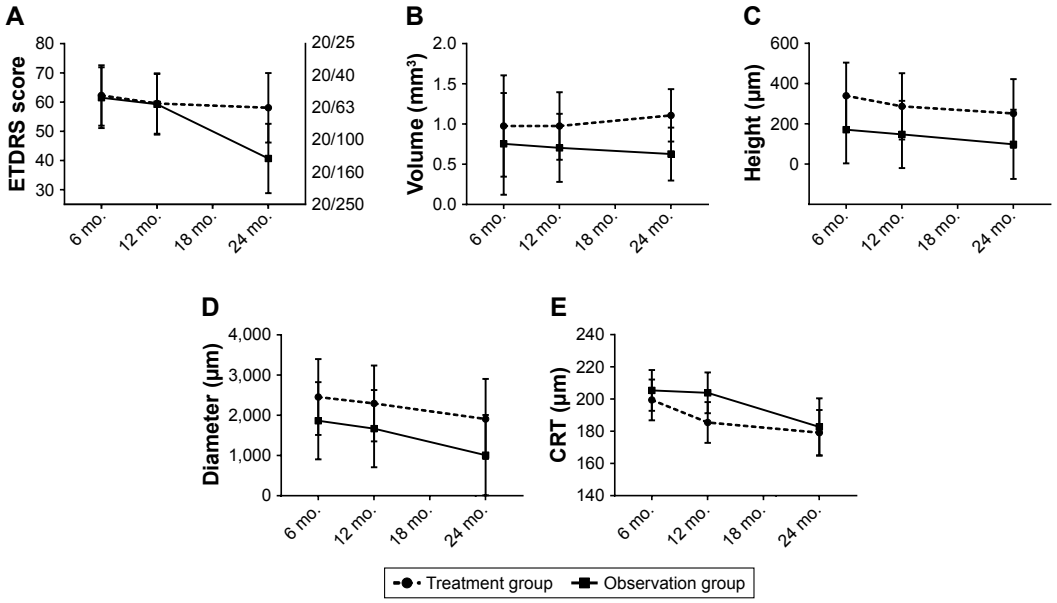

Figure 3 Estimated means of BCVA, PED volume, height and diameter, and CRT from 6 to 24 months.
Notes: (**A**) BCVA; the rightmost y-axis corresponds to Snellen equivalent. (**B**) PED volume. (**C**) PED height. (**D**) PED diameter. (**E**) CRT. The error bars represent 95% CIs (n=22 observations on eight patients).
Abbreviations: BCVA, best-corrected visual acuity; CRT, central retinal thickness; ETDRS, Early Treatment Diabetic Retinopathy Study; mo., months; PED, pigment epithelium detachment.

PED height

After 24 months of follow-up, estimated means of PED height decreased by 88.3 and 72.8 µm in the treatment and observation groups, respectively (Figure 3C). The change of PED height from 6 to 24 months did not differ significantly between the groups (P=0.842, 95% CI 168.6, 137.5). After 6, 12, and 24 months of follow-up, differences in PED height were 168.8 µm (P=0.949, 95% CI 199.7, 537.4), 139.6 µm (P=0.991, 95% CI 229.0, 508.1), and 153.3 µm (P=0.983, 95% CI 226.7, 533.2) between the treatment and observation groups, respectively. Age of patients, baseline PED height, and duration of follow-up were not significant predictors (P=0.483, P=0.075, and P=0.188, respectively).

PED diameter

After 24 months of follow-up, estimated means of PED diameter decreased by 544 and 856 µm in the treatment and observation groups, respectively (Figure 3D). The change of PED diameter from 6 to 24 months did not differ significantly between the groups (P=0.603, 95% CI 863, 1,487). After 6, 12, and 24 months of follow-up, differences in PED diameter were 589 µm (P=1.000, 95% CI 1,478, 2,655), 627 µm (P=0.99, 95% CI 1,440, 2,693), and 900 µm (P=0.976, 95% CI 1,247, 3,048) between the treatment and observation groups, respectively. Baseline diameter and duration of follow-up were significant predictors of decreasing PED diameter (P=0.022 and P=0.044, respectively). Age of patients was not a significant predictor (P=0.218).

Central retinal thickness

After 24 months of follow-up, estimated means of CRT decreased by 20.3 and 22.7 µm in the treatment and observation groups, respectively (Figure 3E). The change in CRT from 6 to 24 months did not differ significantly between the groups (P=0.852, 95% CI 22.8, 27.6). After 6, 12, and 24 months of follow-up, the differences in CRT were 5.9 µm (P=1.000, 95% CI 35.9, 24.0), 18.4 µm (P=0.671, 95% CI 48.4, 11.5), and 3.5 µm (P=1.000, 95% CI 40.8, 33.8) between the treatment and observation groups, respectively. Age of patients and duration of follow-up were significant predictors of decreasing CRT ($P<0.001$ and P=0.019, respectively). A larger baseline value significantly predicted a larger follow-up CRT ($P<0.001$).

Geographic atrophy

GA (defined as iRORA or cRORA) was present in 38%, 75%, 71%, and 86% of patients at baseline and at 6, 12, and 24 months follow-up in both groups combined (Figure 2). After 24 months of follow-up, two patients in the observation group and one patient in the treatment group progressed to cRORA. One patient had identifiable cRORA at baseline in the observation group. A decrease in PED volume was significantly associated with the development of cRORA (Fisher's exact test, P=0.029).

Safety outcomes

There were no cases of endophthalmitis or retinal detachment after the intravitreal injections. Two weeks after injection of triamcinolone acetonide, mean IOP was 13 mmHg (ranging from 11 to 16 mmHg). At baseline, 6 months, 12 months, and 24 months, mean IOP was 16, 15, 13, and 12 mmHg in the treatment group. One patient in the treatment group (Figure 2, ID: 2) was diagnosed with CNV after the first treatment with half-fluence PDT, and was subsequently treated with full-fluence PDT, which led to the development of an RPE tear.

Two patients in the treatment group and one patient in the observation group had an increase of nuclear sclerosis from grade 1 to grade 2 by the end of follow-up. One patient in the observation group (Figure 2, ID: 4) had cataract surgery between 12 and 24 months of follow-up, with no improvement of BCVA because of progression of GA to cRORA.

Discussion

In the present study, we originally set out to investigate the treatment of both serous and drusenoid aPEDs. However, the referred patients with serous PEDs were either excluded because of CNV or central serous chorioretinopathy. The higher risk of CNV in serous PEDs has previously been reported. In a retrospective study, 34% of serous and 9% of drusenoid PEDs developed CNV.[23] In two prospective studies, 32% of serous aPEDs developed CNV after a mean follow-up of 19.6 months,[24] and 23% of drusenoid aPEDs developed CNV over a 5-year period.[15]

Further inclusion and treatment of aPEDs were stopped after the interim analysis of 6 months data. Examination of OCT images showed that 75% of patients in our study were in different stages of GA formation and progression.[25] Treatment with anti-VEGF or PDT is not a viable treatment option for GA, and it is still unclear if the use of anti-VEGF agents increases its progression.[26] PDT has not been shown to directly damage the photoreceptors or RPE. However, PDT induces a selective occlusion of the choriocapillaris,[27] which in turn could lead to atrophy of RPE and photoreceptors.

BCVA decreased during follow-up with no significant differences between groups. The observation group had a greater, although insignificant, loss of ETDRS letters, probably due to the presence of cRORA in three of four patients. Duration of follow-up was a significant predictor of BCVA loss, and this indicates that this study mainly observed the natural course of drusenoid aPEDs. Our results differ from two prospective studies treating aPEDs with anti-VEGF agents, which resulted in stabilization or improvement of BCVA and no progression of GA or development of CNV.[16,17] The drusenoid aPEDs in our treatment group were larger (mean 0.98 mm^3) than in the study conducted by Ritter et al (mean 0.38 mm^3).[16] Large drusenoid aPEDs are probably a sign of more advanced AMD with worse prognosis. Interestingly, the two largest aPEDs in the present study did not progress to cRORA during follow-up, suggesting that PED volume is not the only risk factor for the progression of GA.

Drusenoid aPEDs are thought to be caused by the confluence of soft drusen over time,[5,7] which represents a risk factor for progression of GA or development of CNV.[8] In our study, progression of GA to cRORA was identified in 50% of patients, and development of cRORA was significantly associated with a reduction in PED volume. This is in line with the proposed lifecycle of drusenoid aPEDs with a growth and regression phase that ultimately leads to GA.[28,29] It has been proposed that an increased distance from the RPE to the choriocapillaris in drusenoid aPEDs has a negative impact on the RPE, leading to RPE atrophy and outer retinal atrophy.[30] This theory seems plausible as disruptions of the RPE layer and photoreceptors predominantly occur at the apex of drusenoid aPEDs, which is the point of greatest distance to the choriocapillaris.[28] A reduction in PED volume and distance between the choriocapillaris and RPE may improve the metabolism of the RPE and outer retina. However, a reduction in PED volume will probably only have a positive impact on the RPE and the outer retina if it occurs prior to the progression of GA to cRORA. Two studies on rheopheresis (extracorporeal plasma filtration) in the treatment of drusenoid aPEDs have shown interesting results with improvement of BCVA, a decrease of drusenoid PED volume, and a reduced number of patients with progression of GA or development of CNV.[31,32]

Future studies evaluating new treatment modalities for drusenoid aPEDs should probably aim to reduce PED volume, and assess with high-resolution OCT if the frequency of GA progression to cRORA is reduced.

Conclusion

Although limited by the low number of participants, the present study indicates that multitargeted, primarily antiangiogenic therapy does not favorably alter the natural course of large drusenoid aPEDs.

Abbreviations

Anti-VEGF, anti-vascular endothelial growth factor; aPED, avascular pigment epithelium detachment; BCVA, best-corrected visual acuity; CNV, choroidal neovascularization; cRORA, complete retinal and outer retina atrophy; CRT, central retinal thickness; ETDRS, Early Treatment Diabetic Retinopathy Study Group; FA, fluorescein angiography; FAF, fundus autofluoresence; GA, geographic atrophy; ICG, indocyanine green angiography; iRORA, incomplete retinal and outer retinal atrophy; nPED, neovascular pigment epithelium detachment; OCT, optical coherence tomography; PDT, photodynamic therapy.

Data sharing statement

The datasets used and analyzed during the current study are available from the corresponding author on request.

Acknowledgment

This project has been made possible by the Norwegian Extra-Foundation for Health and Rehabilitation (2016/FO80635). The sponsor had no involvement in any of the stages from study design to submission.

Disclosure

The authors report no conflicts of interest in this work.

References

1. Klein BE, Klein R. Cataracts and macular degeneration in older Americans. *Arch Ophthalmol*. 1982;100(4):571–573.
2. Solomon SD, Lindsley K, Vedula SS, Krzystolik MG, Hawkins BS. Anti-vascular endothelial growth factor for neovascular age-related macular degeneration. *Cochrane Database Syst Rev*. 2014;8:CD005139.
3. Bourne RR, Jonas JB, Flaxman SR, et al. Prevalence and causes of vision loss in high-income countries and in eastern and central Europe: 1990–2010. *Br J Ophthalmol*. 2014;98(5):629–638.
4. Schmidt-Erfurth U, Waldstein SM. A paradigm shift in imaging biomarkers in neovascular age-related macular degeneration. *Prog Retin Eye Res*. 2016;50:1–24.
5. Zayit-Soudry S, Moroz I, Loewenstein A. Retinal pigment epithelial detachment. *Surv Ophthalmol*. 2007;52(3):227–243.
6. Bird AC. Doyne lecture. Pathogenesis of retinal pigment epithelial detachment in the elderly; the relevance of Bruch's membrane change. *Eye (Lond)*. 1991;5(Pt 1):1–12.
7. Casswell AG, Kohen D, Bird AC. Retinal pigment epithelial detachments in the elderly: classification and outcome. *Br J Ophthalmol*. 1985; 69(6):397–403.
8. Roquet W, Roudot-Thoraval F, Coscas G, Soubrane G. Clinical features of drusenoid pigment epithelial detachment in age related macular degeneration. *Br J Ophthalmol*. 2004;88(5):638–642.
9. Lee DK, Kim SH, You YS, Kwon OW. High dose intravitreal bevacizumab for refractory pigment epithelial detachment in age-related macular degeneration. *Korean J Ophthalmol*. 2016;30(4):265–271.
10. Dirani A, Ambresin A, Marchionno L, Decugis D, Mantel I. Factors influencing the treatment response of pigment epithelium detachment in age-related macular degeneration. *Am J Ophthalmol*. 2015;160(4): 732–738.
11. Arora S, McKibbin M. One-year outcome after intravitreal ranibizumab for large, serous pigment epithelial detachment secondary to age-related macular degeneration. *Eye (Lond)*. 2011;25(8):1034–1038.
12. Baba T, Kitahashi M, Kubota-Taniai M, Oshitari T, Yamamoto S. Two-year course of subfoveal pigment epithelial detachment in eyes with age-related macular degeneration and visual acuity better than 20/40. *Ophthalmologica*. 2012;228(2):102–109.
13. Verteporfin in Photodynamic Therapy Study Group. Verteporfin therapy of subfoveal choroidal neovascularization in age-related macular degeneration: two-year results of a randomized clinical trial including lesions with occult with no classic choroidal neovascularization – verteporfin in photodynamic therapy report 2. *Am J Ophthalmol*. 2001;131(5):541–560.
14. Axer-Siegel R, Ehrlich R, Rosenblatt I, et al. Photodynamic therapy for occult choroidal neovascularization with pigment epithelium detachment in age-related macular degeneration. *Arch Ophthalmol*. 2004; 122(4):453–459.
15. Cukras C, Agrón E, Klein ML, et al. Natural history of drusenoid pigment epithelial detachment in age-related macular degeneration: age-related eye Disease Study report no 28. *Ophthalmology*. 2010;117(3): 489–499.
16. Ritter M, Bolz M, Sacu S, et al. Effect of intravitreal ranibizumab in avascular pigment epithelial detachment. *Eye (Lond)*. 2010;24(6):962–968.
17. Gallego-Pinazo R, Marina A, Suelves-Cogollos AM, et al. Intravitreal ranibizumab for symptomatic drusenoid pigment epithelial detachment without choroidal neovascularization in age-related macular degeneration. *Clin Ophthalmol*. 2011;5:161–165.
18. Krishnan R, Lochhead J. Regression of soft drusen and drusenoid pigment epithelial detachment following intravitreal anti-vascular endothelial growth factor therapy. *Can J Ophthalmol*. 2010;45(1):83–84.
19. Kim S, Oh J, Kim K. Morphologic changes in patient with drusen and drusenoid pigment epithelial detachment after intravitreal ranibizumab for choroidal neovascular membrane: a case report. *Open Ophthalmol J*. 2016;10:1–4.
20. Novais EA, Badaró E, Regatieri CV, Duker J, de Oliveira Bonomo PP. Regression of drusen after combined treatment using photodynamic therapy with verteporfin and ranibizumab. *Ophthalmic Surg Lasers Imaging Retina*. 2015;46(2):275–278.
21. Lee NY, Kim KS. Photodynamic therapy treatment for eyes with drusenoid pigment epithelium detachment. *Korean J Ophthalmol*. 2008; 22(3):194–196.
22. Sadda SR, Guymer R, Holz FG, et al. Consensus definition for atrophy associated with age-related macular degeneration on OCT: classification of atrophy report 3. *Ophthalmology*. 2018;125(4):537–548.
23. Hartnett ME, Weiter JJ, Garsd A, Jalkh AE. Classification of retinal pigment epithelial detachments associated with drusen. *Graefes Arch Clin Exp Ophthalmol*. 1992;230(1):11–19.
24. Elman MJ, Fine SL, Murphy RP, Patz A, Auer C. The natural history of serous retinal pigment epithelium detachment in patients with age-related macular degeneration. *Ophthalmology*. 1986;93(2):224–230.

25. Wu Z, Luu CD, Ayton LN, et al. Optical coherence tomography-defined changes preceding the development of drusen-associated atrophy in age-related macular degeneration. *Ophthalmology*. 2014;121(12):2415–2422.
26. Abdelfattah NS, Zhang H, Boyer DS, Sadda SR. Progression of macular atrophy in patients with neovascular age-related macular degeneration undergoing antivascular endothelial growth factor therapy. *Retina*. 2016;36(10):1843–1850.
27. Schlötzer-Schrehardt U, Viestenz A, Naumann GO, Laqua H, Michels S, Schmidt-Erfurth U. Dose-related structural effects of photodynamic therapy on choroidal and retinal structures of human eyes. *Graefes Arch Clin Exp Ophthalmol*. 2002;240(9):748–757.
28. Balaratnasingam C, Yannuzzi LA, Curcio CA, et al. Associations between retinal pigment epithelium and drusen volume changes during the lifecycle of large drusenoid pigment epithelial detachments. *Invest Ophthalmol Vis Sci*. 2016;57(13):5479–5489.
29. Schlanitz FG, Baumann B, Kundi M, et al. Drusen volume development over time and its relevance to the course of age-related macular degeneration. *Br J Ophthalmol*. 2017;101(2):198–203.
30. Mrejen S, Sarraf D, Mukkamala SK, Freund KB. Multimodal imaging of pigment epithelial detachment: a guide to evaluation. *Retina*. 2013;33(9):1735–1762.
31. Blaha M, Rencova E, Langrova H, et al. Rheohaemapheresis in the treatment of nonvascular age-related macular degeneration. *Atheroscler Suppl*. 2013;14(1):179–184.
32. Koss MJ, Kurz P, Tsobanelis T, et al. Prospective, randomized, controlled clinical study evaluating the efficacy of Rheopheresis for dry age-related macular degeneration. Dry AMD treatment with Rheopheresis Trial-ART. *Graefes Arch Clin Exp Ophthalmol*. 2009;247(10):1297–1306.

Paper II

Acta Ophthalmologica

Acta Ophthalmologica 2020

Drusenoid pigment epithelial detachment volume is associated with a decrease in best-corrected visual acuity and central retinal thickness: the Norwegian Pigment Epithelial Detachment Study (NORPED) report no. 1

Arnt-Ole Tvenning,[1,2] Jørgen Krohn,[3,4] Vegard Forsaa,[5] Agni Malmin,[5] Christian Hedels[6] and Dordi Austeng[1,2]

[1]Department of Ophthalmology, St. Olavs Hospital, Trondheim University Hospital, Trondheim, Norway
[2]Department of Neuromedicine and Movement Science, Norwegian University of Science and Technology, Trondheim, Norway
[3]Department of Clinical Medicine, Section of Ophthalmology, University of Bergen, Bergen, Norway
[4]Department of Ophthalmology, Haukeland University Hospital, Bergen, Norway
[5]Department of Ophthalmology, Stavanger University Hospital, Stavanger, Norway
[6]Hedels Eye Clinic, Kristiansund, Norway

ABSTRACT.

Purpose: **To investigate the association of drusenoid pigment epithelial detachment (DPED) volume and change in best-corrected visual acuity (BCVA) and central retinal thickness (CRT) during the growth phase of large DPEDs.**

Methods: **Patients from an ongoing prospective observational study, the Norwegian Pigment Epithelial Detachment Study (NORPED), with 1 year of follow-up and DPEDs ≥1000 μm in diameter, examined with the Heidelberg Spectralis HRA-OCT were included. Patients with DPEDs in the regression phase were excluded. Multicolour, near-infrared reflectance, optical coherence tomography (OCT) and OCT angiography images were obtained every 6 months. Fluorescein angiography and indocyanine green angiography were performed at baseline and yearly to exclude choroidal neovascularization (CNV).**

Results: **Forty-four patients and 66 eyes were included. In the statistical model for BCVA, every 1.0 mm^3 increase in DPED volume led to a decrease in BCVA of 4.0 ETDRS letters (95% CI, −7.0 to −1.0, p = 0.008). A decrease in BCVA was significantly associated with older patient age, the presence of acquired vitelliform lesions and subfoveal location of the DPEDs. In the model for CRT, every 1.0 mm^3 increase in DPED volume led to a decrease in CRT of 26.7 μm (95% CI, −44.4 to −9.0, p = 0.003). Two eyes had progression of geographic atrophy and none developed CNV.**

Conclusion: **The increasing volume of DPEDs during the growth phase is associated with a decrease in BCVA and CRT. The subfoveal location of DPEDs and the presence of acquired vitelliform lesions appear to be associated with a further reduction in BCVA.**

Key words: age-related macular degeneration – best-corrected visual acuity – central retinal thickness – drusenoid pigment epithelial detachment – geographic atrophy – natural history

Acta Ophthalmol.

doi: 10.1111/aos.14423

Introduction

Drusen and retinal pigment epithelium (RPE) abnormalities are the defining features of age-related macular degeneration (AMD) (Bird et al. 1995). The extent of drusen and RPE abnormalities identified on colour fundus photography is a known risk factor for progression to late AMD with choroidal neovascularization (CNV) and geographic atrophy (Gass 1972; Ferris et al. 2013; Chew et al. 2014). Drusenoid pigment epithelial detachment (DPED) is thought to result from the confluence of large drusen and in part by the formation of a hydrophobic barrier in Bruch's membrane resulting in the accumulation of fluid (Casswell et al. 1985; Roquet et al. 2004). Previous retrospective studies have observed that DPEDs could persist, regress with or without the development of geographic atrophy, or develop CNV (Hartnett et al. 1992; Roquet et al. 2004; Alexandre de Amorim Garcia Filho et al. 2013). Other studies of the natural history of eyes with DPED have shown high rates of progression to geographic atrophy, CNV and vision loss (Cukras et al. 2010; Yu et al. 2019). DPEDs are usually located

in the foveal region and associated with a loss of best-corrected visual acuity (BCVA), with or without progression to central geographic atrophy (Cukras et al. 2010; Balaratnasingam et al. 2016b; Yu et al. 2019). DPEDs typically have an initial growth phase followed by a regression phase with progressive outer retinal atrophy on optical coherence tomography (OCT), ultimately leading to complete RPE and outer retinal atrophy (cRORA) (Balaratnasingam et al. 2016b; Sadda et al. 2018). During the last years, several risk factors for the progression of geographic atrophy have been identified. Drusen disrupt the integrity of the photoreceptor layer on OCT (Hartmann et al. 2012), which has been shown to be thinner on top of the drusen (Schuman et al. 2009; Sadigh et al. 2013). Intraretinal hyperreflective foci, loss of RPE and outer photoreceptor segments, increasing DPED volume and abnormal DPED thinning on OCT are associated with progression of geographic atrophy on colour fundus photography (Sleiman et al. 2017). Subretinal drusenoid deposits on OCT are independent risk factors for loss of visual function both with and without associated geographic atrophy and CNV (Garg et al. 2013).

To our knowledge, the present study is the first prospective observational study of DPEDs. In this report, we have investigated which OCT features that could predict a change in BCVA and central retinal thickness (CRT) during the growth phase of DPEDs. We hypothesized, as previously suggested by Mrejen et al. (2013), that the larger the DPED volume the greater the distance from the RPE to the choriocapillaris, resulting in reduced microvascular support and subsequent progressive outer retinal atrophy with a decrease in BCVA and CRT.

Material and Methods

This is the first study report on the 1-year results from an ongoing prospective, observational, multicentre study, the Norwegian Pigment Epithelial Detachment Study (NORPED). The patients were included from March 2016 to December 2017, and the planned follow-up period is 5 years. Ophthalmologists in central and western Norway referred patients with DPEDs to the University Hospitals of Trondheim, Bergen and Stavanger. The research study was approved by the Regional Committee for Medical and Health Research Ethics Central Norway (2012/1743) and followed the tenets of the Declaration of Helsinki. Written informed consent was obtained from the study participants after explanation of the nature and possible consequences of the study.

Only patients examined with the Spectralis HRA-OCT (Heidelberg Engineering GmbH, Heidelberg, Germany) were included in this report. Other inclusion criteria were age of ≥50 years, DPED with a diameter ≥1000 μm and BCVA ≥20/400. Exclusion criteria were previous vitrectomy, corticosteroid therapy, intravitreal anti-vascular endothelial growth factor injections and photodynamic therapy. Eyes with subfoveal fibrosis, central geographic atrophy, CNV on fluorescein angiography (FA) or indocyanine green angiography (ICGA), glaucoma with central visual field defects, diabetic macular oedema, proliferative diabetic retinopathy and uveitis were also excluded.

Patients with a pigment epithelial detachment that appeared yellow on clinical fundus examination, with predominantly hyperreflective contents on OCT, staining on FA and hypofluorescence on ICGA were diagnosed with DPED (Casswell et al. 1985; Arnold et al. 1997). Patients with subretinal fluid and intraretinal cysts were not excluded if FA and ICGA did not exhibit features of CNV. Baseline FA and ICGA images were pseudonymized and sent to an external reading centre to ensure a correct diagnosis of avascular DPED. Eyes with leakage on FA and 'hotspots' or 'plaques' on ICGA were diagnosed with CNV. Central geographic atrophy was defined as a well-demarcated circular lesion with visible choroidal vasculature, early hyperfluorescence on FA and ICGA, and ≥250 μm in size measured on OCT with foveal involvement.

Patients were examined by slit-lamp biomicroscopy and multimodal imaging at baseline, 6 and 12 months. The multimodal imaging was performed with the Spectralis HRA-OCT and consisted of FA, ICGA, near-infrared reflectance imaging, multicolour imaging, fundus autofluorescence imaging and OCT. Macular cube scans were acquired with the follow-up mode, and a dense scan pattern of 49 scans with eye-tracking enabled. Each line of the macular cube scans consisted of 18–30 averaged images recorded with the automatic real-time function. High definition line scans centred on the fovea with 100 averaged images were also obtained. OCT angiography (OCTA) was performed at every study visit with the Cirrus HD-OCT (Carl Zeiss Meditec AG, Jena, Germany) (Fig. 1). FA and ICGA were done at baseline and after 12 months and if CNV was suspected.

BCVA was measured with an Early Treatment Diabetic Retinopathy Study (ETDRS) chart in an illuminated cabinet (ESV3000; Good-Lite, Elgin, IL, USA) at 4 m. The cabinet automatically adjusts lighting to 85 cd/m^2. Room lighting was dimmed so that 100−110 Lux could be measured directly in front of the cabinet. The refraction was measured at baseline and yearly by the investigating physician.

Volumetric measurements of the DPEDs and intraretinal hyperreflective foci were done with a semi-automatic segmentation program (ReV Analyzer version 3.0.5; ADCIS SA, Saint-Contest, France). The DPEDs and intraretinal hyperreflective foci were in each OCT scan manually delineated, which enabled automatic calculation of their volumes. Intraretinal hyperreflective foci were defined as hyperreflective areas in the retina above the ellipsoid zone on OCT (Fig. 2A). The calliper available in the viewing software of the Spectralis HRA-OCT (Spectralis Viewing Module version 6.0.9.0; Heidelberg Engineering GmbH, Heidelberg, Germany) was used to measure subfoveal DPED height, diameter and CRT. The three centremost scans, centred in the middle of fovea guided by OCT, were used for measurements, and the mean was used for statistical analysis. The fovea was defined as the innermost guiding circle (712 μm in diameter) of the ETDRS grid, available in the Spectralis Viewing Module, centred in the middle of the fovea guided by OCT. The DPEDs were classified as subfoveal if their location were within this circle. CRT was measured from the

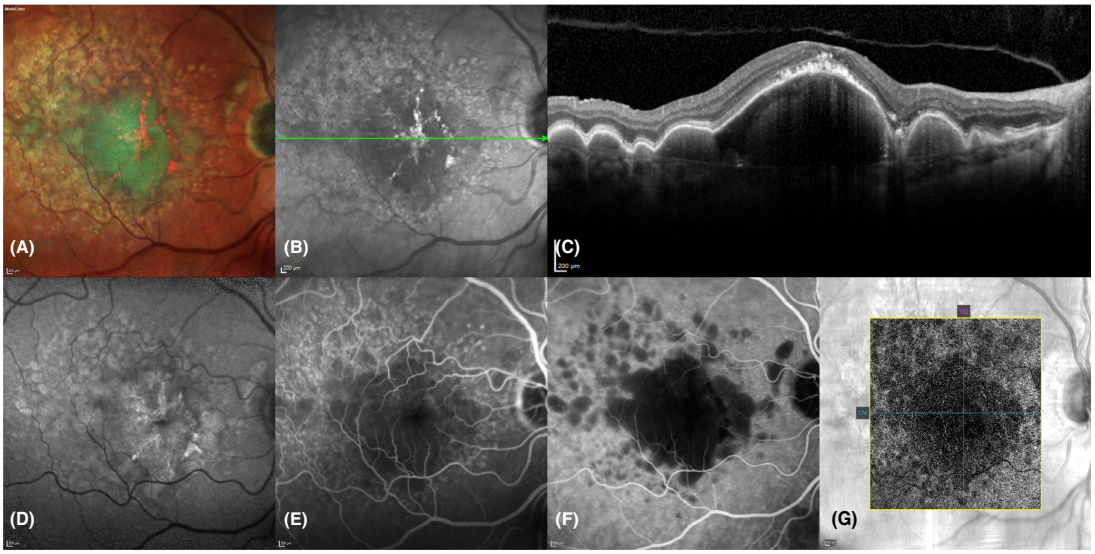

Fig. 1. Multimodal imaging of a drusenoid pigment epithelial detachment. (A) Multicolour image. (B) Near-infrared reflectance image. (C) Optical coherence tomography scan. (D) Fundus autofluorescence image. (E) Fluorescein angiography image. (F) Indocyanine green angiography image. (G) Optical coherence tomography angiography scan. Scale bar = 200 μm.

internal limiting membrane to, but not including, the RPE. Subfoveal thickening of the RPE, subretinal fluid and acquired vitelliform lesions were not included in the measurements. DPED height was measured from the RPE to Bruch's membrane. During measurement, the OCT images were magnified 400−800% in the 1:1 μm format.

Subretinal drusenoid deposits (Fig. 2D) were present if there were ≥5 subretinal deposits in >1 OCT scan identified on OCT as previously described by Zweifel et al. (2010). Acquired vitelliform lesions were defined as present if there was foveal subretinal hyperreflective material on OCT (Fig. 2A). Foveal thickening of the RPE (Fig. 2B) was defined on OCT as thickened RPE, with shadowing of the sub-RPE structures, also visible as hyperreflective areas on near-infrared reflectance images.

Grading of atrophy on OCT was done as described by the Classification of Atrophy Meeting consensus group (Sadda et al. 2018; Guymer et al. 2020). cRORA (Fig. 2D); (1) region of hypertransmission of at least 250 μm in diameter in any lateral dimension, (2) zone of attenuation or disruption of the RPE of at least 250 μm in diameter and (3) evidence of overlying photoreceptor degeneration. Complete outer retinal atrophy (cORA) (Fig. 2C); evidence of photoreceptor degeneration, but with intact or discontinuous RPE. Features of photoreceptor degeneration included all of the following: loss of interdigitation zone, ellipsoid zone, and external limiting membrane, and thinning of the outer nuclear layer, which also could be identified by a descending outer plexiform layer. Incomplete RPE and outer retinal atrophy (iRORA) (Fig. 2B); the criteria for cRORA were not met, but there was hypertransmission <250 μm in diameter and the RPE-line was discontinuous with evidence of photoreceptor degeneration.

Statistical analysis

Descriptive statistics and linear mixed models were used for statistical analysis. In the linear mixed model, eyes of patients were nested within patients with repeated measurements to account for the correlated eye data (Ying et al. 2017). Restricted maximum likelihood estimation was used for the calculation of fixed effects. R^2 statistics were calculated by running the full models and models including only DPED volume, diameter and height with restricted maximum likelihood estimation. The variance of the fixed effects was calculated after predicting fitted values based on the fixed effects alone. As described by Nakagawa and Schielzeth, R^2 for the fixed effect(s) and for the full model including random effects were calculated and named R^2 marginal and R^2 conditional, respectively (Nakagawa & Schielzeth 2013). The residuals were visually inspected regarding normal distribution with histograms and Q–Q plots. In the building of the statistical models, only observations in the growth phase of the DPED life cycle were included. The DPEDs were determined to be in the regression phase if the DPED volume decreased and atrophy progressed after 6−12 months of follow-up. Three of 188 observations were excluded due to the regression of DPED volume and foveal cRORA or cORA. Predictors with a p-value ≥0.05 were excluded from the statistical models unless the exclusion worsened model fit. The model fit was evaluated with Akaike's information criterion (Akaike 1974). The primary statistical models had DPED volume as the measurement unit of DPED size. However, secondary analyses of foveal DPED diameter and height

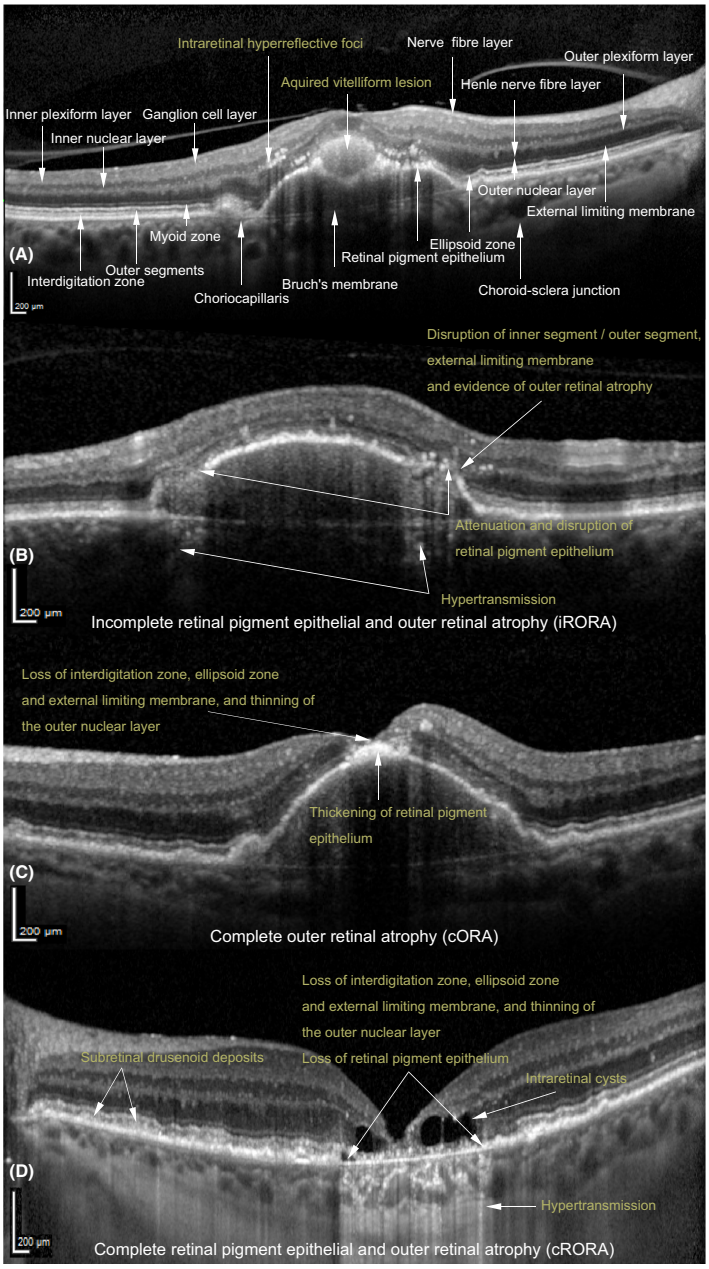

Fig. 2. Pathological findings and classification of atrophy in drusenoid pigment epithelial detachments on optical coherence tomography scans. (A) Retinal layers, intraretinal hyperreflective foci and acquired vitelliform lesion. (B) Incomplete retinal pigment epithelial and outer retinal atrophy (iRORA). (C) Complete outer retinal atrophy (cORA) and thickening of retinal pigment epithelium. (D) Complete retinal pigment epithelial and outer retinal atrophy (cRORA), intraretinal cysts and subretinal drusenoid deposits. Scale bar = 200 µm.

were also performed as these parameters were readily available and considered clinically relevant. STATA 15.1 (StataCorp LLC, College Station, TX, USA) was used for statistical analysis.

Results

A total of 66 eyes from 44 patients were included in the study. Four eyes (6%) in three patients (7%) were lost to follow-up. One patient died, another was diagnosed with dementia, and the last patient did not want further follow-up. One observation at 6 months was missing because the OCT image could not be found in the database. In two eyes (3%), we observed regression of the DPED and development of geographic atrophy, where one progressed to foveal cORA and the other to cRORA. There was no foveal iRORA, cORA or cRORA at baseline. Three eyes (5%) had extrafoveal iRORA at baseline, which increased to six (10%) at 12 months. None of the eyes developed CNV. Baseline patient and OCT characteristics are summarized in Tables 1 and 2, respectively.

Best-corrected visual acuity and drusenoid pigment epithelial detachment volume

In the linear mixed model, each 1.0 mm^3 increase in DPED volume led to a decrease in BCVA of 4.0 ETDRS letters (95% CI, −7.0 to −1.0, p = 0.008) (Fig. 3A), and every patient-year led to a decrease in BCVA of 0.4 ETDRS letters (95% CI, −0.6 to −0.2, p < 0.001). The presence of acquired vitelliform lesions reduced BCVA by 5.6 ETDRS letters (95% CI, −8.1 to −3.1, p < 0.001), and subfoveal location of the DPEDs

Table 1. Baseline patient characteristics (*n* = 44 patients).

		Range
Age, years, mean (SD)	72.6 (7.5)	54.9–87.5
BCVA, ETDRS letters, mean (SD)	76.8 (7.5)	58.0–93.0
Metamorphopsia, *n* (%)	9 (21)	
Pseudophakia, *n* (%)	9 (21)	
Female sex, *n* (%)	33 (75)	
Diabetes mellitus, *n* (%)	2 (5)	
Hypertension, *n* (%)	18 (42)	
Hypercholesterolaemia, *n* (%)	11 (26)	
History of smoking, *n* (%)	24 (56)	
Cardiovascular disease, *n* (%)	7 (16)	

BCVA = best-corrected visual acuity, ETDRS = Early Treatment Diabetic Retinopathy Study, *n* = number; SD = standard deviation.

Table 2. Baseline optical coherence tomography characteristics (n = 66 eyes).

		Range
DPED volume, mm^3, median (IQR)	0.24 (0.40)	0.01–2.40
HRF volume, mm^3, median (IQR)	0.001 (0.04)	0–0.051
Subfoveal DPED height, µm, median (IQR)	134 (102)	13–531
Subfoveal DPED diameter, µm, mean(SD)	1929 (853)	129–3932
Central retinal thickness, µm, median (IQR)	158 (60)	49–280
Subfoveal DPED, n (%)	62 (94)	
HRF, n (%)	56 (85)	
Interruption of ellipsoid zone, n (%)	52 (79)	
Subretinal drusenoid deposits, n (%)	42 (64)	
Subfoveal thickening of the RPE, n (%)	27 (41)	
Aquired vitelliform lesion, n (%)	18 (27)	
Subretinal fluid, n (%)	7 (11)	
Intraretinal cysts, n (%)	6 (9)	

DPED = drusenoid pigment epithelial detachment, HRF = intraretinal hyperreflective foci, IQR = interquartile range, n = number of eyes, RPE = retinal pigment epithelium, SD = standard deviation.

reduced BCVA by 5.5 ETDRS letters (95% CI, −10.6 to −0.3, p = 0.036). Follow-up duration, the presence of subretinal drusenoid deposits, foveal subretinal fluid and intraretinal cysts, and the volume of hyperreflective foci were not significant predictors of BCVA. The proportion of the variance in BCVA predicted by the fixed effects in the model was 0.40 (R^2 marginal) and by the full model 0.83 (R^2 conditional).

Best-corrected visual acuity and foveal drusenoid pigment epithelial detachment diameter

In the linear mixed model, each 1000 µm increase in foveal DPED diameter led to a decrease in BCVA of 2.1 ETDRS letters (95% CI, −3.5 to −0.6, p = 0.005) (Fig. 3B), and every patient-year led to a decrease in BCVA of 0.4 ETDRS letters (95% CI, −0.6 to −0.1, p = 0.003). The presence of acquired vitelliform lesions reduced BCVA by 5.6 ETDRS letters (95% CI, −8.2 to −3.1, p < 0.001), whereas the presence of subretinal drusenoid deposits increased BCVA by 3.5 ETDRS letters (95% CI, 0.4 to 6.6, p = 0.027). Follow-up duration, the presence of foveal subretinal fluid and intraretinal cysts, and the volume of hyperreflective foci were not significant predictors of BCVA. R^2 marginal and R^2 conditional were 0.35 and 0.84, respectively.

Best-corrected visual acuity and foveal drusenoid pigment epithelial detachment height

In the linear mixed model, each 100 µm increase in foveal DPED height led to a decrease in BCVA of 1.8 ETDRS letters (95% CI, −3.0 to −0.5, p = 0.005) (Fig. 3C), and every patient-year led to a decrease in BCVA of 0.3 ETDRS letters (95% CI, −0.6 to −0.1, p = 0.005). The presence of acquired vitelliform lesions reduced BCVA by 6.1 ETDRS letters (95% CI, −8.6 to −3.6, p < 0.001). Follow-up duration, the presence of subretinal drusenoid deposits, foveal subretinal fluid and intraretinal cysts, and the volume of hyperreflective foci were not significant predictors of BCVA. R^2 marginal and R^2 conditional were 0.36 and 0.82, respectively.

Central retinal thickness and drusenoid pigment epithelial detachment volume

In the linear mixed model, each 1.0 mm^3 increase in DPED volume led to a decrease in CRT of 26.7 µm (95% CI, −44.4 to −9.0, p = 0.003) (Fig. 4A). Patient age, subfoveal location of the DPEDs, follow-up duration, the presence of acquired vitelliform lesions, subretinal drusenoid deposits, foveal subretinal fluid and intraretinal cysts, and the volume of hyperreflective foci were not significant predictors of CRT. R^2 marginal and R^2 conditional were 0.10 and 0.95, respectively.

Central retinal thickness and foveal drusenoid pigment epithelial detachment diameter

In the linear mixed model, each 1000 µm increase in foveal DPED diameter led to a decrease in CRT of 13.1 µm (95% CI, −19.5 to −6.6, p < 0.001) (Fig. 4B), and the presence of subretinal fluid in the fovea led to an increase in CRT of 8.8 µm (95% CI, 0.4 to 17.3, p = 0.042). Patient age, subfoveal location of the DPEDs, follow-up duration, the presence of acquired vitelliform lesions, subretinal drusenoid deposits and intraretinal cysts, and the volume of hyperreflective foci were not significant predictors of

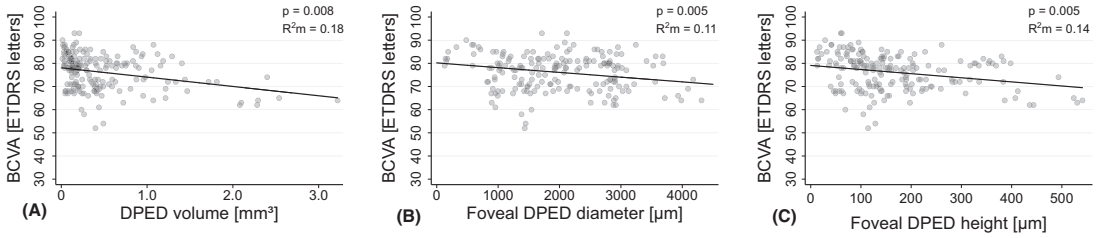

Fig. 3. The associated decrease in best-corrected visual acuity (BCVA) with increasing drusenoid pigment epithelial detachment (DPED) volume, foveal diameter and height. (A) BCVA and DPED volume. (B) BCVA and foveal DPED diameter. (C) BCVA and foveal DPED height. Statistical analysis; linear mixed models. The lines represent linear predictions. Scatter plots of BCVA and DPED volume, diameter and height. The marginal coefficient of determination (R^2m) is the proportion of the variance in BCVA predicted by the fixed effects of DPED volume, diameter and height. N = 185 observations, 66 eyes and 44 patients. A p-value <0.05 was considered statistically significant.

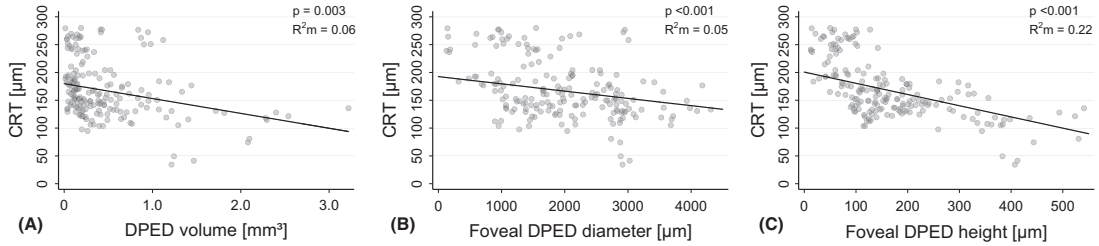

Fig. 4. The associated decrease in central retinal thickness (CRT) with increasing drusenoid pigment epithelial detachment (DPED) volume, foveal diameter and height. (A) CRT and DPED volume. (B) CRT and foveal DPED diameter. (C) CRT and foveal DPED height. Statistical analysis; linear mixed models. The lines represent linear predictions. Scatter plots of CRT and DPED volume, diameter and height. The marginal coefficient of determination (R^2m) is the proportion of the variance in CRT predicted by the fixed effects of DPED volume, diameter and height. $N = 185$ observations, 66 eyes and 44 patients. A p-value <0.05 was considered statistically significant.

CRT. R^2 marginal and R^2 conditional were 0.08 and 0.95, respectively.

Central retinal thickness and foveal drusenoid pigment epithelial detachment height

In the linear mixed model, each 100 µm increase in foveal DPED height led to a decrease in CRT of 20.2 µm (95% CI, −26.6 to −13.7, $p < 0.001$) (Fig. 4C). Patient age, subfoveal location of the DPEDs, follow-up duration, the presence of acquired vitelliform lesions, subretinal drusenoid deposits, foveal subretinal fluid and intraretinal cysts, and the volume of hyperreflective foci were not significant predictors of CRT. R^2 marginal and R^2 conditional were 0.23 and 0.95, respectively.

Discussion

This is the first prospective observational study of DPEDs examined with multimodal imaging including OCT. The main findings of this study are that the increasing volume of DPEDs during their growth phase is associated with a reduction in both BCVA and CRT. Further analysis showed that the increasing foveal DPED diameter and height had a similar effect on BCVA and CRT.

The natural history of large DPEDs is typically characterized by a growth phase, followed by a regression phase leading to geographic atrophy (Balaratnasingam et al. 2016b). The observations from our study suggest that within 1 year, there is progressive atrophy and a reduction in visual function in the majority of eyes with DPEDs during the growth phase. These findings support the hypothesis that the RPE function decreases over time as a consequence of the long-term separation from the underlying choriocapillaris, leading to RPE atrophy and photoreceptor loss (Mrejen et al. 2013). In a previous study, it has also been observed that retinal atrophy is associated with DPEDs, as patients with DPED and poor visual acuity at baseline had focal foveal atrophy within the DPED (Roquet et al. 2004). The association between decreasing BCVA and increasing DPED volume is in part supported by the retrospective DPED cohort studies of the Age-Related Eye Disease Study (AREDS) Research Group, where a decline in visual function was observed in eyes not progressing to late AMD (Cukras et al. 2010; Yu et al. 2019). In the study by Yu et al., there was a 26% estimated proportion of patients without progression to late AMD who would lose ≥15 ETDRS letters, and in the study by Cukras et al., patients not progressing to late AMD lost eight ETDRS letters over 5 years (Cukras et al. 2010; Yu et al. 2019). These studies used stereoscopic colour fundus photography to assess late AMD, and some of the DPEDs may thus have been in the regression phase, explaining the vision loss. A study that used OCT to retrospectively measure DPED height, diameter and volume in 21 eyes, found that maximum DPED size was inversely correlated with final visual acuity. However, the final visual acuity measurements in this study were performed during the regression phase of the DPEDs (Balaratnasingam et al. 2016b). A cross-sectional study evaluating macular function in patients with DPED found a reduction in visual acuity, microperimetry sensitivity and multifocal electroretinography responses in patients with DPEDs compared to healthy controls (Ogino et al. 2014), and our results support these findings.

There was an association between decreasing CRT and increasing DPED volume, which is plausible as there is a gradual progression of geographic atrophy related to the DPED life cycle. Previous natural history studies of DPEDs have not reported CRT changes when evaluating the progression of geographic atrophy. However, a few studies based on stereoscopic fundus photography have shown that the presence of DPEDs and increasing DPED area are significant risk factors for the development of geographic atrophy (Cukras et al. 2010; Yu et al. 2019).

The occurrence of acquired vitelliform lesions on top of the DPEDs was in the present study associated with an additional reduction in BCVA. This finding is in part supported by a retrospective study where patients with both AMD and acquired vitelliform lesions had a higher risk of foveal geographic atrophy and a decline in BCVA compared to those with only adult-onset foveomacular dystrophy (Balaratnasingam et al. 2016a). The vitelliform lesions are thought to arise from defective phagocytosis of the RPE, resulting in the accumulation of outer segment debris and RPE organelles, and can be considered as a marker of maximal RPE disturbance with a focal loss of photoreceptors (Arnold et al. 2003; Chen et al. 2016; Balaratnasingam et al. 2017).

The results of our study suggest that the subfoveal location of the DPEDs is unfavourable for visual function. Even though the majority of DPEDs were located in the fovea (94%), the few perifoveal located DPEDs had markedly better BCVA, which demonstrates the negative impact of DPED volume on the foveal outer retina.

The presence of intraretinal hyperreflective foci is a known risk factor for the progression to late AMD (Nassisi et al. 2018). Interestingly, we did not find that increasing volume of intraretinal hyperreflective foci predicted a change in BCVA or CRT. On the other hand, intraretinal hyperreflective foci are probably a late manifestation of the disease. The DPEDs in this report have only 1 year of follow-up, and the DPEDs in the regression phase were excluded from the statistical models, which may explain why we were unable to document such an association.

DPED is a well-known risk factor for the development of CNV (Cukras et al. 2010; Yu et al. 2019). However, none of our patients developed CNV during the first year. This may be due to the relatively short follow-up and the exclusion of patients with CNV based on several types of angiography at baseline.

The strength of this study is its prospective design, the use of multimodal imaging and a low loss to follow-up. The number of eyes included was fairly large, considering the asymptomatic nature of intermediate AMD and the rarity of large DPEDs. Only 3% of the patients in the AREDS study had DPED at baseline (Cukras et al. 2010). The patients were also thoroughly investigated with FA, ICGA and OCTA to exclude patients with CNV. Subtle type 1 CNV could still have been missed since 11% and 9% of the eyes at baseline had sub- and intraretinal fluid, respectively. Limitations of the study include the absence of a control group of AMD patients without DPED and the lack of blinding of the study investigator when measuring the primary outcomes. Another limitation and future direction is the possibility to measure the rod-mediated dark adaptation function. Rod-mediated vision is affected earlier and more severely with progression of AMD, especially in the presence of subretinal drusenoid deposits (Chen et al. 2019).

In conclusion, this study has shown that increasing DPED volume and foveal DPED diameter and height are associated with a reduction of BCVA and CRT during the growth phase of DPEDs. The subfoveal location of DPEDs and the presence of acquired vitelliform lesions appear to be associated with a further reduction in BCVA.

References

Akaike H (1974): A new look at the statistical model identification. IEEE Trans Automat Contr **19**: 716–723.

Alexandre de Amorim Garcia Filho C, Yehoshua Z, Gregori G, Farah ME, Feuer W & Rosenfeld PJ (2013): Spectral-domain optical coherence tomography imaging of drusenoid pigment epithelial detachments. Retina **33**: 1558–1566.

Arnold JJ, Quaranta M, Soubrane G, Sarks SH & Coscas G (1997): Indocyanine green angiography of drusen. Am J Ophthalmol **124**: 344–356.

Arnold JJ, Sarks JP, Killingsworth MC, Kettle EK & Sarks SH (2003): Adult vitelliform macular degeneration: a clinicopathological study. Eye (Lond) **17**: 717–726.

Balaratnasingam C, Hoang QV, Inoue M et al. (2016a): Clinical characteristics, choroidal neovascularization, and predictors of visual outcomes in acquired vitelliform lesions. Am J Ophthalmol **172**: 28–38.

Balaratnasingam C, Yannuzzi LA, Curcio CA et al. (2016b): Associations between retinal pigment epithelium and drusen volume changes during the lifecycle of large drusenoid pigment epithelial detachments. Invest Ophthalmol Vis Sci **57**: 5479–5489.

Balaratnasingam C, Messinger JD, Sloan KR, Yannuzzi LA, Freund KB & Curcio CA (2017): Histologic and optical coherence tomographic correlates in drusenoid pigment epithelium detachment in age-related macular degeneration. Ophthalmology **124**: 644–656.

Bird AC, Bressler NM, Bressler SB et al. (1995): An international classification and grading system for age-related maculopathy and age-related macular degeneration. The International ARM Epidemiological Study Group. Surv Ophthalmol **39**: 367–374.

Casswell AG, Kohen D & Bird AC (1985): Retinal pigment epithelial detachments in the elderly: classification and outcome. Br J Ophthalmol **69**: 397–403.

Chen KC, Jung JJ, Curcio CA, Balaratnasingam C, Gallego-Pinazo R, Dolz-Marco R, Freund KB & Yannuzzi LA (2016): Intraretinal hyperreflective foci in acquired vitelliform lesions of the macula: clinical and histologic study. Am J Ophthalmol **164**: 89–98.

Chen KG, Alvarez JA, Yazdanie M et al. (2019): Longitudinal study of dark adaptation as a functional outcome measure for age-related macular degeneration. Ophthalmology **126**: 856–865.

Chew EY, Clemons TE, Agron E, Sperduto RD, Sangiovanni JP, Davis MD & Ferris FL (2014): Ten-year follow-up of age-related macular degeneration in the age-related eye disease study: AREDS report no. 36. JAMA Ophthalmol **132**: 272–277.

Cukras C, Agrón E, Klein ML, Ferris FL, Chew EY, Gensler G & Wong WT, Age-Related Eye Disease Study Research Group (2010): Natural history of drusenoid pigment epithelial detachment in age-related macular degeneration: age-related eye disease study report no. 28. Ophthalmology **117**: 489–499.

Ferris FL, Wilkinson CP, Bird A, Chakravarthy U, Chew E, Csaky K & Sadda SR (2013): Clinical classification of age-related macular degeneration. Ophthalmology **120**: 844–851.

Garg A, Oll M, Yzer S, Chang S, Barile GR, Merriam JC, Tsang SH & Bearelly S (2013): Reticular pseudodrusen in early age-related macular degeneration are associated with choroidal thinning. Invest Ophthalmol Vis Sci **54**: 7075–7081.

Gass JD (1972): Drusen and disciform macular detachment and degeneration. Trans Am Ophthalmol Soc **70**: 409–436.

Guymer RH, Rosenfeld PJ, Curcio CA et al. (2020): Incomplete retinal pigment epithelial and outer retinal atrophy in age-related macular degeneration: classification of atrophy meeting report 4. Ophthalmology **127**: 394–409.

Hartmann KI, Gomez ML, Bartsch DU, Schuster AK & Freeman WR (2012): Effect of change in drusen evolution on photoreceptor inner segment/outer segment junction. Retina **32**: 1492–1499.

Hartnett ME, Weiter JJ, Garsd A & Jalkh AE (1992): Classification of retinal pigment epithelial detachments associated with drusen. Graefes Arch Clin Exp Ophthalmol **230**: 11–19.

Mrejen S, Sarraf D, Mukkamala SK & Freund KB (2013): Multimodal imaging of pigment epithelial detachment: a guide to evaluation. Retina **33**: 1735–1762.

Nakagawa S & Schielzeth H (2013): A general and simple method for obtaining R^2 from generalized linear mixed-effects models. Methods Ecol Evol **4**: 133–142.

Nassisi M, Fan W, Shi Y, Lei J, Borrelli E, Ip M & Sadda SR (2018): Quantity of intraretinal hyperreflective foci in patients with intermediate age-related macular degeneration correlates with 1-year progression. Invest Ophthalmol Vis Sci **59**: 3431–3439.

Ogino K, Tsujikawa A, Yamashiro K et al. (2014): Multimodal evaluation of macular function in age-related macular degeneration. Jpn J Ophthalmol **58**: 155–165.

Roquet W, Roudot-Thoraval F, Coscas G & Soubrane G (2004): Clinical features of drusenoid pigment epithelial detachment in age related macular degeneration. Br J Ophthalmol **88**: 638–642.

Sadda SR, Guymer R, Holz FG et al. (2018): Consensus definition for atrophy associated with age-related macular degeneration on OCT: classification of atrophy report 3. Ophthalmology **125**: 537–548.

Sadigh S, Cideciyan AV, Sumaroka A et al. (2013): Abnormal thickening as well as thinning of the photoreceptor layer in intermediate age-related macular degeneration. Invest Ophthalmol Vis Sci **54**: 1603–1612.

Schuman SG, Koreishi AF, Farsiu S, Jung SH, Izatt JA & Toth CA (2009): Photoreceptor layer thinning over drusen in eyes with age-related macular degeneration imaged in vivo with spectral-domain optical coherence tomography. Ophthalmology **116**: 488–496.

Sleiman K, Veerappan M, Winter KP et al. (2017): Optical coherence tomography predictors of risk for progression to non-neovascular atrophic age-related macular degeneration. Ophthalmology **124**: 1764–1777.

Ying GS, Maguire MG, Glynn R & Rosner B (2017): Tutorial on biostatistics: linear regression analysis of continuous correlated eye data. Ophthalmic Epidemiol **24**: 130–140.

Yu JJ, Agron E, Clemons TE et al. (2019): Natural History of drusenoid pigment epithelial detachment associated with age-related macular degeneration: age-related eye disease study 2 report no. 17. Ophthalmology **126**: 261–273.

Zweifel SA, Imamura Y, Spaide TC, Fujiwara T & Spaide RF (2010): Prevalence and significance of subretinal drusenoid deposits (reticular pseudodrusen) in age-related macular degeneration. Ophthalmology **117**: 1775–1781.

Received on November 21st, 2019.
Accepted on March 8th, 2020.

Correspondence:
Arnt-Ole Tvenning
Department of Ophthalmology
St. Olavs Hospital
Trondheim University Hospital
7006 Trondheim
Norway
Tel: +47 72575012
Fax: +47 72574833
Email: arnt.o.tvenning@ntnu.no

This study was presented in part as a poster at the 2019 ARVO Annual Meeting in Vancouver, Canada, 28 April–2 May 2019. The project has been made possible by the Dam Foundation (2016/FO80635). The sponsor had no influence on the study design or implementation.

Paper III

Retinal nerve fibre and choroid layers are signified as age-related macular degeneration by deep learning in classification of spectral-domain optical coherence tomography macular volumes

Arnt-Ole Tvenning*,[1,3] Stian Rikstad Hanssen*,[2] Dordi Austeng,[1, 3] and Tora Sund Morken[1, 3]

[1] Department of Ophthalmology, St. Olavs Hospital, Trondheim University Hospital, Trondheim, Norway

[2] Department of Computer Science, Norwegian University of Science and Technology, Trondheim, Norway

[3] Department of Neuromedicine and Movement Science, Norwegian University of Science and Technology, Trondheim, Norway

Correspondence**:** Arnt-Ole Tvenning

Department of Ophthalmology, St. Olavs Hospital, Trondheim University Hospital, 7006 Trondheim, Norway

Tel: +47 72575012 Fax: +47 72574833

Email: arnt-ole.tvenning@stolav.no ORCID 0000-0002-6890-7376

*Arnt-Ole Tvenning and Stian Hanssen co-authored this paper.